NEW IN-PLANE AND INTERLAMINAR SHEAR TEST METHODS FOR FIBER REINFORCED COMPOSITES

by

Peter G. Ifju

Thesis submitted to the Faculty of the

Virginia Polytechnic Institute and State University

in partial fulfillment of the requirements for the degree of

Master of Science

in

Engineering Science and Mechanics

APPROVED:

D. Post, Chairman

R. Czarnek

C. W. Smith

June, 1989

Blacksburg, Virginia

NEW IN-PLANE AND INTERLAMINAR SHEAR TEST METHODS FOR FIBER REINFORCED COMPOSITES

by

Peter G. Ifju

D. Post, Chairman

Engineering Science and Mechanics

(ABSTRACT)

A new compact double-notched specimen for in-plane shear testing of isotropic, anisotropic and composite materials was developed. A preliminary test of the specimen was performed on a cross-ply laminate. High sensitivity moire interferometry was used to determine the shear and normal strains on the entire face of the specimen. The results of the test were compared to those of the Iosipescu specimen on the same material. The compact specimen produced a more uniform and more pure shear distribution than the Iosipescu specimen. Stiffness measurements of the composite material were made. A detailed investigation of the specimen was performed and it revealed important attributes and defficiencies of the specimen. Recommendations for future work are cited.

The interlaminar shear response of a cross-ply composite was investigated. Shear strains on a ply-by-ply basis were measured using moire interferometry. Qualitative and quantitative information of the interlaminar shear characteristics of the material were obtained. The interlaminar shear modulus of individual plies and the effective modulus for the laminate were determined. Variations of nominally equal plies were observed.

Acknowledgements

The author wishes to express thanks to the many people who have been supportive throughout the masters program.

- A special thanks to Prof. Dan Post, the chairman of the committee, for his suggestions and knowledge on the technical issues of this thesis. Also his patience and support throughout the masters program is greatly appreciated.
- To Dr. Czarnek and Prof. Morton whose knowledge and support were helpful.
- To my fellow students in the photomechanics group whose cooperation, patience and most importantly friendship is greatly appreciated. Special thanks to , , , , , , and .
- To my family who have supported me throughout my academic career.
- To my close friends who I could always count on to raise my spirits especially, , , , , , , , , and .
- Also to the machine shop personel , , , , and who have helped greatly over the years with their skills and suggestions.
- To , and whose friendship was appreciated.

Table of Contents

INTRODUCTION

Current interest in fiber reinforced composites has resulted in efforts to characterize the mechanical behavior of these materials. Material properties for design and analysis include tensile, compressive and shear characteristics to name a few. The measurement of shear properties has proved to be more difficult than other tests such as tension and compression. Because of this, shear testing of composites has received a considerable amount of attention. Many experimental methods have been developed to test the in-plane shear properties of composites. Yet none has received widespread acceptance and as a result there is no generally accepted method to measure in-plane shear properties such as shear stiffness and strength. In addition only low resolution methods exist to determine the interlaminar shear response of fiber reinforced composites.

The objective of this study was to develop new test methods for the determination of in-plane and interlaminar shear properties of composite materials and to obtain corresponding material properties for a cross-ply laminate. This text is divided into two main portions followed by an appendix. The first part documents the development of a new compact specimen for the measurement of in-plane shear properties of composites. In the second section a study on the interlaminar shear response of a composite is documented.

In the first section the motivation for the development of a new in-plane shear test will be reviewed. This includes a brief description of other tests suited for in-plane shear testing of multi-direction composite laminates. Next, a new compact shear specimen will be proposed. An initial test of the specimen and its performance will be studied on a thick cross-ply laminate and the results are compared to those of the Iosipescu shear specimen. Qualitative and quantitative analysis of the specimen deformation will be determined. The deformation of both the new compact specimen and the Iosipescu specimen will be

analyzed in detail. A section on recommendations and specimen refinement will then follow.

The second section of this text will be devoted to the study of interlaminar shear of a cross-ply laminate. Two specimen configurations and loading fixtures will be proposed and investigated. A detailed qualitative and quantitative analysis will be presented for the interlaminar shear characteristics of a thick crossed-ply laminate.

Finally an appendix will detail the experimental techniques used in this work. This section will include a brief description of moire interferometry, the experimental technique used in this work, and applications of this method in the testing machine environment.

PART 1

IN-PLANE SHEAR TESTING

BACKGROUND

In-plane shear testing of fiber reinforced composites has received a considerable amount of attention. Shear properties are needed in the composites community as design parameters and for testing existing laminates for strength and quality control. Numerous test methods have been developed to obtain shear stiffness and strength measurements for composite materials, yet none has been widely accepted in the materials testing community [1]. In fact, at the present time no shear test method has been adopted for standardization by the American Society for Testing and Materials [2]. This is because each of the existing tests suffer from disadvantages associated with testing, analysis and/or versatility.

To test a material for in-plane shear stiffness and strength, ideally the material should be in a state of pure and uniform shear stress [3]. The illustration in Fig. 1 shows a cubic element of composite material where the three states of shear exist, one state of in-plane and two states of interlaminar shear. When one of these states exist without the presence of another or the presence of normal stresses then a state of pure shear stress exists [4]. When the shear state uniquely exists in the plane of the laminate plies then the

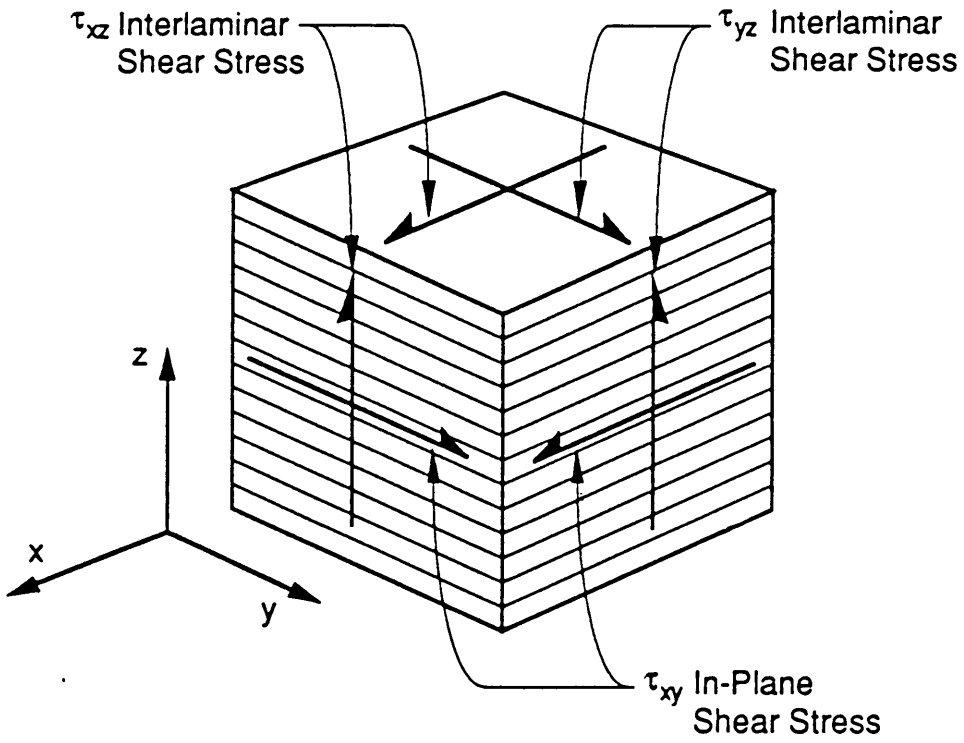

Fig. 1. The three independent states of shear stress which act on a composite. There is one state of in-plane and two states of interlaminar.

stress state is pure in-plane shear. In addition, if the shear is constant across the entire length of the material the shear stress state is both pure and uniform.

From a mechanics viewpoint the most pure and uniform shear stress state can be achieved by applying a torsional loading to a thin walled cylinder [5]. However for composites this scheme is limited to testing only specially made cylindrical specimens and extrapolating the results to flat laminates or existing laminated structures. This is expensive and often inaccurate. Therefore many different shear tests have been developed which use specimens cut from flat laminates. These tests sacrifice, to a small degree, pure and uniform shear stress in favor of convenience, and versatility. Among these methods are the off-axis tensile test, ± 45 degree tensile, Iosipescu test, Arcan test, rail shear, cross-sandwich beam test, and the picture-frame shear tests [3].

The off-axis tensile and the ±45 degree shear test work well for determining shear properties of unidirectional composites, however they cannot be applied to multi-directional composites [6,7]. This greatly reduces the usefulness of these tests and excludes them from quality control and shear testing of existing multi-directional laminates.

The ideal shear test method is one which is simple and inexpensive to conduct, measures both stiffness and strength, and incorporates a small, easy to fabricate specimen. There are instances when a small specimen would be advantageous. Composite materials are expensive to produce and small specimens would reduce the cost of multiple tests to determine its shear response. At times only a limited amount of material is available for testing. Often the shear characterization of only a small portion of an existing structure is needed. In addition some structures may have a slight curvature in the area where shear response characteristics are sought. In these instances large specimens could not be used.

At the present time there are few shear test methods available that incorporate a small specimen and provide the versatility to test a variety of material systems for both

shear stiffness and strength. The following three sections will review the most popular and/or promising existing shear test methods, the two rail shear, the Arcan shear test method, and the Iosipescu shear test method. The shear tests will be briefly described along with their advantages and disadvantages.

Two-rail Shear Test

The two rail shear test was one of the most widely used shear test methods in the aerospace industry [8]. This method consists of bolting rails along the sides of a rectangular specimen as illustrated in Fig. 2. Stresses are transmitted as shear by the relative displacement of one rail with respect to the other. A universal testing machine in compression is used to introduce the load.

The test method has gained popularity for various reasons. Rail shear tests are simple, inexpensive, and do not require much specialized equipment. Nevertheless the test has not gained total acceptance in the materials testing community because it does suffer from some serious disadvantages.

Whitney et al [8] conducted an extensive theoretical stress analysis on the rail shear specimen using Fourier series solutions. He concluded the test was not valid for specimens with an aspect ratio (length/width) less than 10. Because of this, the specimen size would need to be quite large. Specimens are commonly around six or seven inches long and two or three inches wide. Garcia et al [9] found that certain ply orientations caused irregular shear distributions. Chang et al [10] found the failure of a thick composite was initiated by interlaminar shears and normal stresses at the free edge. A round robin survey of the effectiveness of the rail shear test showed an alarming scatter in test results [11]. This brings to question the validity of the two rail shear test. Lee and Munro [3] conducted a comparison of the popular shear tests and rated the rail shear test below the

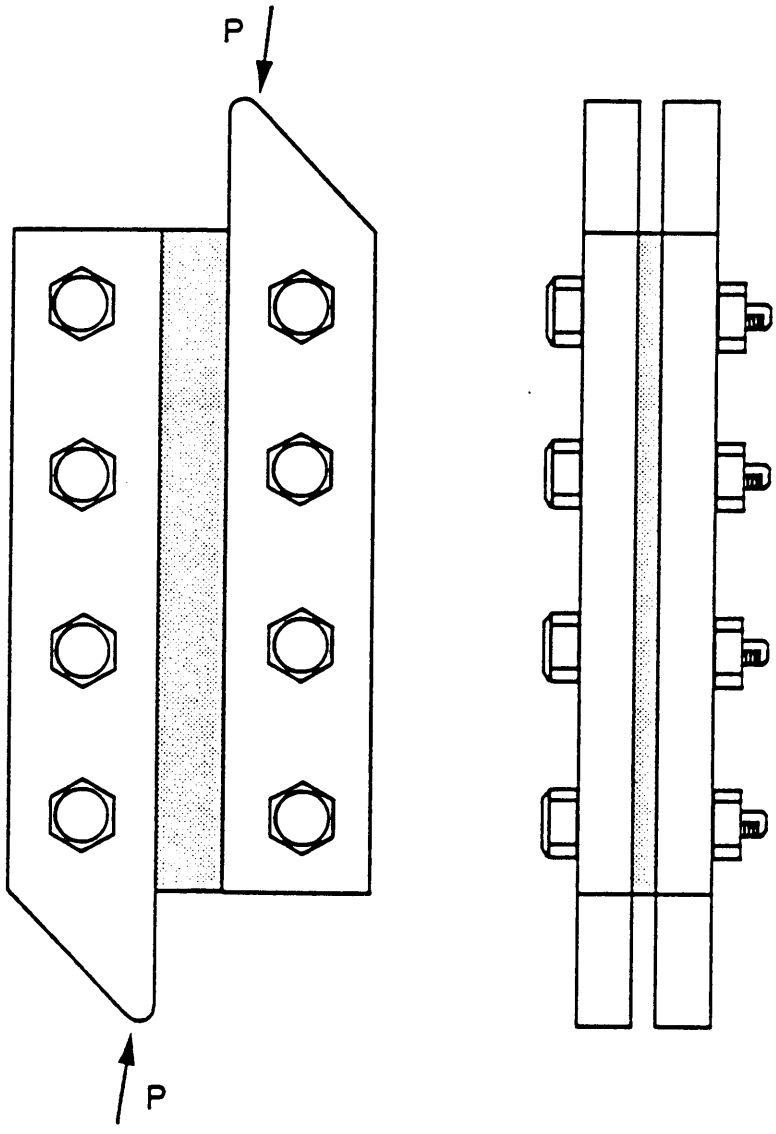

Fig. 2. The two rail shear test consists of a rectangular specimen with rails bolted to opposite sides. The loads are applied as shown by a universal testing machine resulting in shear along a vertical line down the center of the specimen.

average. Another disadvantage of the rail shear test includes the use of bolts for clamping the specimen to the rails. This is generally not an efficient or effective means of joining composites because of high stress concentrations around the bolts.

The Arcan Specimen

The Arcan specimen and loading fixture has been used to test composites to determine shear stiffness and strength [12]. Some liken the Arcan specimen to the Iosipescu specimen discussed in the next section. The test fixtures consists of two identical parts that are designed to clamp on both sides of a butterfly shaped specimen as shown in Fig. 3. A tensile load on the fixture is transmitted to the specimen as shear in the narrow section of the specimen.

Major advantages of this test method include easy specimen preparation, simple fixturing, and straight-forward testing. A wide variety of testing machines can be used. Additionally, biaxial testing can be performed with this test method. Arcan claims the shear in the test section is pure and uniform [13].

The Arcan test method nevertheless has not been widely accepted by the materials testing community for reasons which are not clear. Some disadvantages though are sighted here. First the test method uses bolts to secure the specimen to the loading fixtures. Failure of some laminates are believed to be initiated at the bolts. Shear strain concentrations occur as well as uneven bolting pressures. In addition the shear stress distributions of the Arcan specimen have yet to be confirmed uniform in the test section and it is believed they vary greatly with fiber orientation [13]. Another disadvantage of the Arcan specimen is its size. The specimen is 3.5 in. by 2.75 in. with a test section length of around 0.75 in.. With the amount of material needed for one Arcan specimen three Iosipescu specimens could be made.

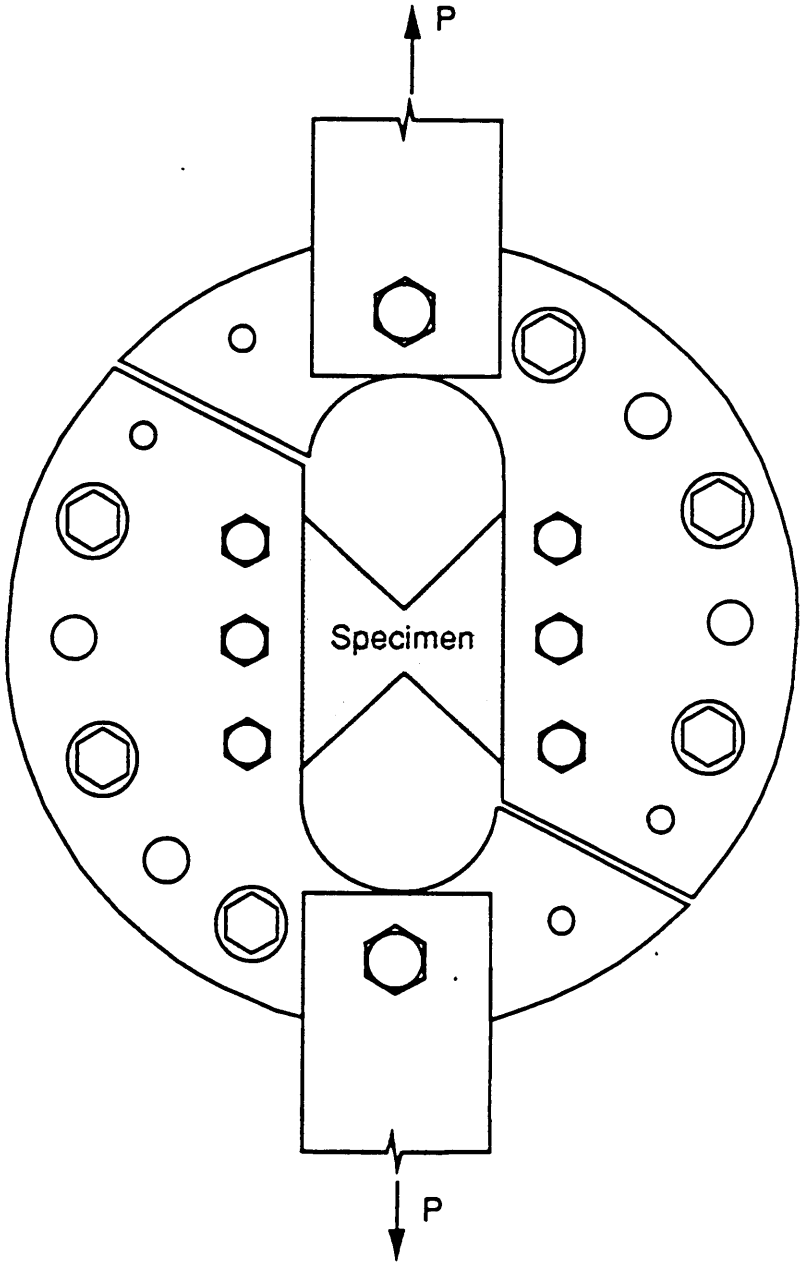

Fig. 3. The Arcan test uses a butterfly shaped specimen with load fixtures bolted to its sides. The strains are obtained from gages located in the test section between the notches.

The Iosipescu Test

The Iosipescu shear test is one of the most popular methods used today for composite materials. The test is used for determining the shear stiffness and strengths of both unidirectional and multidirectional laminates [14-16]. The test method was devised by Nicolae Iosipescu of Bucharest, in the early 1960's [17]. The Iosipescu specimen shown in Fig. 4 is rectangular with two opposing notches centered on its top and bottom. A specialized fixture clamps the specimen, then applies a shearing action between the notches. Numerous loading fixtures have been developed for use with the Iosipescu specimen. Walrath and Adams at the University of Wyoming [16] have developed two fixtures. The second or modified Walrath-Adams test fixture is the most widely used. Slepetz et al [18] developed an asymmetric four point bend loading fixture, as an alternative.

The Iosipescu test has some clear advantages. The specimen is small and therefore, it can be extracted from existing laminated structures efficiently. It is also simple to prepare [19]. Shear strength measurements are thought to be accurate [20]. In a study of the available shear test methods by Lee and Munro [3], the Iosipescu test rated the best.

The Iosipescu specimen and loading fixtures have been studied extensively using experimental and numerical approaches. Finite element (FE) studies have been performed on the specimen. Herakovich et al used FE [21] to determine the extent of the zone of uniform shear. They concluded that only a small region of uniform shear existed between the notches. Additionally, they found that the shear strain distributions were far from uniform in the test section and that specimens with differing ply orientations produce markedly different distributions. This was verified experimentally by Pindera et al [22] using moire interferometry, a whole field displacement technique. In another study Pindera et al [20] suggested the use of correction factors to compensate for nonuniform shear stress

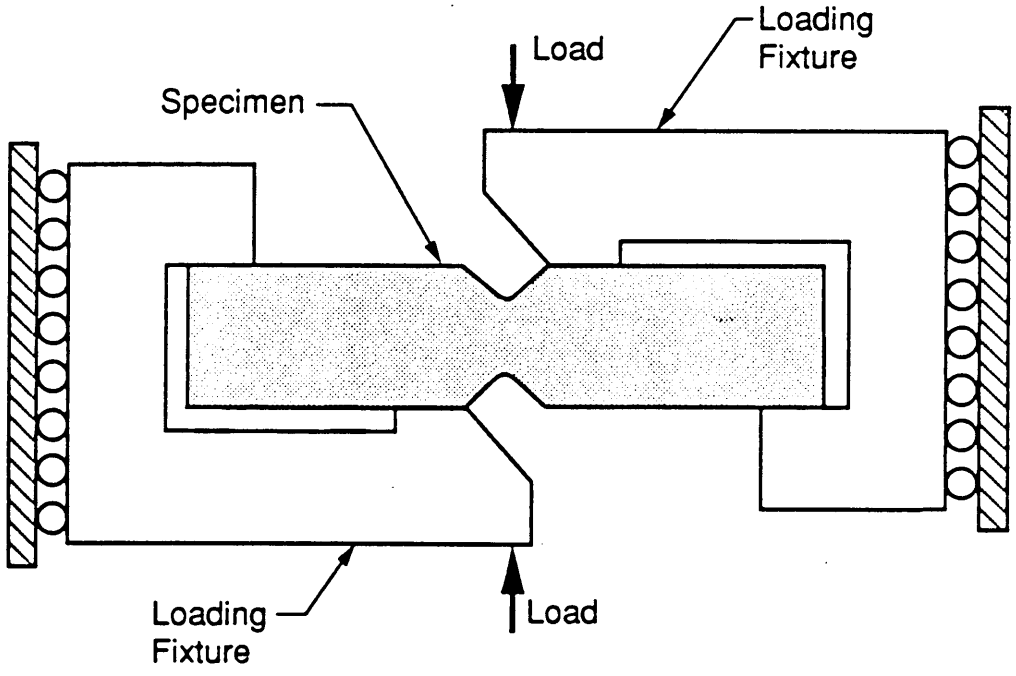

Fig. 4. The Iosipescu specimen is rectangular with opposing notches centered on the top and bottom. A special fixture applies the loads creating shear in the test section between the notches.

distributions. Correction factors on the order of 20% were used to improve the stiffness results measured by strain gages. Wang et al [23] also determined the shear strain extent and distributions for unidirectional laminates using FE analysis. They found that the notch angle and radius affected the uniformity of shear strain in the test section. They also determined that the optimum notch angle and radius was a function of the ply orientation. Abdallah [24] combined moire interferometry, photoelasticity and finite element analysis to investigate three loading fixtures commonly used--the two Wyoming fixtures, and the asymmetric four point bend fixture. He concluded that each fixture produced unique shear, and normal stress distribution in the test section. Normal strains existed in the test sections of all the specimens, but they were larger with the Wyoming fixtures. Abdallah concluded the assymetric four point bend fixture gave better results than the Wyoming fixtures. He concluded that specimen placement or alignment had a large influence on the state of stress in the test section of each fixture.

From these studies it was clear that the Iosipescu specimen did not produce a large region of pure and uniform shear. Because of this, stiffness results can be accurate only if the right correction factor is used. Strength measurements are also questionable since again the maximum shear strain exceeded the average shear strain. The degree to which pure shear exists in the test section is also questionable. This point casts further doubt on the shear strength measuring capabilities of the Iosipescu specimen loaded in some fixtures.

The American Society for Testing and Materials is in the process of standardizing a shear test method. The Iosipescu specimen and the second or modified Walrath, Adams fixture have been proposed for that standard [2]. Unanimous support for this test method is not present, and as a result, there has been a delay in its ratification.

It is evident that at the present time the most effective shear test methods suffer from serious shortcomings. As a result, the composites community is forced to compromise the

accuracy of material characterization. The development of a superior shear test method could have an important impact on the materials testing community.

DEVELOPMENT OF A NEW SHEAR SPECIMEN

A new shear specimen and loading system is proposed to measure the shear response of engineering materials. The specimen is called the compact double-notched specimen. However it will be referred to at times as the compact specimen. It was developed to offer a simple alternative to the existing test methods. Key issues such as specimen size, uncomplicated fixturing, specimen material variety and reliable measurements of shear response served as the objective for its development. The compact specimen appears to be superior for most routine shear response measurements, including stress-strain properties in shear and shear strength measurements. Figures 5 and 6 show the specimen and loading fixtures used in this initial test. The specimen was 1.5 in. long, 0.75 in. wide and 0.25 in thick with 0.25 in. wide notches. The distance between the notches was 0.75 in. The overall size of the compact specimen was half that of the Iosipescu specimen yet its test section was larger by more than 40%.

The loading system of the compact specimen was simple and inexpensive to manufacture. The specimen was loaded by two load transfer fixtures clamped to its sides as shown in Fig. 5 by special clamping devices. These clamping devices act to keep the specimen in static equilibrium and help alignment as compressive loads were applied to the specimen at two opposite corners. The load was then redistributed in the specimen resulting as shear in the test section located between the notches.

The compact specimen was developed to be used with strain gages located halfway between its notches much like the Iosipescu test. The gages would be used to record shear

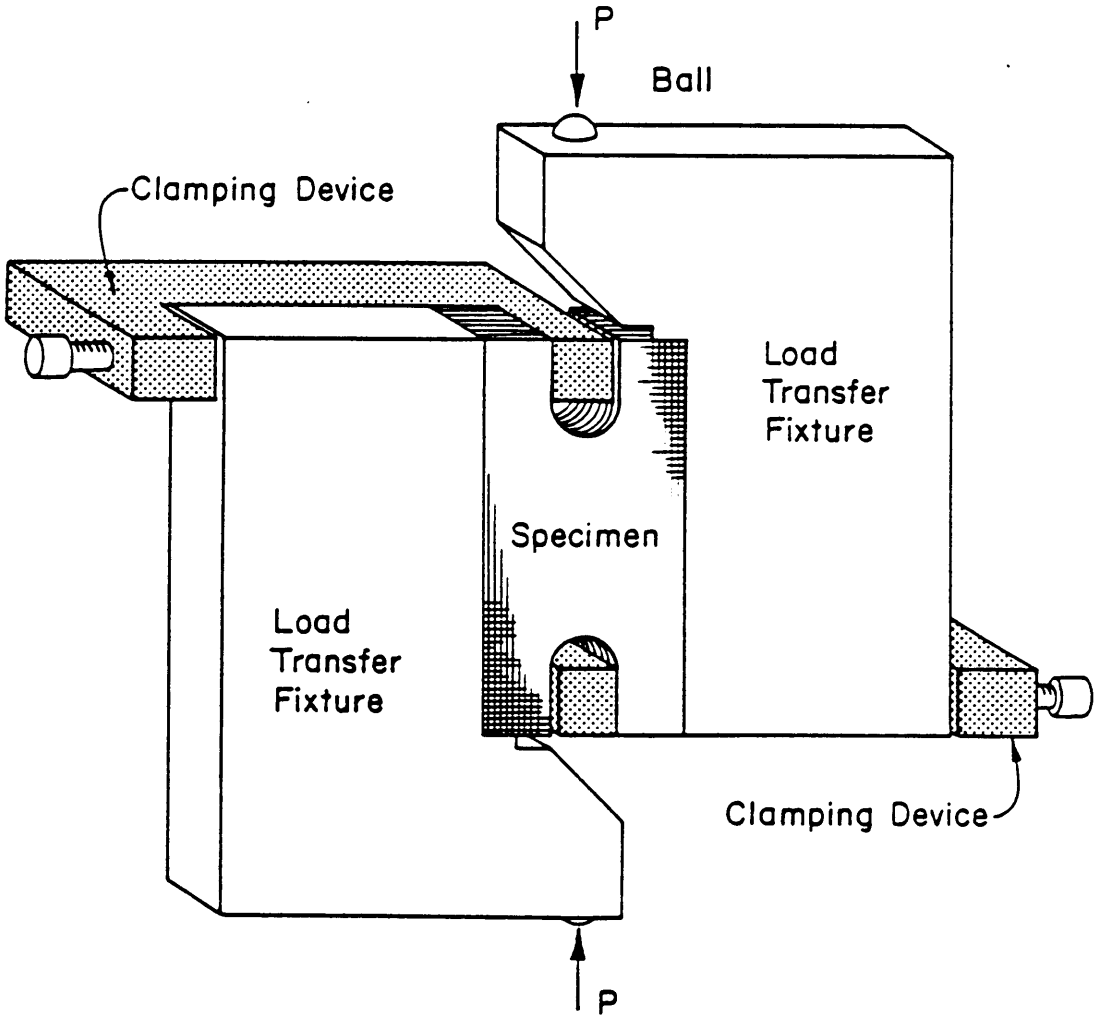

Fig. 5. The compact double-notched specimen and loading fixtures. The specimen is loaded at its corners by direct compression and held in static equilibrium by special clamping devices.

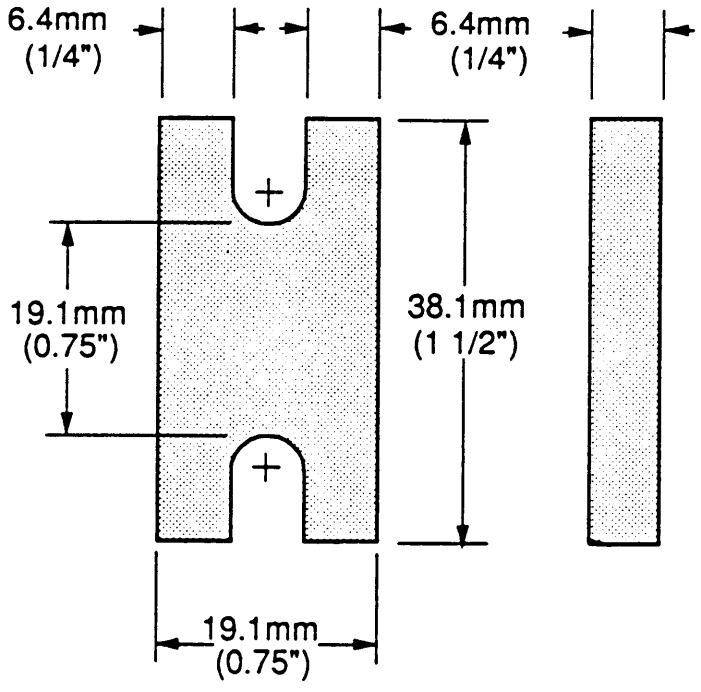

Fig. 6. An engineering drawing of the compact specimen used in this initial test.

and normal strains. Strain gages provide an inexpensive method of extracting shear strain information on a routine basis from a small area called the gage zone located half way between the notches. Gages are used often in the materials testing community for repetitive testing. Even though strain gages are proposed for routine testing, moire interferometry was used in these experiments to evaluate the specimen. Moire interferometry [25] is an optical technique discussed in detail in the appendix section of this text. It can measure deformations on a whole field basis and therefore it is suited for evaluating test methods. Moire interferometry was used in these experiments to provide shear and normal strain distributions on the entire face of the specimen. Accurate strain distributions and shear stress-strain information were acquired with the help of moire. Although it is an excellent method for specimen evaluation, moire interferometry is not a recommended technique for routine testing. Also few labs have the capability of using moire interferometry. Therefore it was used to monitor the compact specimen to evaluate its applicability for strain gage use.

INITIAL VERIFICATION OF THE COMPACT SPECIMEN

An initial test on a cross-ply laminate was performed to evaluate the merits of the compact specimen. The results were compared to that of the Iosipescu specimen shown in Fig. 7, which was taken from the same laminate. One Iosipescu and two compact specimens were removed from a thick graphite/epoxy, cross-ply composite cylinder as shown in Fig. 8. The material specifications are given in Fig. 8 also. Because of its small size the compact specimen could be removed from the cylinder aligned in either the hoop or axial directions. Both orientations were investigated. The orientation that had the test section of the specimen aligned in the hoop direction was known as compact specimen I. The specimen which had the test section aligned in the axial direction was specimen II, as

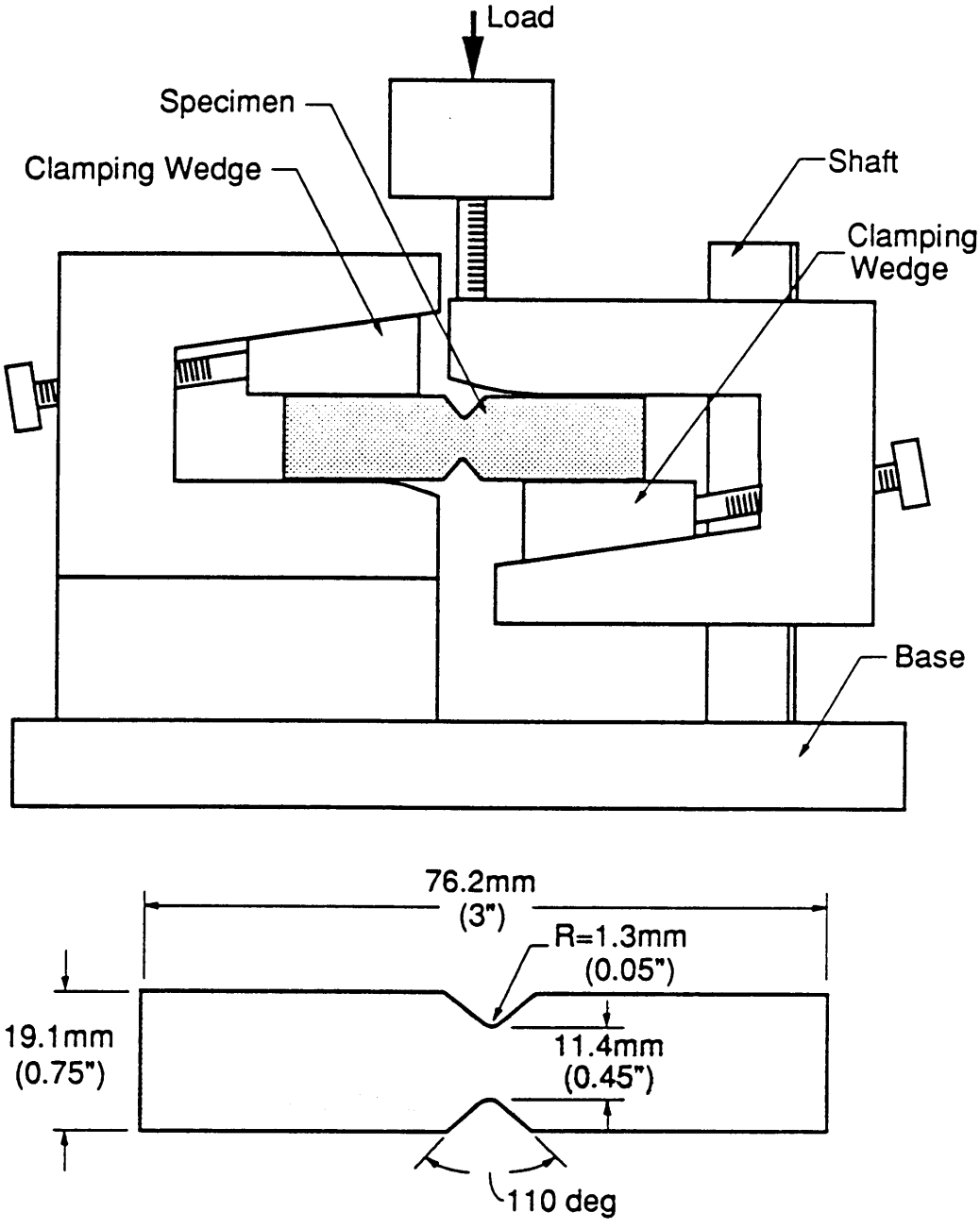

Fig. 7. The Iosipescu specimen and loading fixture used in these experiments. The fixture was the second or modified Wyoming fixture.

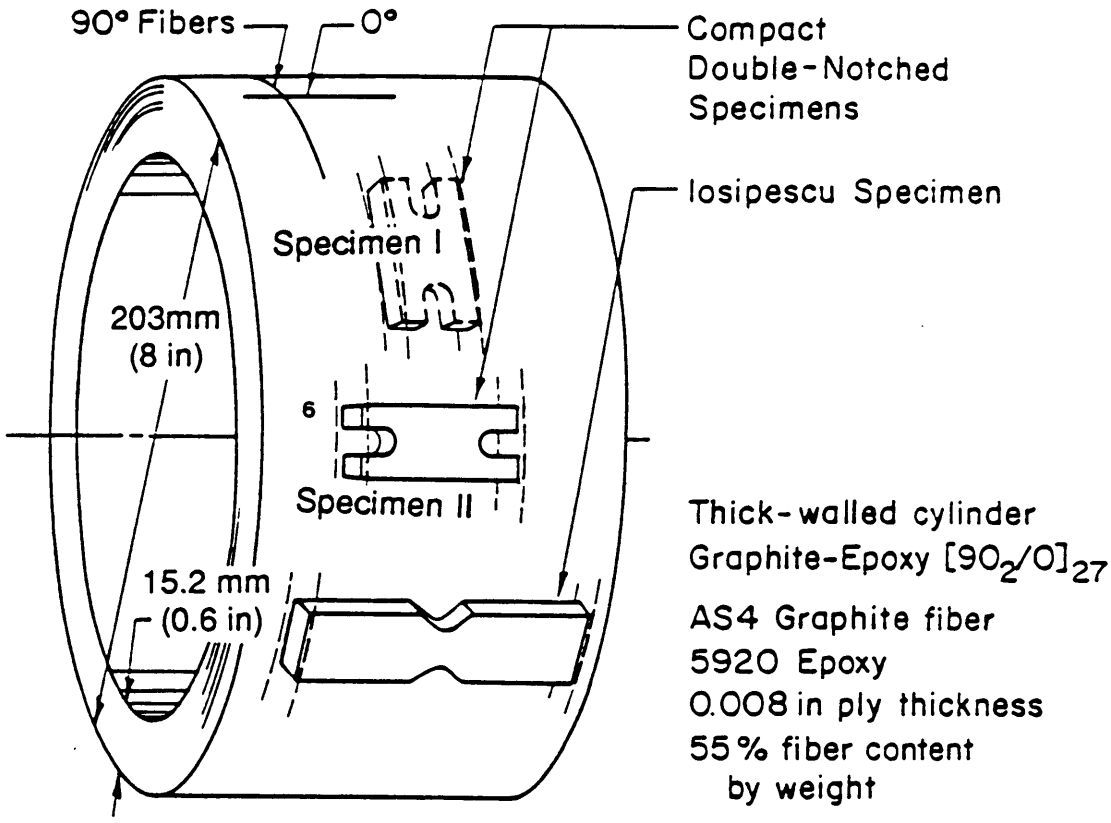

Fig. 8. The specimens were cut from a thick-walled cross-ply graphite/epoxy cylinder. Two orientations were investigated for the compact specimen as show.

shown in the figure. The Iosipescu specimen could be extracted from the cylinder aligned in only one direction, that which had the test section in the hoop direction. Since both test methods (compact and Iosipescu) apply loads in a vertical plane, ideally the plies in the test section should coincide with that plane. Therefore pure shear in the test section would most likely occur in compact specimen II since the effects of ply curvature are circumvented by this orientation. Undesirable curvature in the other two specimens existed, but the effects are thought to be small since the cylinder diameter was large compared to the length of the test sections. The effects of ply curvatures is discussed in a following section.

All three specimens were cut from the cylinder with a diamond saw. The edges were ground flat and the notches were cut with a diamond-impregnated hole saw. In addition to the ply orientations, only one other difference existed between the two compact double-notch tests. Specimen I was cemented to the load transfer fixtures with epoxy and clamped whereas specimen II was just clamped. The cement in specimen I failed at an intermediate load level. The deformation of the specimen then became almost identical to that of specimen II since the loading conditions were the same.

The load P shown in Fig. 5 for the compact specimens was applied with a simple wedge type loading fixture shown in Fig. 9. Loads were recorded by a strain gage indicator connected to calibrated strain gages on the wedge fixture. This fixture was used to allow testing on a vibration isolation table which greatly simplified the moire setup.

The Iosipescu specimen shown in Fig. 7 was tested in the second or modified Walrath, Adams loading fixture. The fixture clamped both ends of the specimen with a wedge type grip. One half of the fixture held the specimen stationary while the other half slid on a linear bearing down a shaft upon loading. The relative motion of the two halves of the specimen create shear in the test section. Loads were introduced to this fixture with a

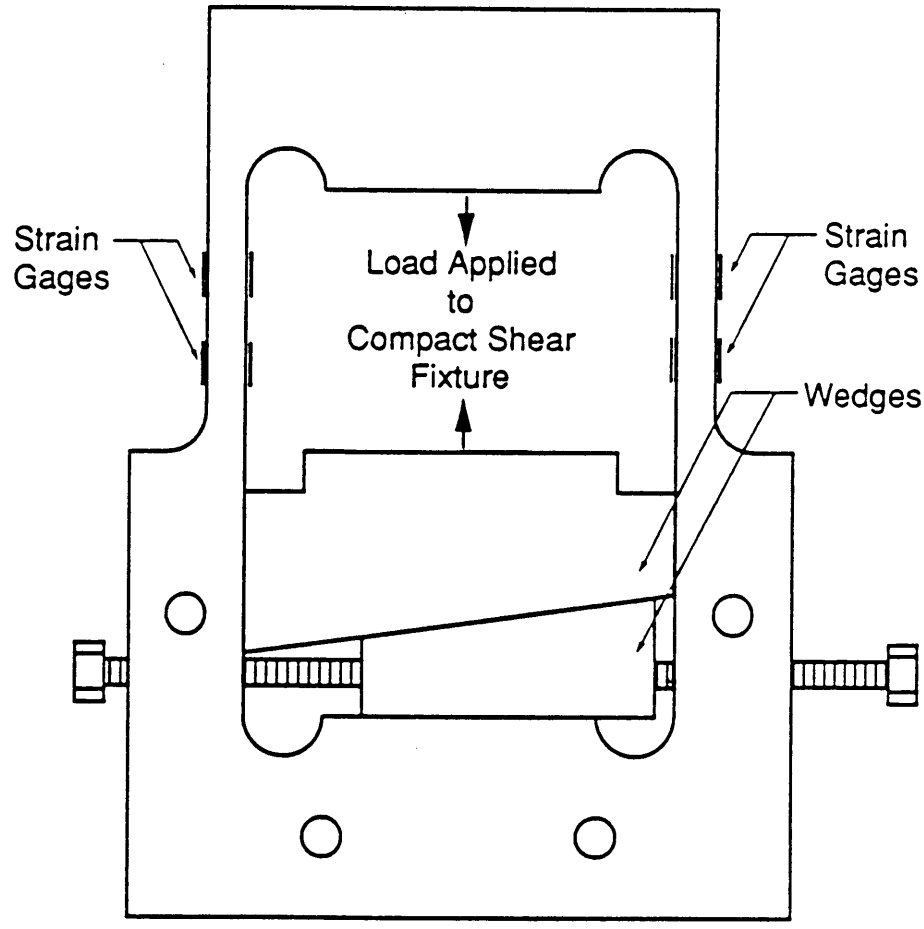

Fig. 9. The loads were applied to the compact specimen fixtures by a simple wedge type loading fixture.

Tinius Olsen screw driven testing machine. A special moire interferometer, discussed in the appendix, was built for testing on the Tinius Olsen.

The three specimens were loaded well into the nonlinear region of shear deformation. The load levels tested are shown in Table 1. Only compact specimen II was loaded to failure.

DEFORMATION ANALYSIS USING MOIRE INTERFEROMETRY

Contour maps of the in-plane displacements were recorded for the entire face of both of the compact specimens and for the central third of the Iosipescu specimen. The shear and normal strains could be calculated from these displacement fields. The appendix section on experimental techniques discusses in more detail the principals of moire interferometry.

Qualitative Analysis of Deformation

The Compact Double-Notched Specimen

The fringe patterns in Figs. 10 through 12 obtained through the use of moire interferometry, depict the U (horizontal) and V (vertical) displacements of compact specimen I for various load levels. Figures 13 through 15 are the U and V displacement fields for specimen II. As can be seen in Figs 10 and 13, at the zero load level the deformation in the test section located between the notches was almost zero for both specimens . As the loads increased, a predominant state of shear was observed in the test section as can be seen in Figs 11, 12, 14, and 15. This was revealed by the vertical fringes in the V field patterns. All points along any fringe in the test section had displaced vertically with respect to points along a neighboring fringe. This result can be seen in both

Table. 1. The load steps recorded for the two compact specimens and the Iosipescu specimen.

Load Steps for Compact Specimen I

Load, N (lb)		Average Stress, kPa (psi)		Average Strain (με)
0	(0)	0	(0)	0
655	(147)	5516	(800)	1406
1735	(390)	14630	(2122)	4102
2869	(645)	24200	(3510)	7884
3025	(680)	25510	(3700)	9260
3914	(880)	33020	(4789)	13670

Load Steps for Compact Specimen II

Load, N (lb)		Average Stress, kPa (psi)		Average Strain (με)
0	(0)	0	(0)	0
655	(147)	5536	(803)	897
1690	(380)	14310	(2076)	3440
2869	(645)	24300	(3524)	7130
3914	(880)	33160	(4809)	12440

Load Steps for the Iosipescu Specimen

Load, N (lb)		Average Stress, kPa (psi)		Average Strain (με)
0	(0)	0	(0)	0
214	(48)	2930	(425)	530
436	(98)	6005	(871)	1171
890	(200)	12260	(1778)	2283
1325	(298)	18260	(2649)	4145
1780	(400)	24510	(3555)	6610
2602	(585)	35850	(5200)	14364

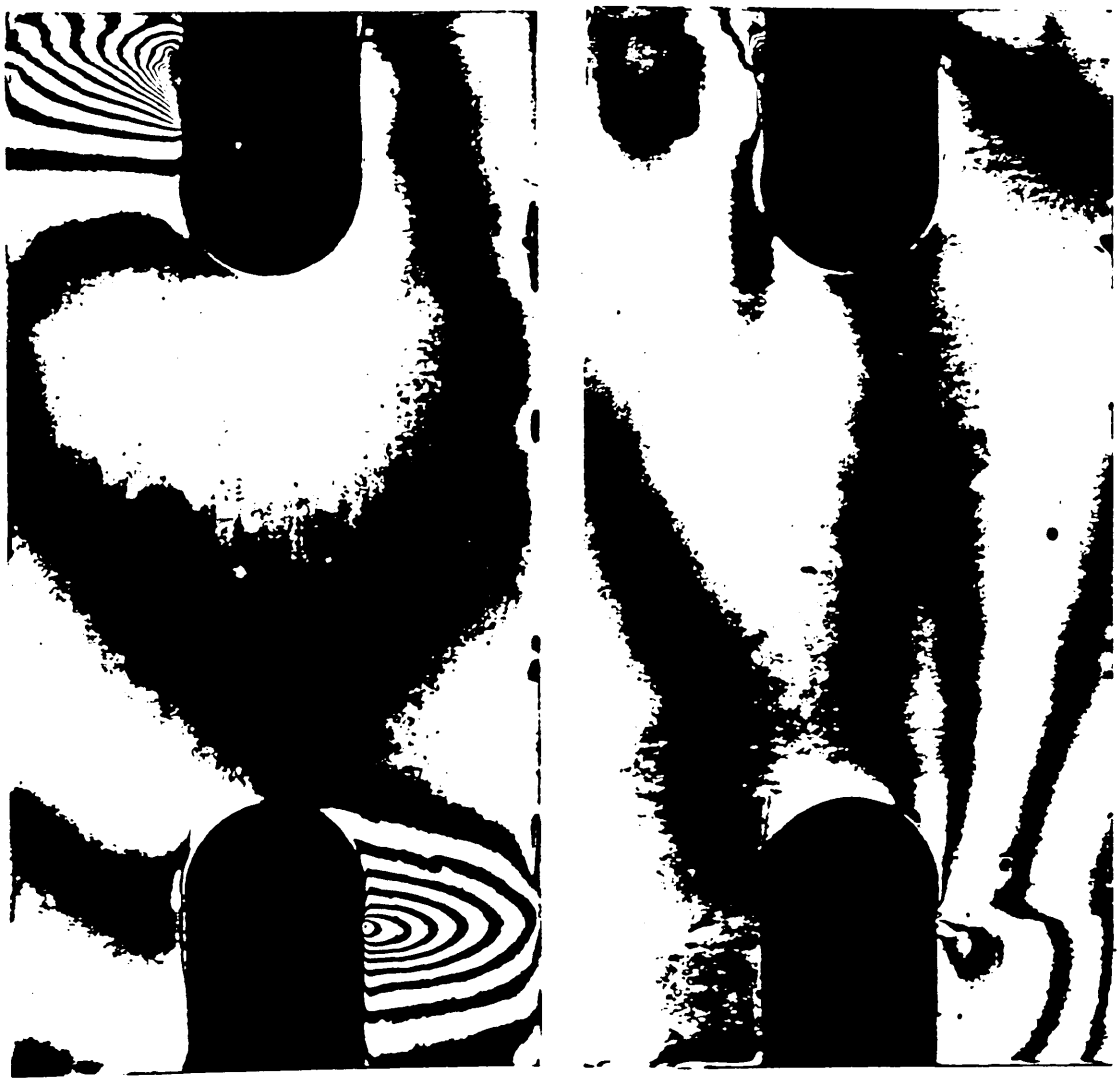

Fig. 10. The U and V displacement fields for compact specimen I at 0 kPa (0 psi.).

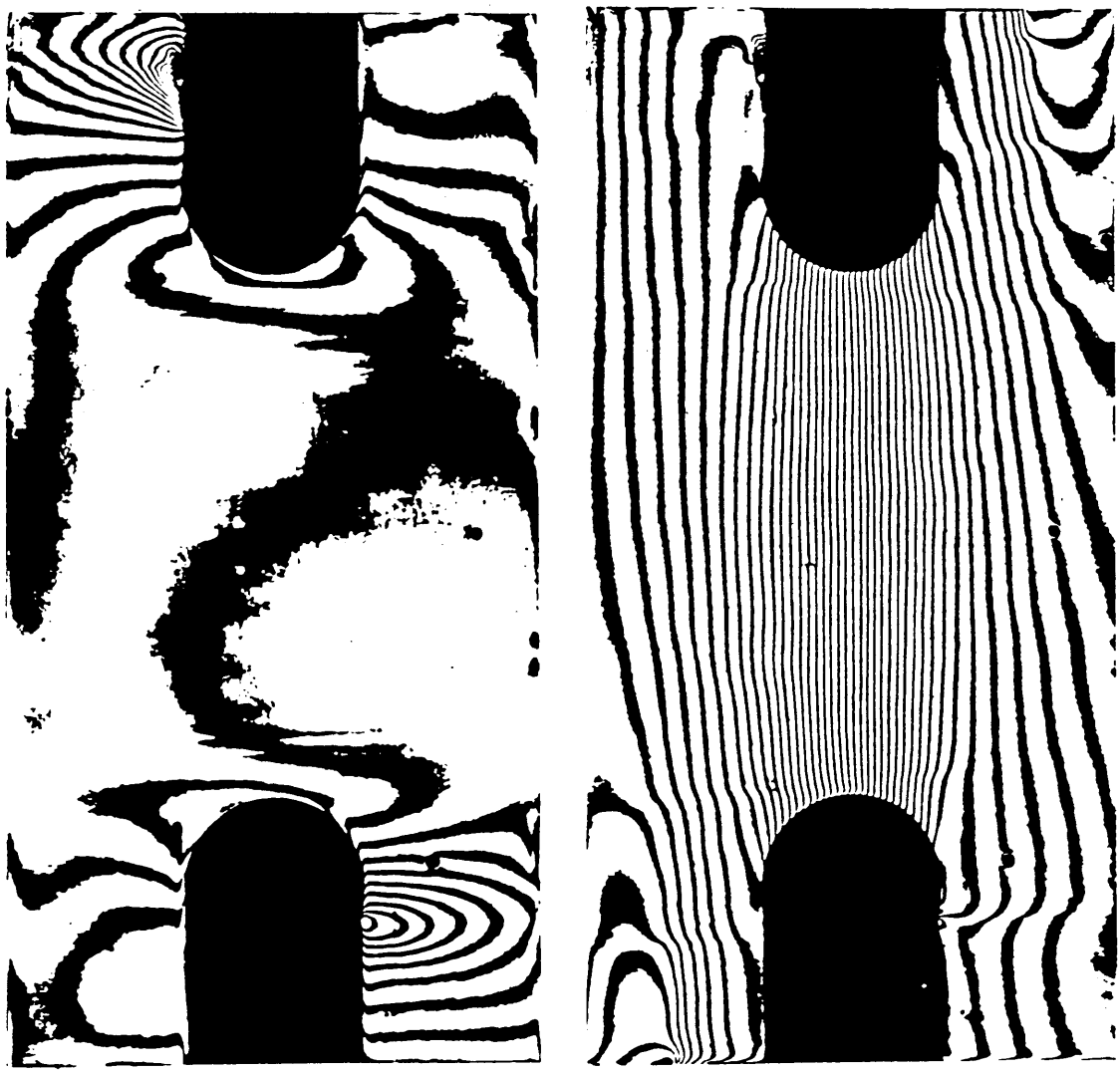

Fig. 11. The U and V displacement fields for compact specimen I at 5516 kPa (800 psi.).

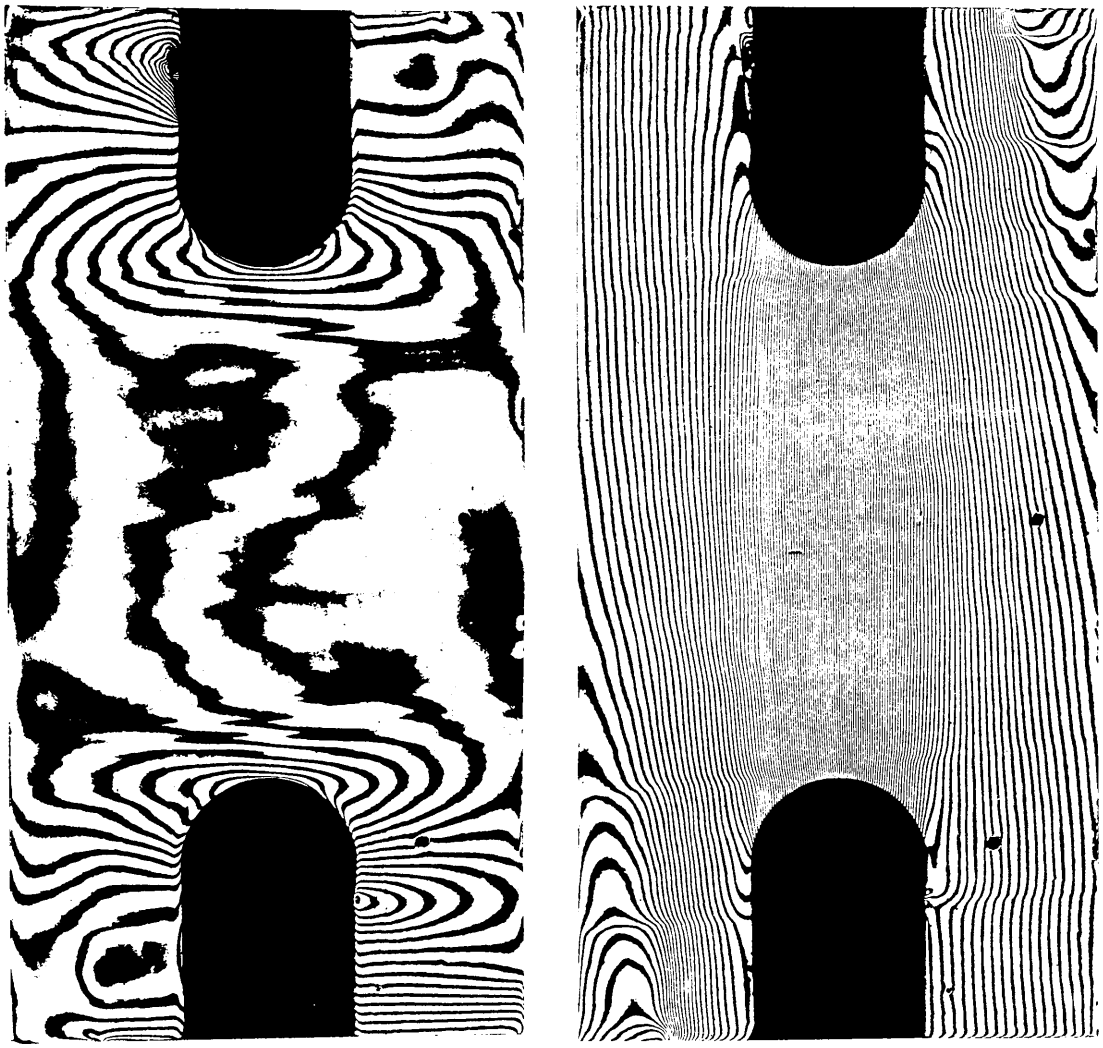

Fig. 12. The U and V displacement fields for compact specimen I at 14630 kPa (2120 psi.).

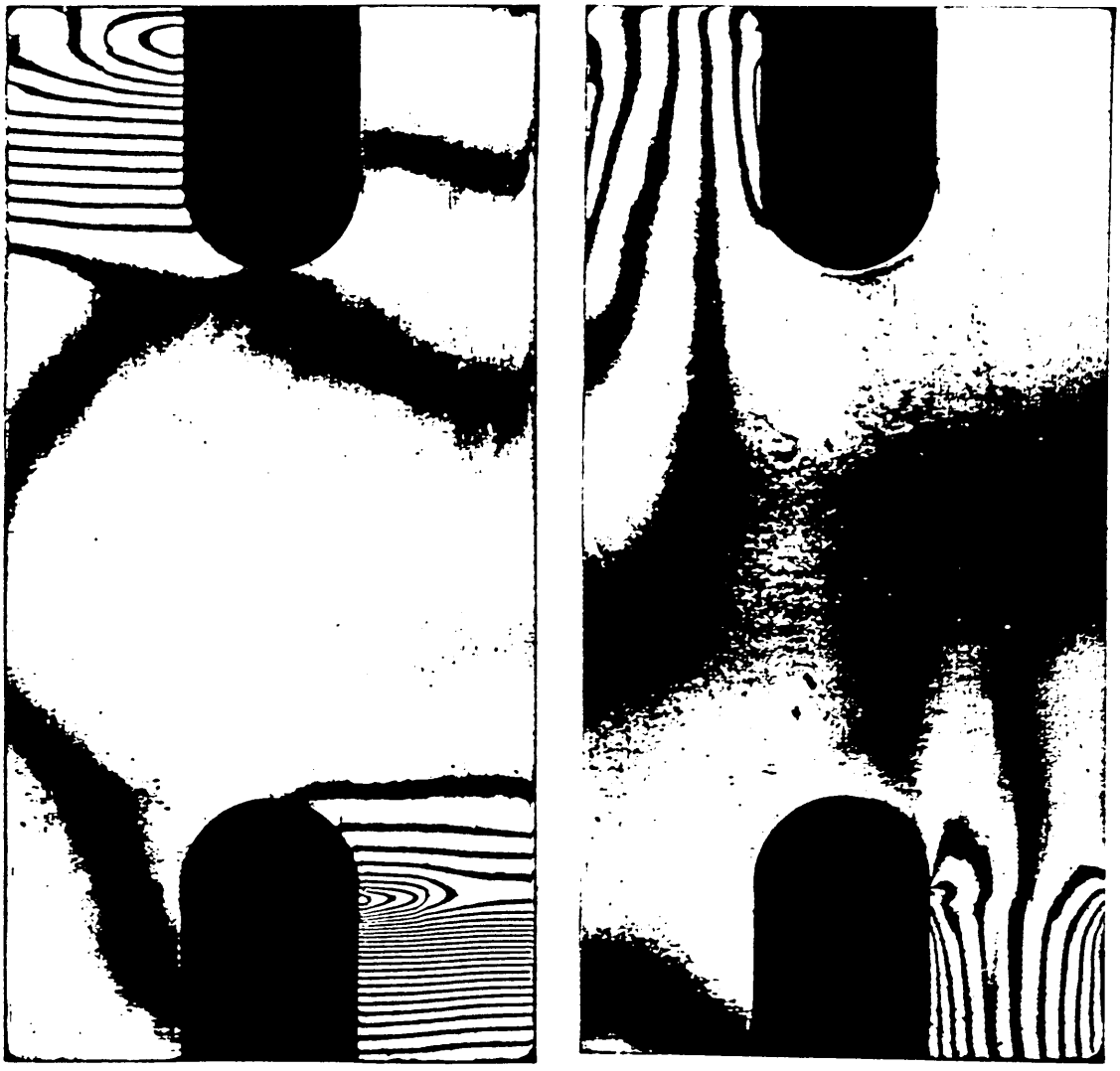

Fig. 13. The U and V displacement fields for compact specimen II at 0 kPa (0 psi.).

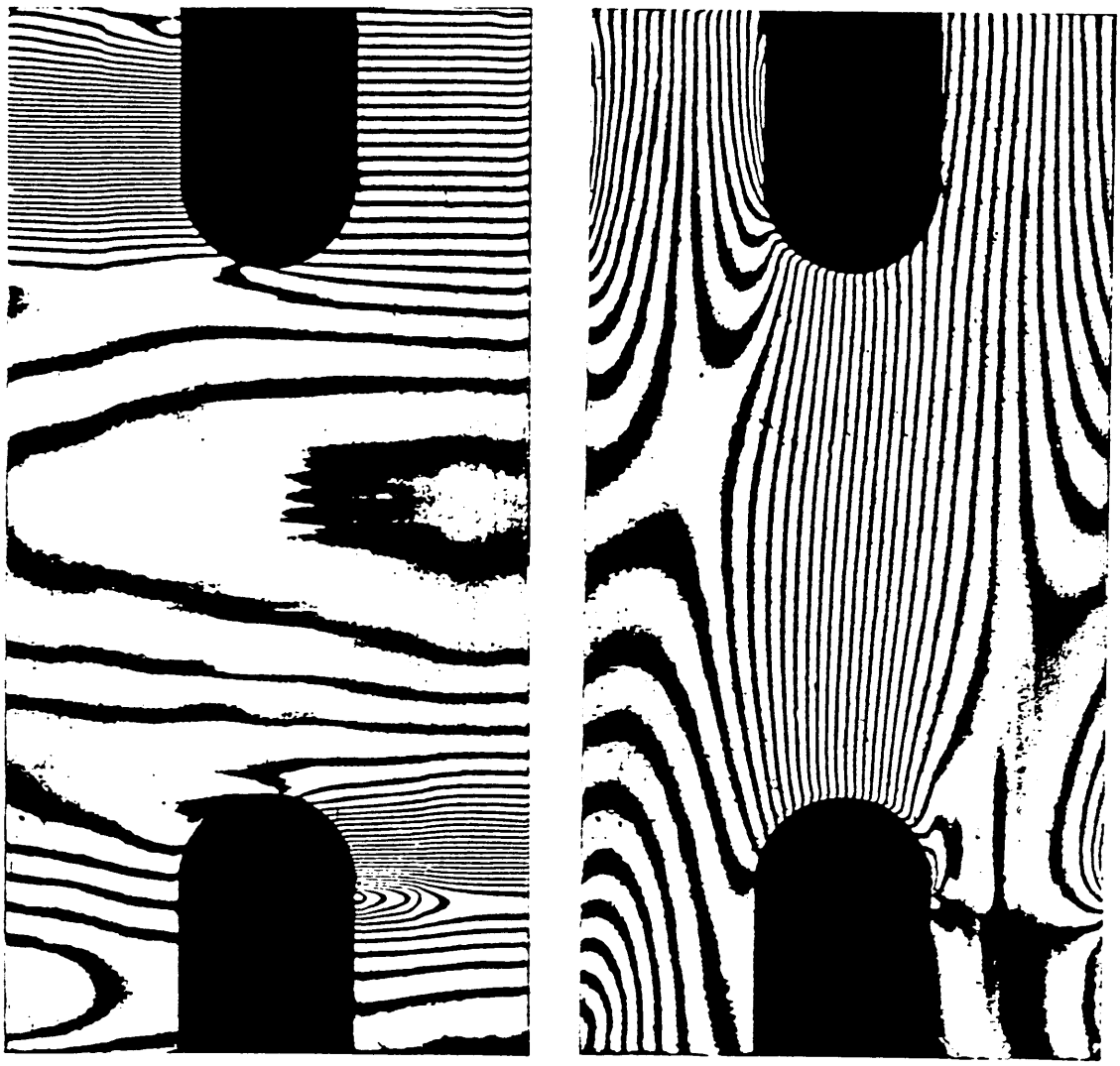

Fig. 14. The U and V displacement fields for compact specimen II at 5536 kPa (803 psi.).

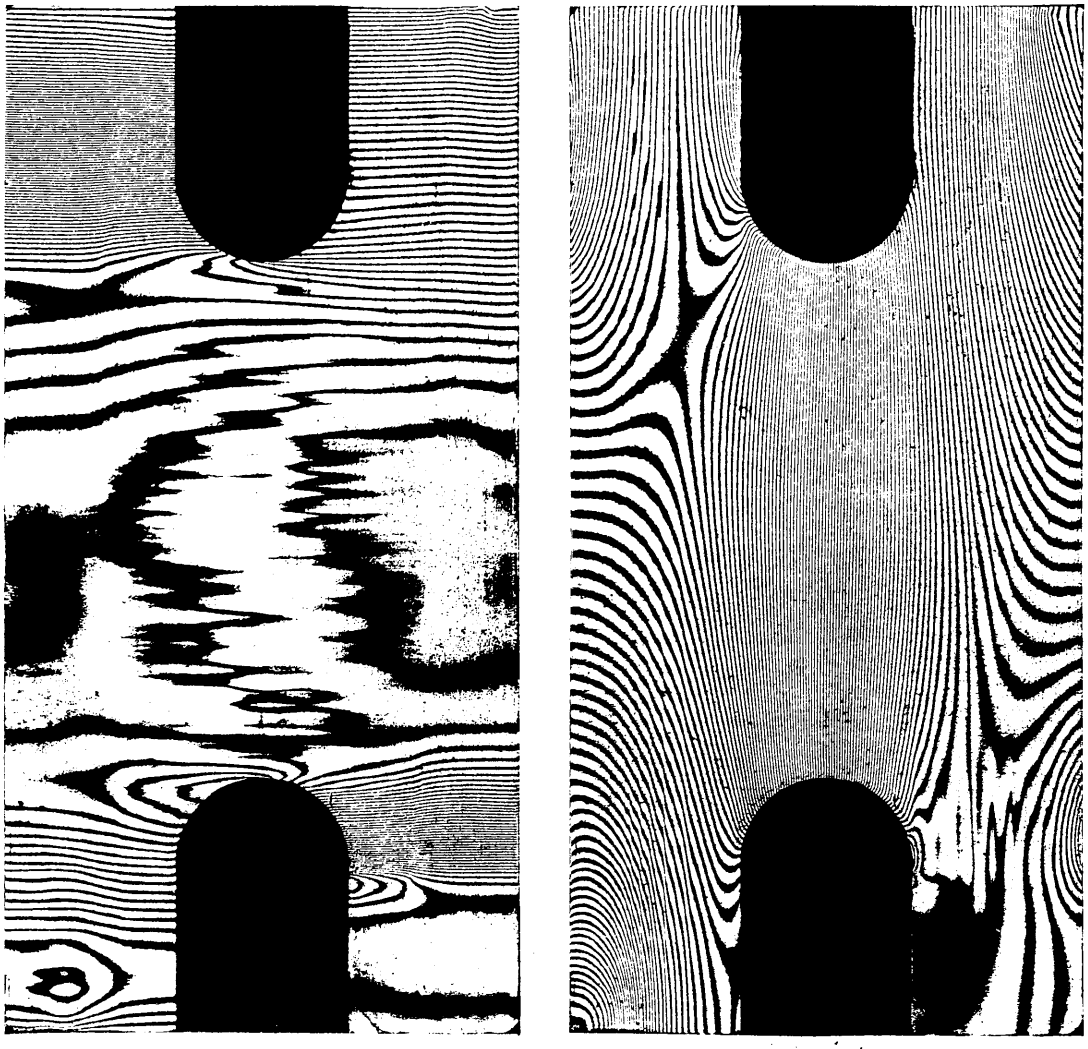

Fig. 15. The U and V displacement fields for compact specimen II at 14310 kPa (2080 psi.).

specimens. The fringes in specimen II are almost perfectly vertical and evenly spaced, whereas there is some nonuniformity seen in specimen I, This variation in the fringe spacing will be discussed in more detail in the section on shear strain nonuniformities. It is believed that the varying fringe gradient was a result of specimen nonuniformities and was not load induced.

Still focusing on the area between the notches of both specimens in Figs 11, 12 14, and 15, it was apparent that the normal strains ε_y and ε_x were small compared to the shear strains. Since the fringes in the V field are basically vertical there is little fringe gradient in the vertical direction and therefore ε_y is small. Now looking at the U field for both specimens, the horizontal fringe gradient was small or zero in the area between the notches signifying small ε_x. Nearing the notch tips, though, normal strain ε_x was observed in compact specimen II. The magnitude of this normal strain was much less than the shear strains. Because of the absence of significant normal strains in the test section of the specimen it was apparent that a relatively pure state of shear existed.

In the arms of both specimens there was some compressive strain resulting from the direct bearing of the load transfer fixture. This is evidenced by the V field patterns which revealed strong vertical fringe gradients in the affected areas. Also in the other two arms of specimen II there were some strong shear strains caused by the clamping devices. The strains outside the test section will be discussed later in this text under the heading, high strains remote from the test section.

The Iosipescu Specimen

Figures 16, 17, and 18 show the U and V displacement patterns for the central third of the Iosipescu specimen at various load levels. At the zero load level in Fig. 16 there was an initial state of deformation in the test section of the specimen. The vertical

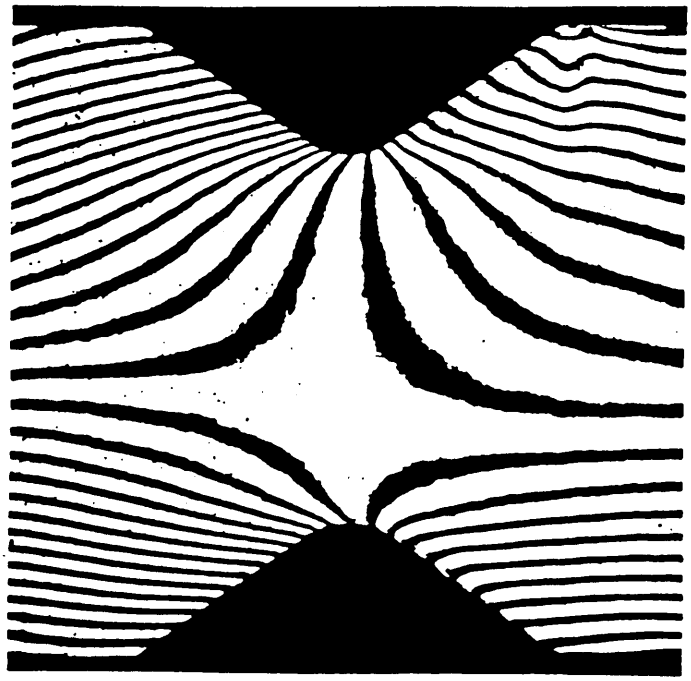

U Field

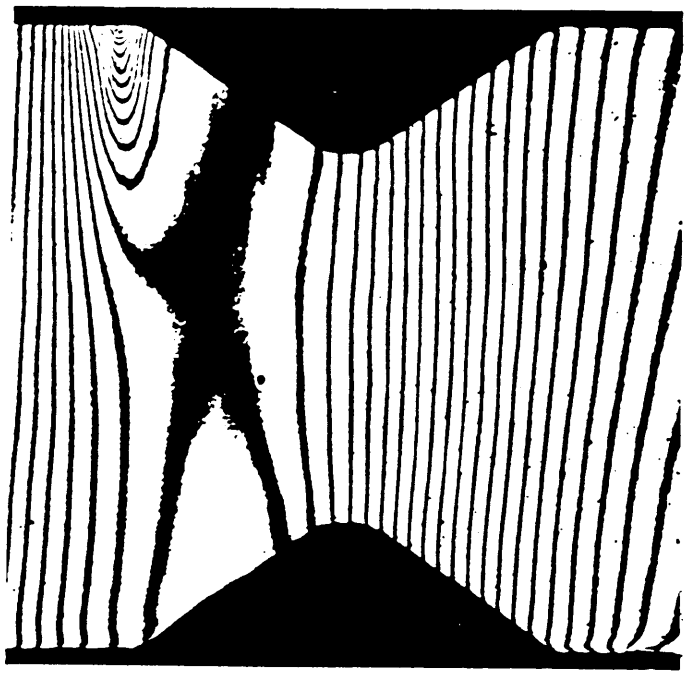

V Field

Fig. 16. The U and V displacement fields for the Iosipescu specimen at 0 kPa (0 psi.).

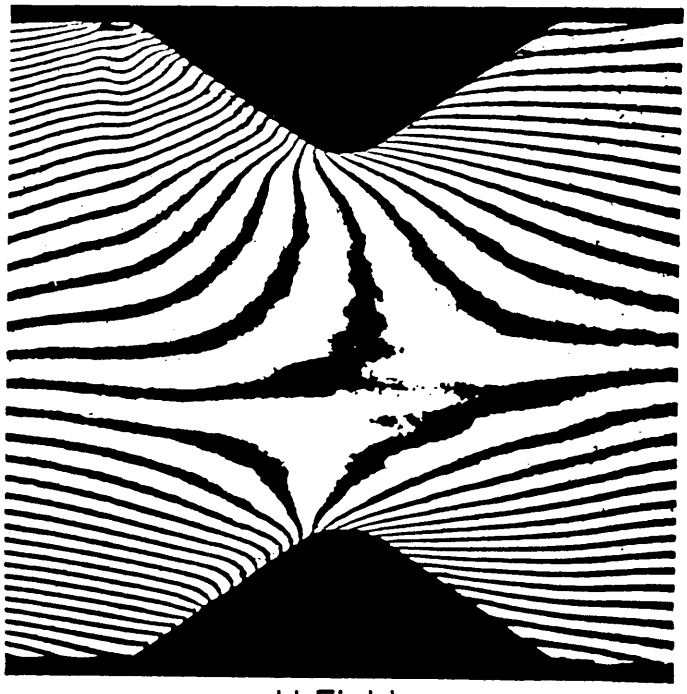

U Field

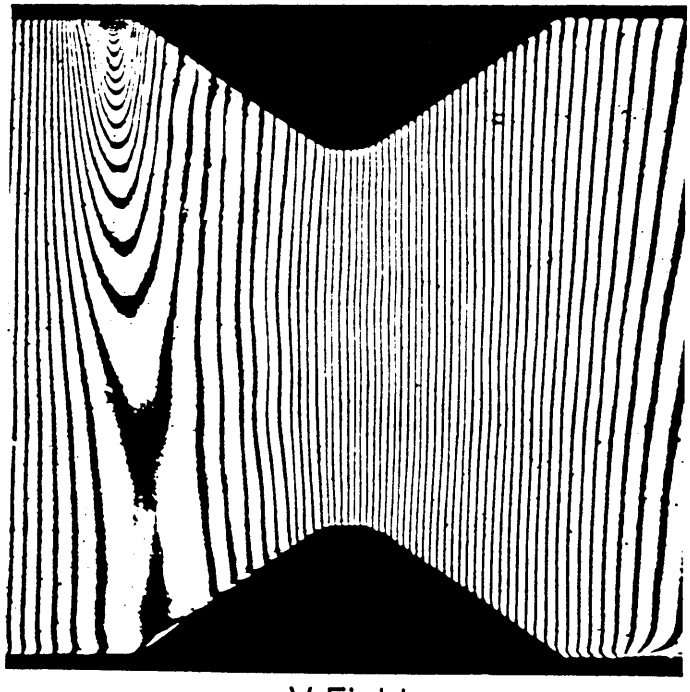

V Field

Fig. 17. The U and V displacement fields for the Iosipescu specimen at 6005 kPa (871 psi.).

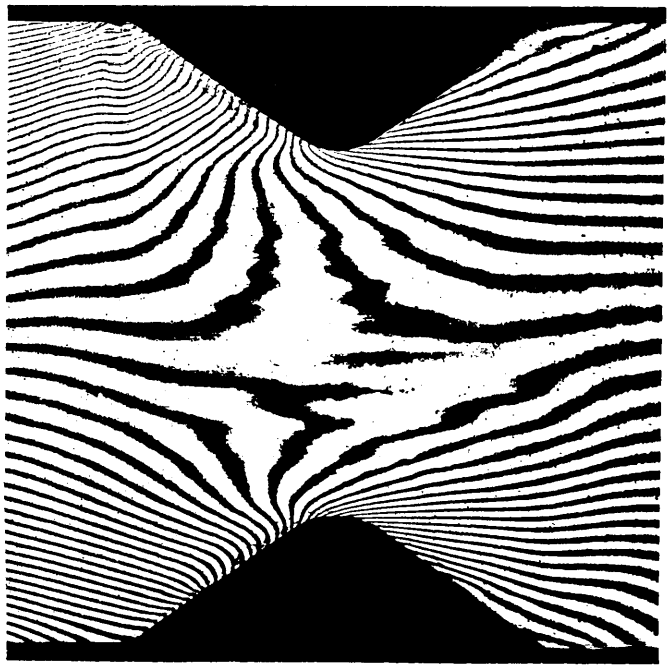

U Field

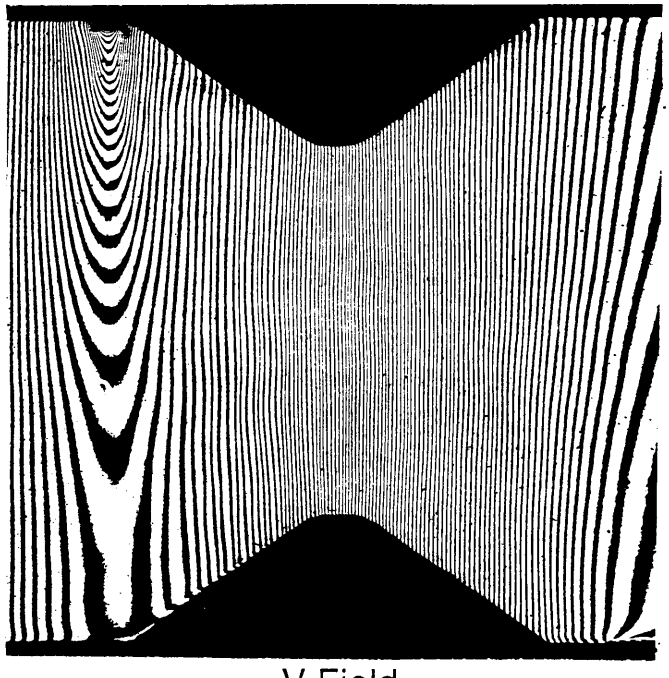

V Field

Fig. 18. The U and V displacement fields for the Iosipescu specimen at 12260 kPa (1778 psi.).

gradient in the V field indicates shear. The star shaped pattern in the U field resulted from bending with tension and compression on the top and bottom of the test section, respectively. As the loads were increased (Fig. 17 and 18), the V field showed that a state of shear existed (by virtue of vertical fringes) in the test section located between the notches. The shear strain had some nonuniformity as can be seen by the cyclic variations of fringe gradient. Just as in compact specimen I, it was not believed to be load induced but rather a material property inconsistency.

The normal strain ε_y was virtually zero. The normal strain ε_x though, indicates bending in the test section as evidenced by the gradient of the U fringes in the x direction near the notch tips. The bending was caused by the loading fixture producing tension and compression on the lower and upper ends of the test section respectively with the neutral axis near the center. A truly pure state of shear did not exist across the entire test section.

Quantitative Analysis

Shear Stiffness Measurements with the Compact Specimens

Fringe patterns of displacement were recorded for the load levels in Table 1. Shear strains along a line connecting the notch roots were extracted for each load level. The strains were extracted at 19 locations between the notch roots of the three specimens. These strains were plotted along a line connecting the notches and are illustrated in Figs 19 through 25. The scatter of data points near the notch tips in specimen I indicates nonuniform shear strains. This was caused by changing plies on the surface of the specimen resulting from the ply curvatures. The curves have been smoothed to reveal the load-induced response. As can be seen for the two compact specimens the shear strains rise abruptly from zero at the notch tips to form a fairly uniform distribution. The shape of the distributions do not change greatly with load level. The differences in the shapes of the

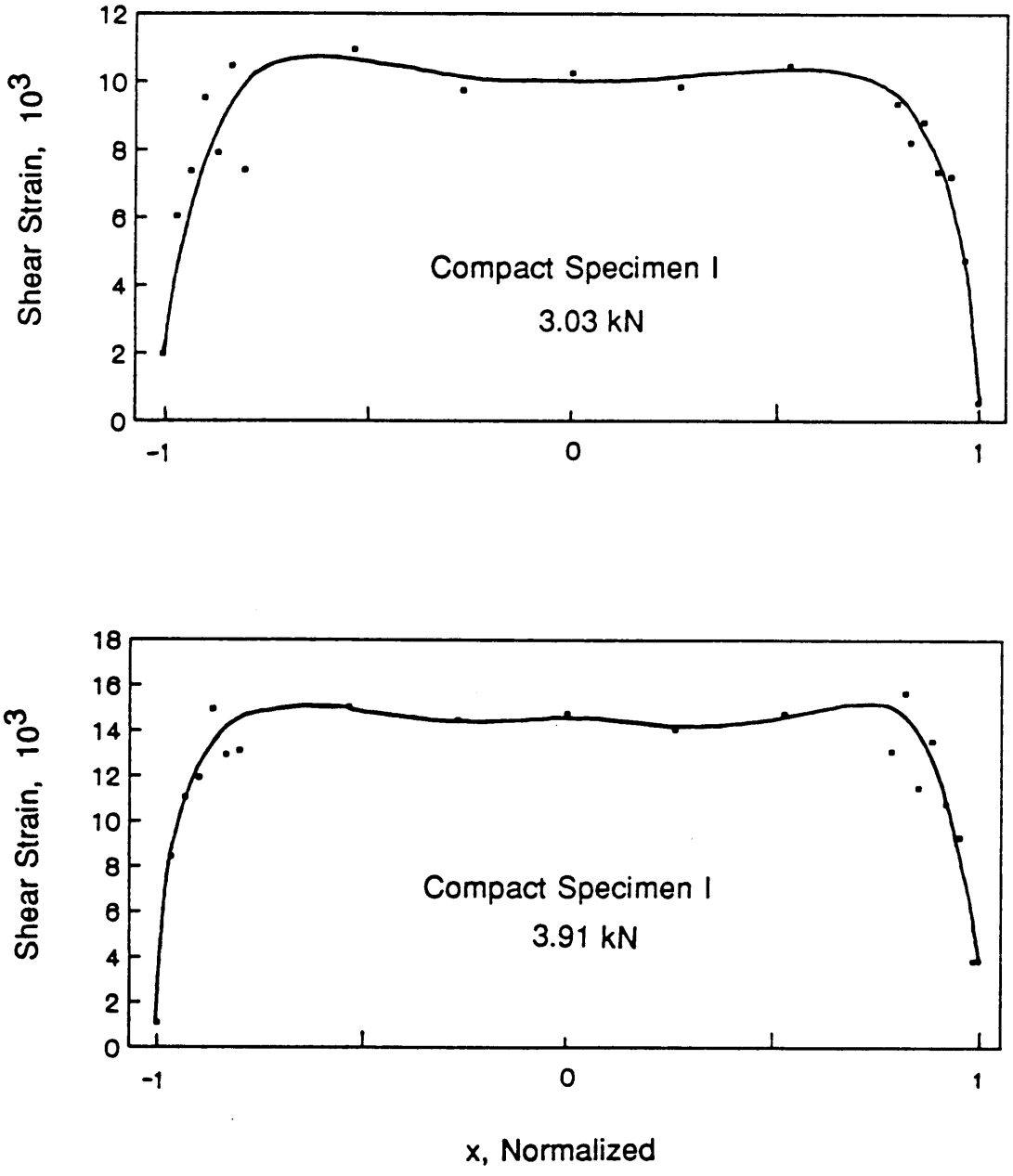

Fig. 20. Shear strain distributions along a line connecting the notch tips for compact specimen I at 3.03, 3.91 kN (680, and 880 lb.).

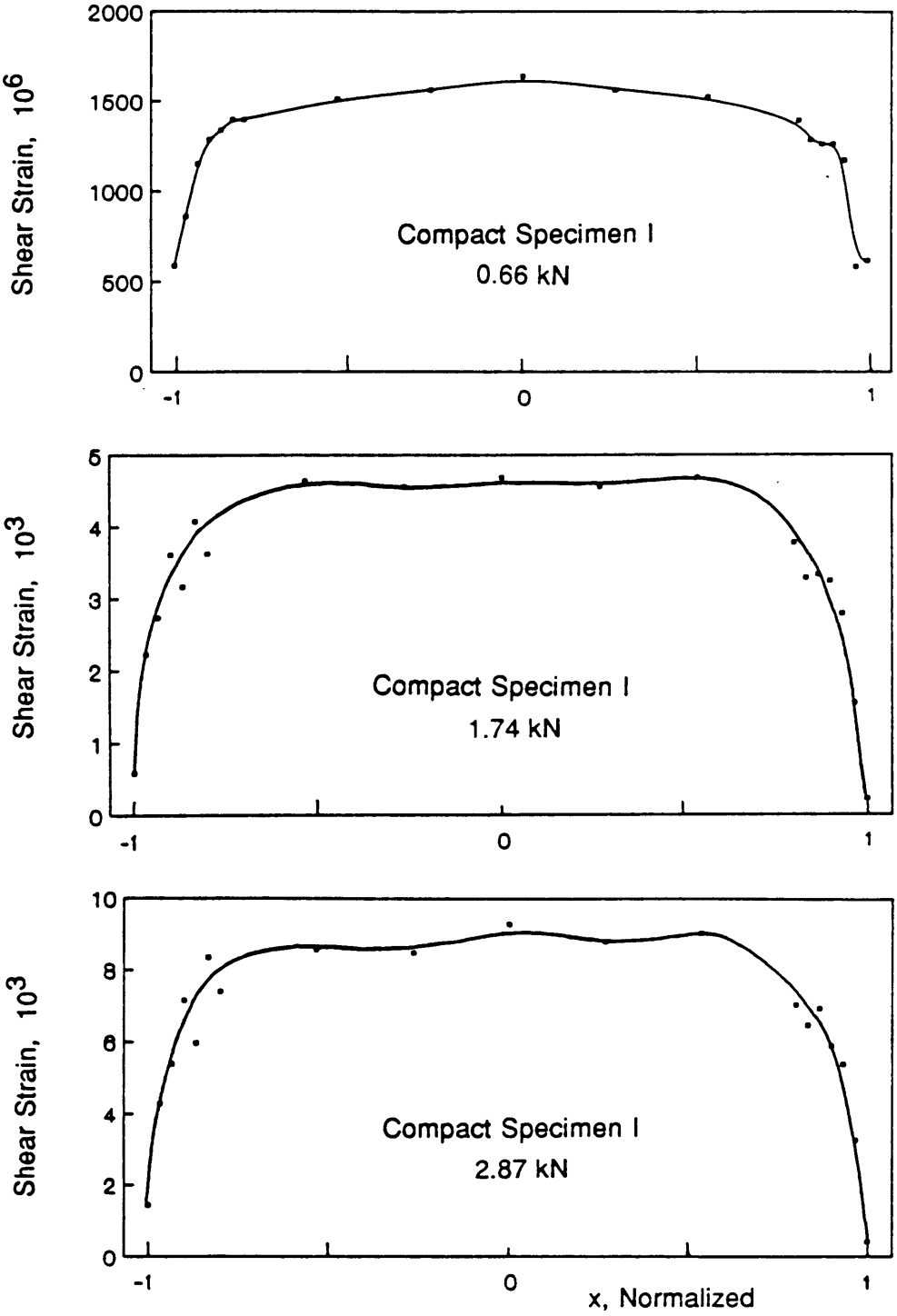

Fig. 19. Shear strain distributions along a line connecting the notch tips for compact specimen I at 0.66, 1.74, 2.87 kN (147, 390, and 645 lb.).

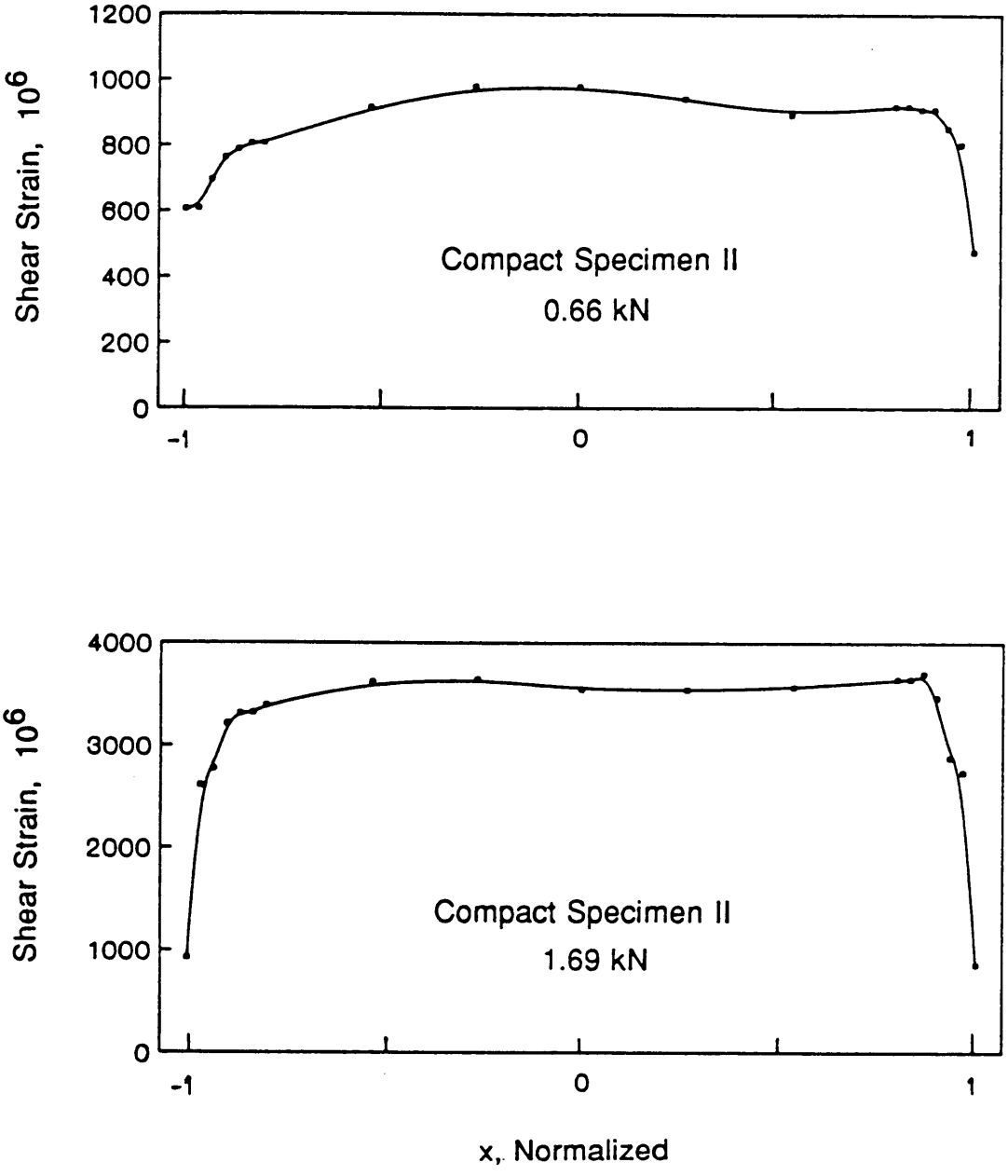

Fig. 21. Shear strain distributions along a line connecting the notch tips for compact specimen II at 0.66, 1.69 kN (147, and 380 lb.).

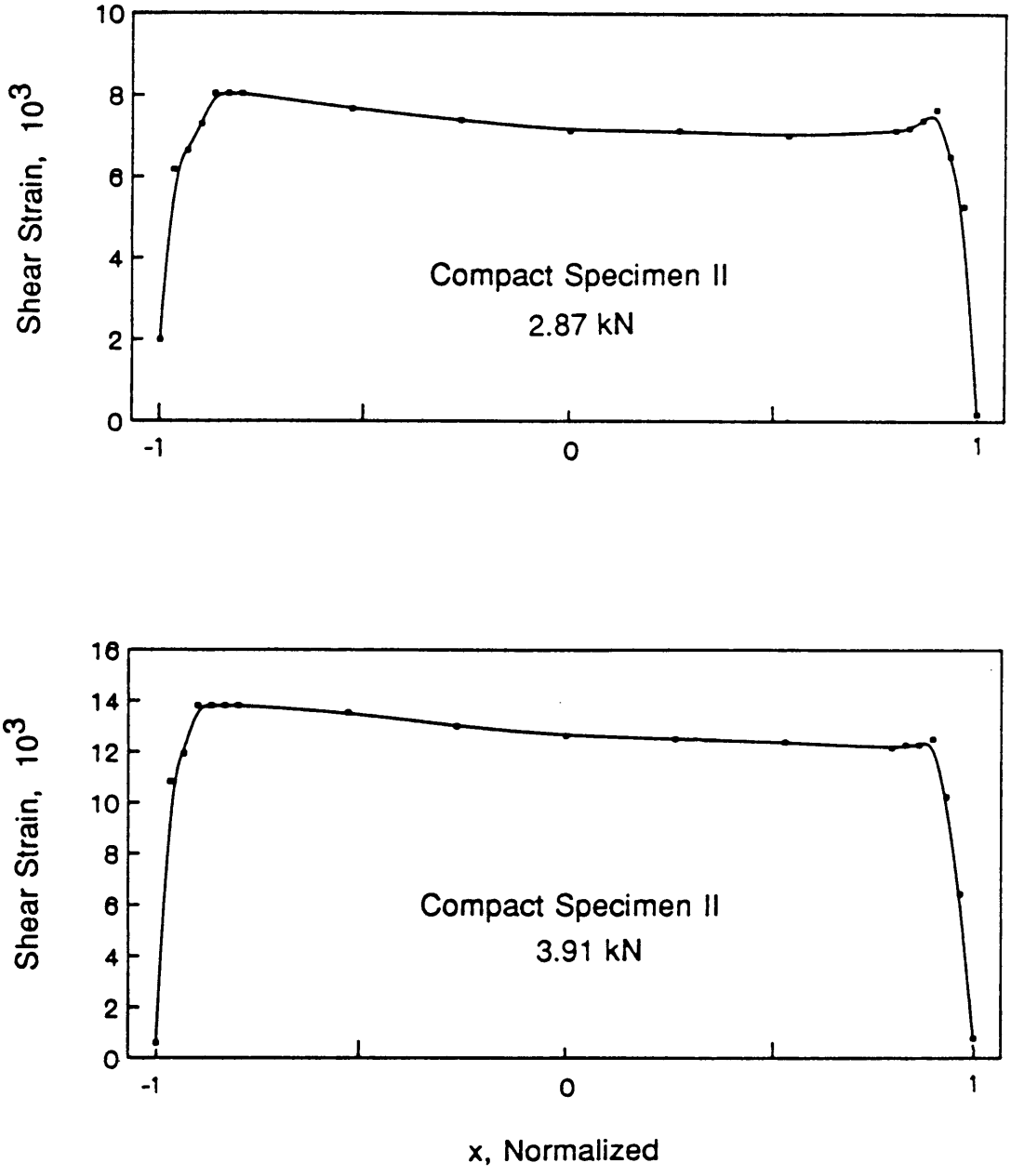

Fig. 22. Shear strain distributions along a line connecting the notch tips for compact specimen II at 2.87, 3.91 kN (645, and 880 lb.).

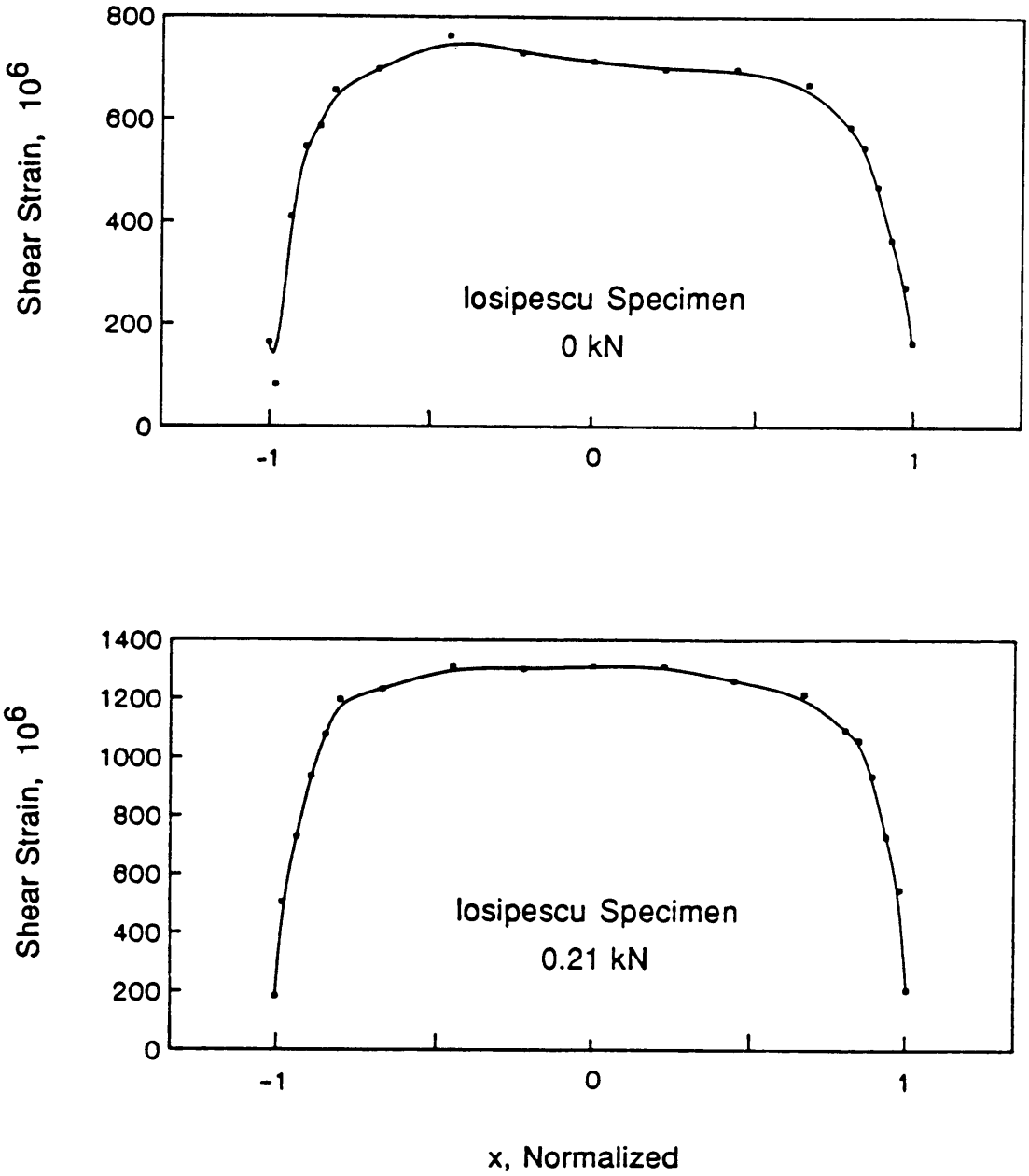

Fig. 23. Shear strain distributions along a line connecting the notch tips for the Iosipescu specimen at 0, 0.21 kN (0, and 48 lb.).

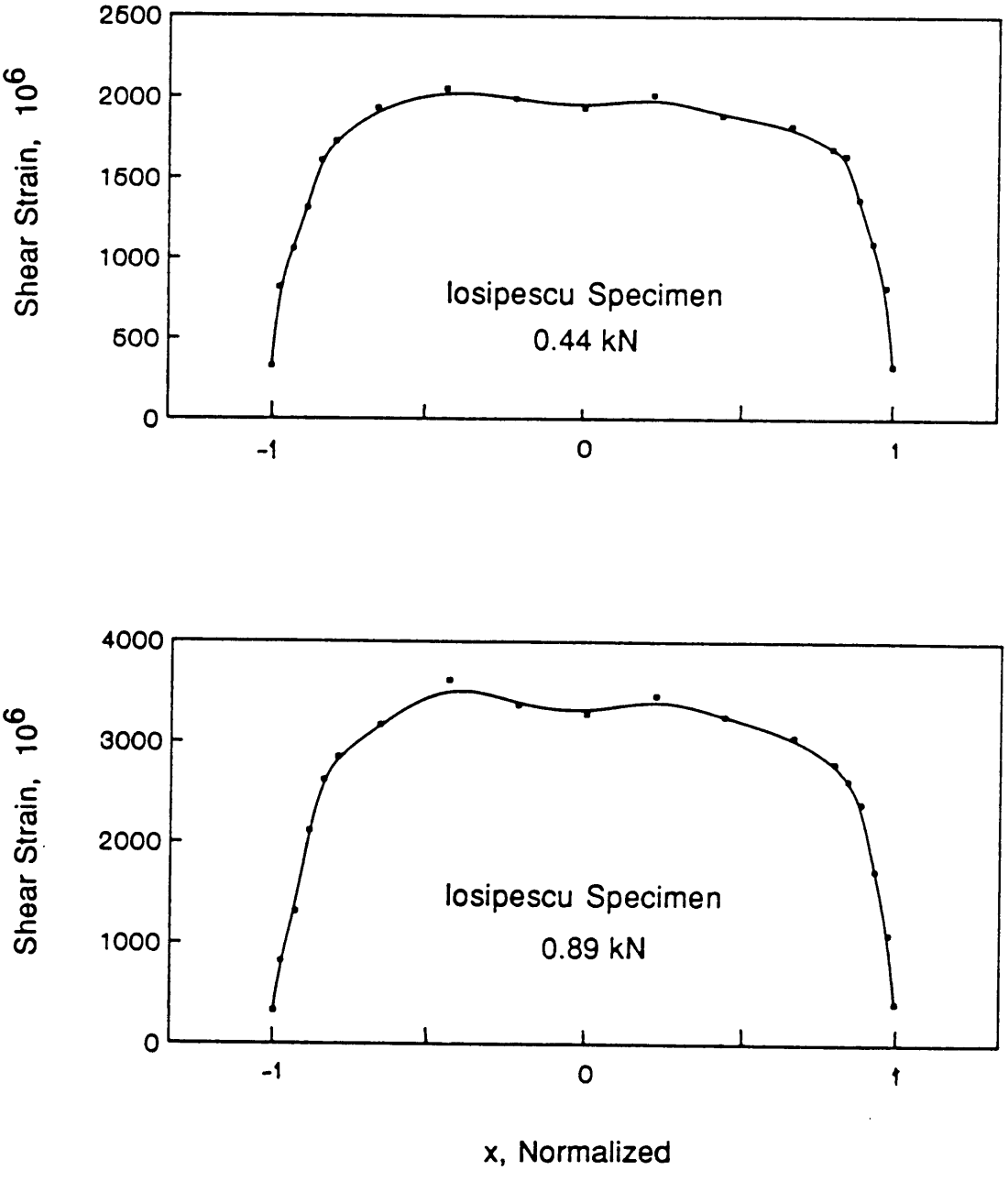

Fig. 24. Shear strain distributions along a line connecting the notch tips for the Iosipescu specimen at 0.44, 0.89 kN (98, and 200 lb.).

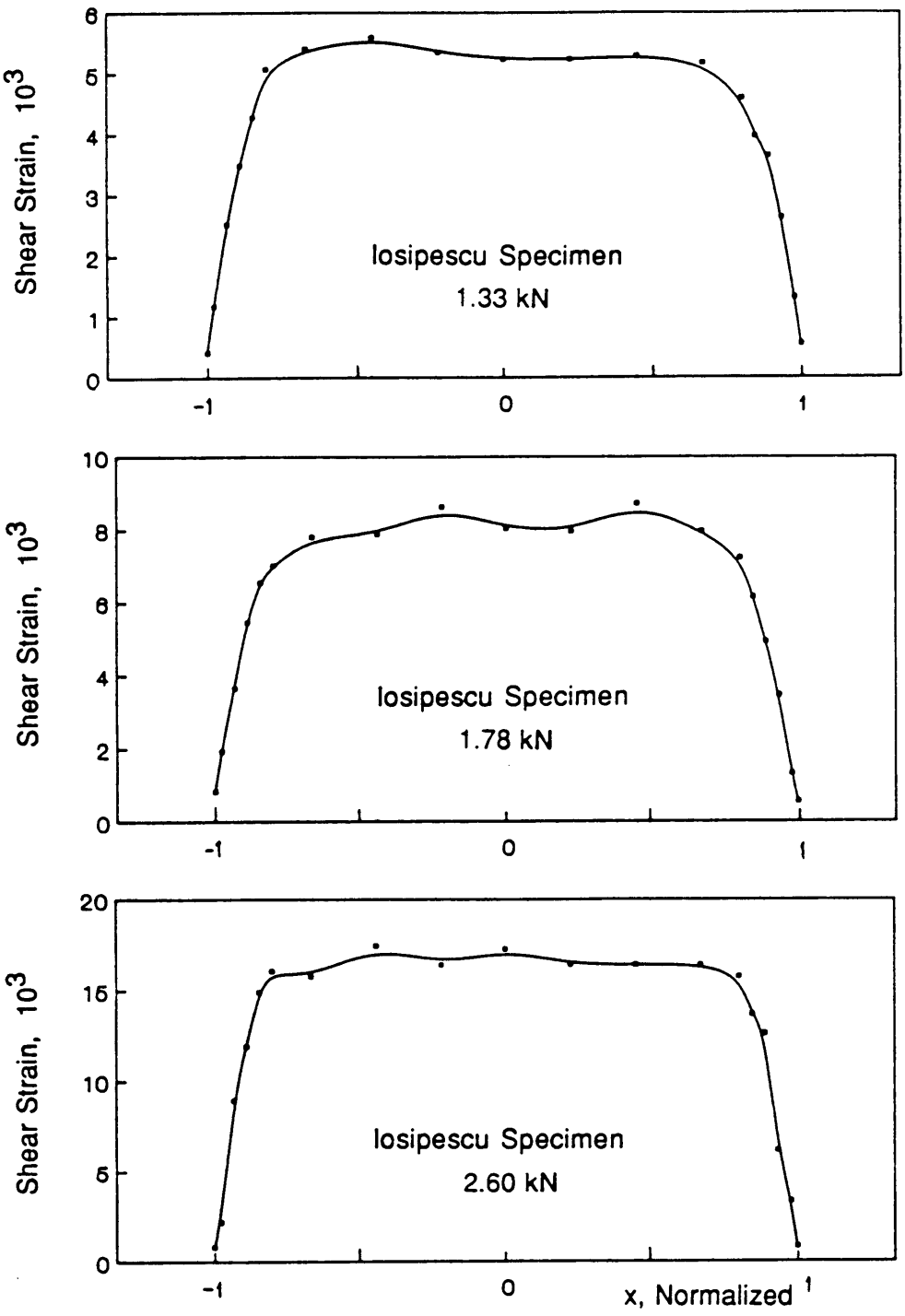

Fig. 25. Shear strain distributions along a line connecting the notch tips for the Iosipescu specimen at 1.33, 1.78, 2.60 kN (298, 400, and 585 lb.).

curves for the two specimens was a result of the ply orientations. Considering the distributions for the Iosipescu specimen, again, the shape is consistent throughout the load range. The shear strain distribution of the Iosipescu specimen, though, is noticeably different than those of the two compact specimens. Strains do not rise as quickly from the notch tips and the shape was less uniform. Figure 26 compares the shear distributions for the two compact specimens and the Iosipescu specimen at similar load levels. It can be seen clearly that the two compact specimens exhibit similar distributions while the Iosipescu distribution is different. The compact specimens provided a more uniform distribution than the Iosipescu specimen. Also the deviations from the average shear strain of the compact specimens were less than that for the Iosipescu specimen.

When using strain gages centered on the line connecting the notch tips, the shear strain values obtained for the Iosipescu specimen would be higher than those obtained for the compact specimens and higher than the average values. A correction factor should be used for the strain reading of the gages in order to obtain accurate stiffness measurements. Correction factors were used by Pindera et al [20] to account for the nonuniform shear stress. Similar correction factors for the compact specimens would be smaller than the Iosipescu specimen since the strains at the gage location were closer to the average strain. In fact a correction of less than 5% would be used for the compact specimens while about 20% would be used for the Iosipescu specimen.

Since moire interferometry was used in these experiments the average strains could be determined accurately from the shear strain distributions at every load level. Accurate shear stiffness measurements of a material could be obtained from the average shear strain and average shear stress (P/A) where P is the load level and A is the cross-sectional area between the notches. A plot of the average shear stress and the average shear strain for the three specimens is illustrated in Fig. 27. The initial state of shear at the zero load level for

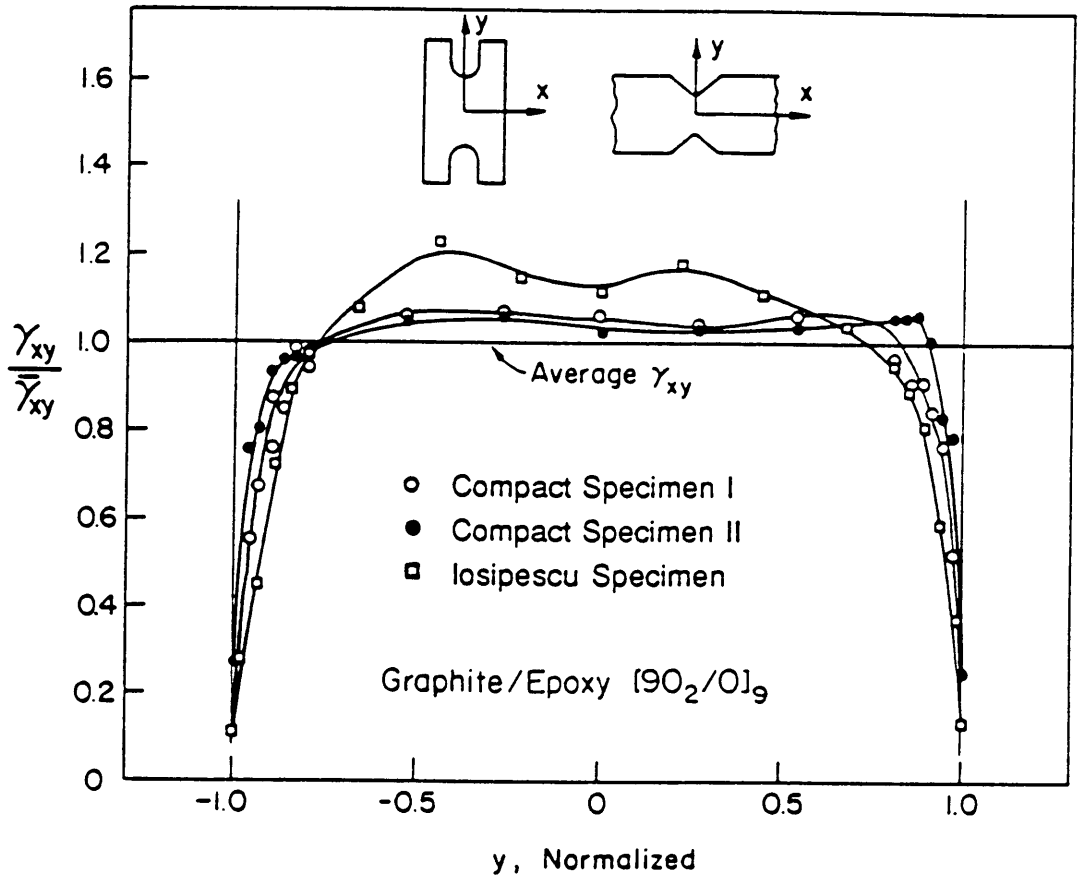

Fig. 26. The shear strain distributions along a line connecting the notch tips for the three specimens. The shear stress levels for compact specimens I, II, and the Iosipescu specimen were 14630, 14310, 12260 kPa (2122, 2076, and 1778 psi) respectively

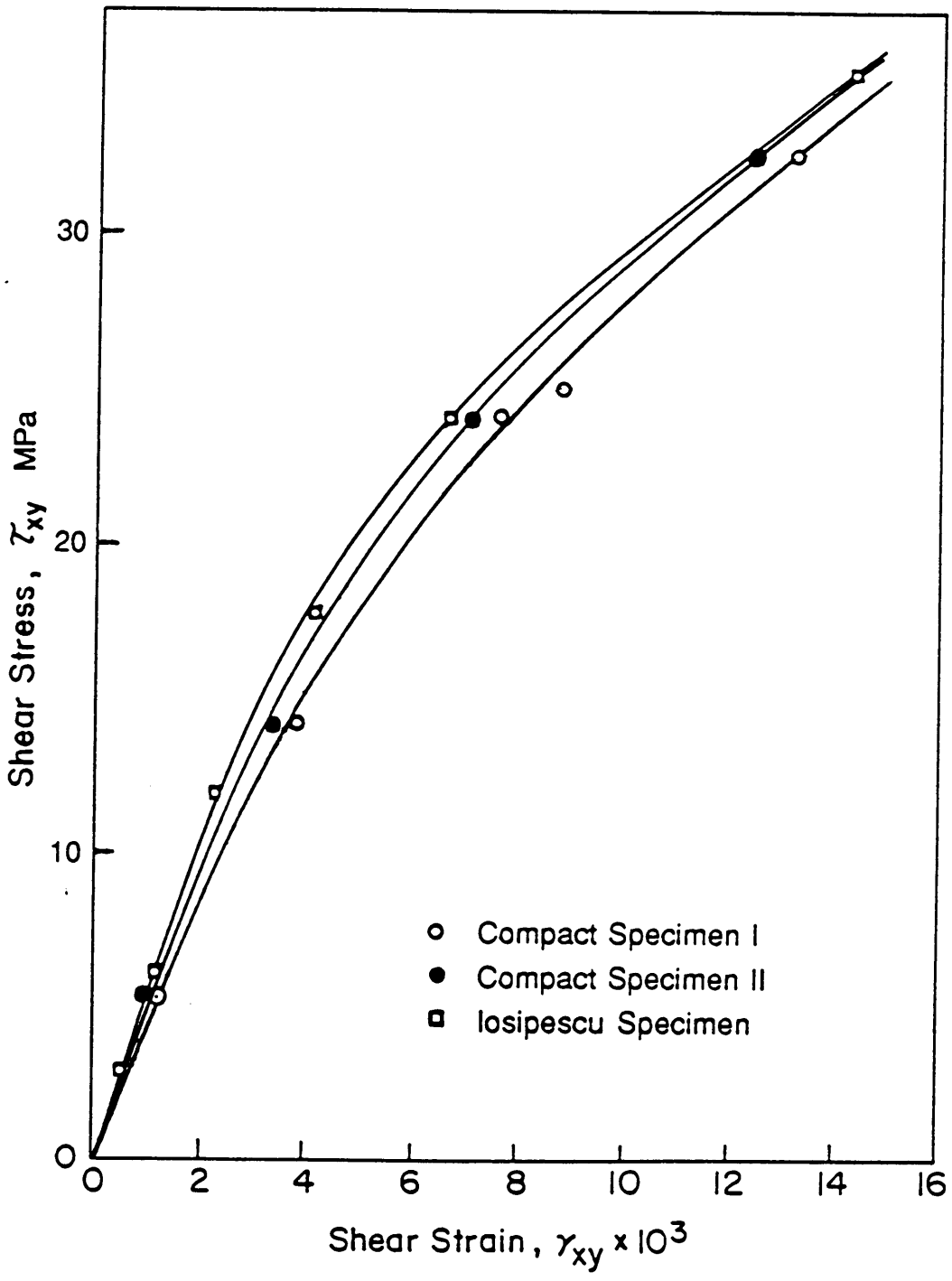

Fig. 27. The shear stress, shear strain curves for the three specimens tested.

the Iosipescu specimen was subtracted from subsequent load levels, while this was not required for the compact specimens. Differences in the curves could be a result of varying material properties from region to region of the composite cylinder. Also a state of plane stress may not have been present in each of these tests as a result of nonuniform bearing forces on the specimens. The specimen thickness may have influenced this. Finally the ply curvature in the test section may have influenced the shear stiffness.

Normal Strains in the Test Section

The normal strains in the test sections of the three specimens were determined. The normal strain ε_y was found to be small and negligible. This will be discussed in a following section entitled normal strain ε_y. The normal strain ε_x however was not considered negligible and could enter into strength results by causing a complex stress state. A plot of ε_x is shown in Fig. 28 for the Iosipescu specimen and for the two compact specimens at similar stress levels. Compact specimen I exhibits virtually no normal strains while specimen II has ε_x only in the region near the notch tips. For specimen II the maximum ε_x was 16% of the average shear strain in the test section. This value is considered small and would not effect the shear strength significantly. Since the magnitude of the normal strain was small compared to the shear strain, and since it is localized only at the notch tips, ε_x was considered negligible for the compact specimen.

Normal strain ε_x was present in the test section of the Iosipescu specimen in the form of bending. Figure 28 shows the distribution of these strains compared to the compact specimen. The top half of the test section was in tension while the bottom half was in compression. The magnitude of the maximum strain was more than twice that of the compact specimen. Normal strain ε_x was 52% of the average shear strain in the test section. This may lead to premature failure of the specimen resulting from a complex stress

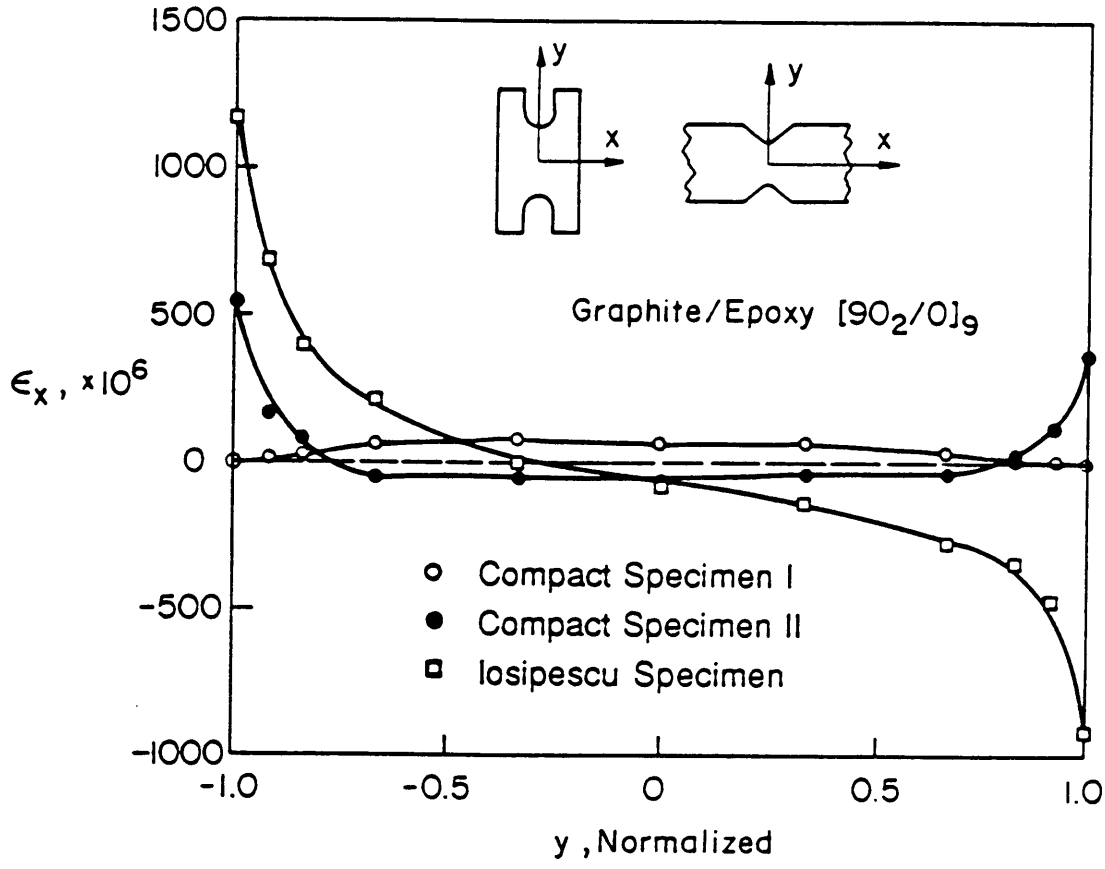

Fig. 28. The Normal strain ε_x distridutions along the line connecting the notch tips for the three specimens. The shear stress levels for compact specimens I, II, and the Iosipescu specimen were 14630, 14310, 12260 kPa (2122, 2076, and 1778 psi) respectively

state. The normal strain was observed at the zero load level and it increased with load. It was believed to have resulted from the loading fixture, wherein the right side of the fixture could have rotated as a result of clearance or deformation of the linear bearing system that supports the fixture.

From the plot in Fig. 28 it was apparent that the compact specimen produced a more nearly pure state of shear in the specimen. It is likely therefore to provide excellent shear strength measurements, as will be discussed in the section entitled shear strength measurements using the compact double-notched specimen.

DETAILED ANALYSIS OF DEFORMATION

Although these experiments are considered preliminary, a detailed analysis of the results can help to refine the specimen and test method. This section contains a number of topics which were observed during the analysis of the shear test.

Transverse Shear Strain

The shear strain distribution across the specimen at the proposed location of the strain gage was investigated for the two compact specimens and the Iosipescu specimen. Figure 29 shows this distribution over a 0.25 in. length for all three specimens at comparable stress levels. The plots have been smoothed slightly to eliminate the nonuniform shear strains in order to reveal the load-induced trend. From the plot it is apparent that all three specimens exhibit distributions of similar shape. The shear strain distributions from the two compact specimens are well aligned with the center of the specimen. The maximum shear strain coincided with the line connecting the notch tips. This result was not surprising since the loading conditions on the specimen were

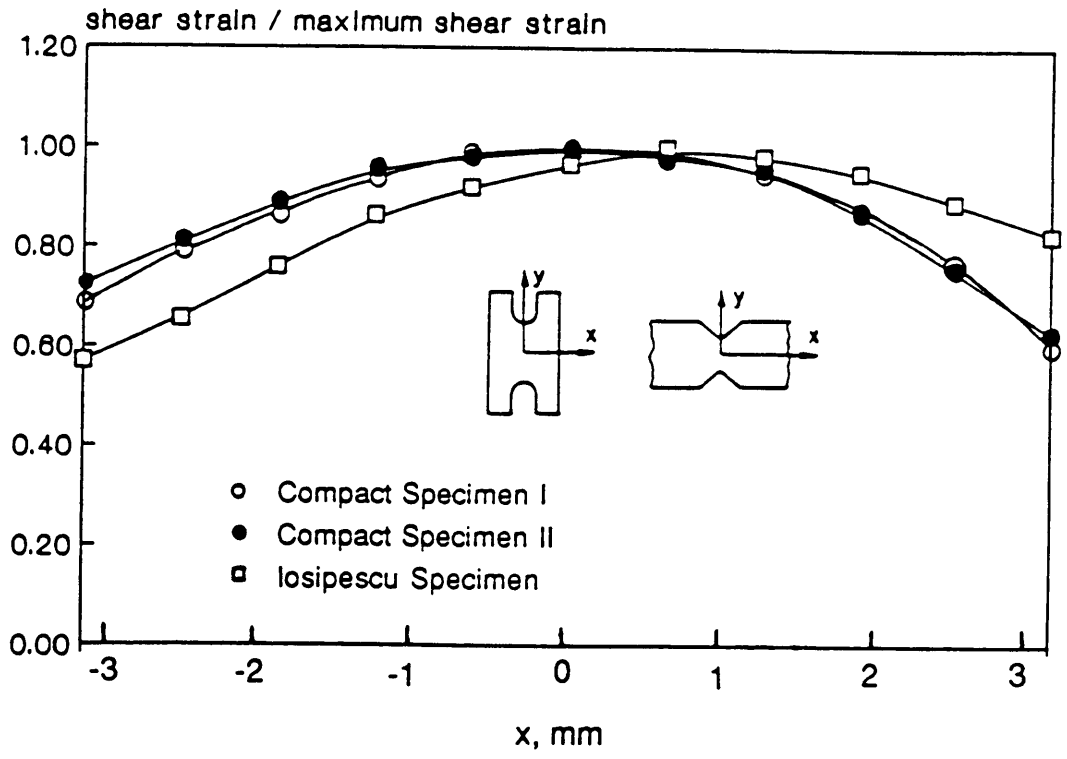

Fig. 29. Normalized shear strain distibutions along the x axis for the three specimens. The shear stress levels for compact specimens I, II, and the Iosipescu specimen were 14630, 14310, 12260 kPa (2122, 2076, and 1778 psi) respectively

symmetric. The distribution for the Iosipescu specimen was slightly shifted so that the maximum shear strain was not centered between the notch tips. This indicates that specimen alignment in the Wyoming test fixture may be important, or that the fixture could not produce symmetric shear. The non-symmetric shear strain distribution introduces some error into the shear stress-strain calculations for the material investigated, since the shear strains between the notch tips were extracted along the center of the specimen and not the location of the maximum shear strain. If the shear strains were extracted slightly to the right the average shear strains would have been higher at each load level. This change would act to bring the results for the Iosipescu test closer to those for the compact tests. The offset transverse strain distribution of the Iosipescu test may introduce serious error when measuring the strain with gages.

When using strain gages for these three specimens a correction factor may be needed to account for the finite size of the gage, since the gage would read a strain value averaged across a finite area. This correction factor would depend on the size of the strain gage used. From the plot in Fig. 29 a correction factor of 3% to 6% for the compact specimens would be needed to improve the accuracy of strain readings for a well placed eighth inch (3 mm) gage. The correction for the Iosipescu specimen would depend on the placement of the strain gage. If the gage was aligned directly between the notches the correction would be about 10%.

For this initial experiment on the cross-ply material a decreased strain reading resulting from the transverse strain distribution would tend to compensate for the shear strain distribution along a line connecting the notch tips. For this material, strain gage results would average the shear strains over a finite area, thus the nonuniform shear strain distribution effect in the two directions would self compensate to some degree. This assumes that both of the shear distributions are convex in shape. It should be noted that

care must be taken to know the shear distributions in both directions for the material under investigation. On a 0 deg unidirectional laminate, for instance, the two distributions may not be self compensating as they are for this specimen [22].

Shear strain Nonuniformities

Shear strain nonuniformities could be seen in the V field of compact specimen I (Fig. 12) and the Iosipescu specimen (Fig. 18) but curiously not in compact specimen II. These nonuniformities appear as varying fringe densities across the specimens in the test sections. The two specimens which showed shear variability were cut from the cylinder with the same orientation. Also the surface for all three specimens consisted of plies that were aligned with the hoop direction of the composite cylinder. It is believed that the plies have more shear variability in their transverse fiber directions than their longitudinal fiber directions. This effect may be attributed to the manufacturing process. Shear strain nonuniformities were believed to be caused by varying fiber volume content in the composite cylinder. For example Fig. 30 shows a section of the cylinder where noticeable resin-rich regions appear. In these localized areas of high resin content the shear stiffness was believed to be low. These variations of the stiffness in the outer plies of the specimen appear in the displacement patterns as nonuniform fringe gradients.

The magnitude of the variations was not large except for some highly localized zones. From the fringe patterns the ratio of the highest recorded strain to the lowest was 1.5. While this exhibits the extreme case, it is probable that initiation of failure would occur in one such localized zone of low stiffness.

Shear strain distributions were extracted from the fringe patterns smoothing through the nonuniform effects. The distributions represent the average properties of the material in order to evaluate the test fixtures. It was found that the positioning of the vertical line

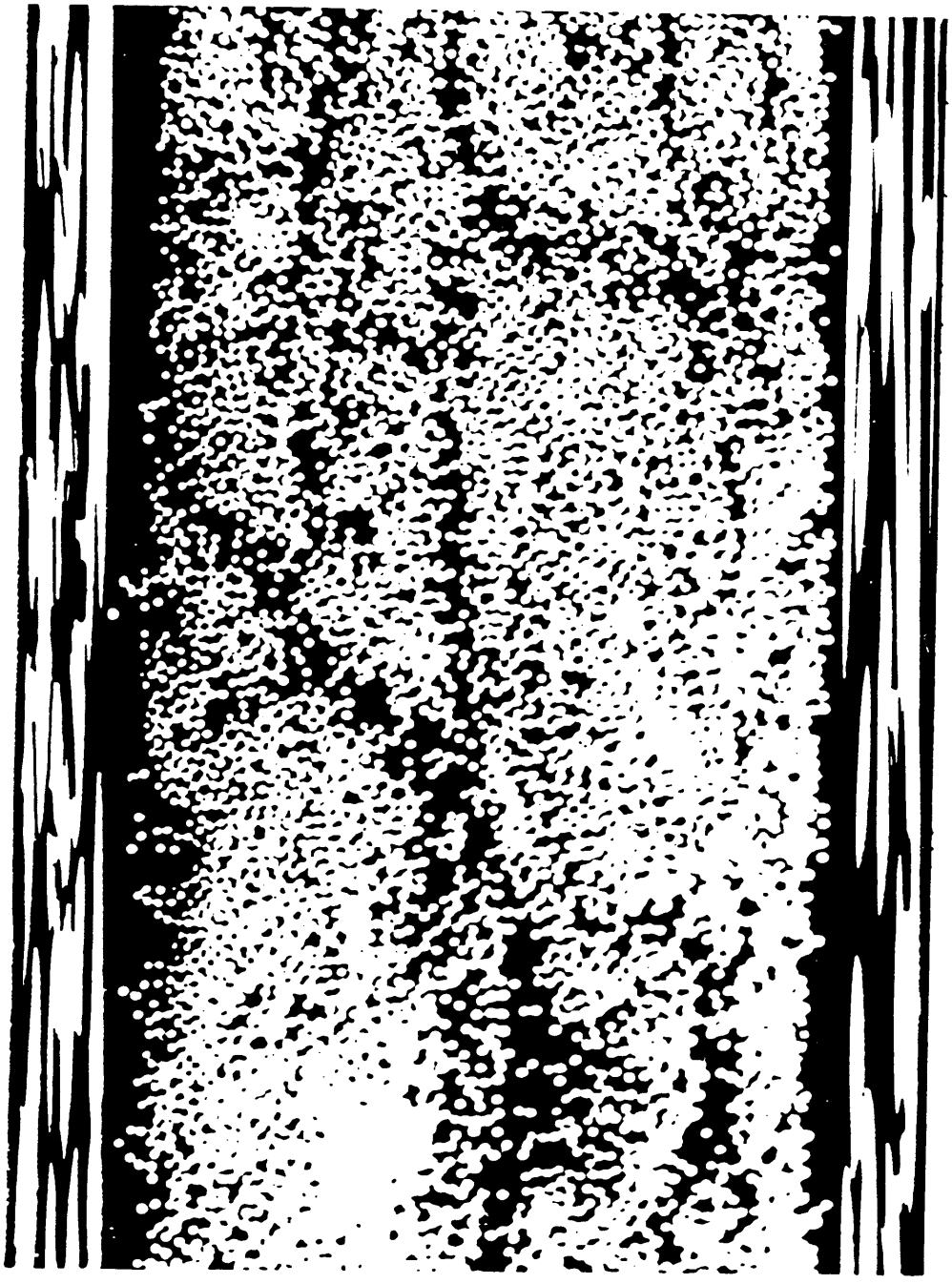

Fig. 30. A magnified view of the cross section of the composite cylinder. The photograph reveals areas of high resin content.

where the shear strains were extracted had an effect on the distribution. Therefore, in order to extract the average shear strains, carrier patterns were used. Carrier patterns are discussed in detail in the appendix section. It was found that in compact specimen I and the Iosipescu specimen the V field showed the nonuniform shear in the test section as varying fringe density. A carrier of rotation was used to subtract the uniform part of the shear strain from the V field. As a result an equal carrier of rotation was imposed on the U field. These carrier patterns don't effect the shear strain information [25]. Then the U field fringe pattern changed so that in the test section there was a series of well spaced horizontal fringes. In fact the U field showed little nonuniform shear except for the region near the notches of compact specimen I. This variation though was associated with changing plies on the surface of the specimen resulting from the ply curvatures. The V field then contained the nonuniform part of the shear strain while the U field contained the uniform part. This can be seen in Figs 31 and 32 which are fringe patterns for compact specimen I and the Iosipescu specimen. The shear strains for compact specimen I and the Iosipescu specimen were taken primarily from the U field in order to gain representative shear strain distributions.

For compact specimen II the nonuniform shear strain information was contained in the U field and the uniform shear strains were contained in the V field. Therefore the shear strains were predominantly taken from the V field.

Shear Strength Measurements using the Compact Specimen

For accurate shear strength measurements, a state of pure and uniform shear stress should exist in the test section. From the plots of shear and normal strain distributions in the test section it was apparent that if the specimen failure occurred in the test section that the strength measurements would be reliable. Since the normal strains in the test section

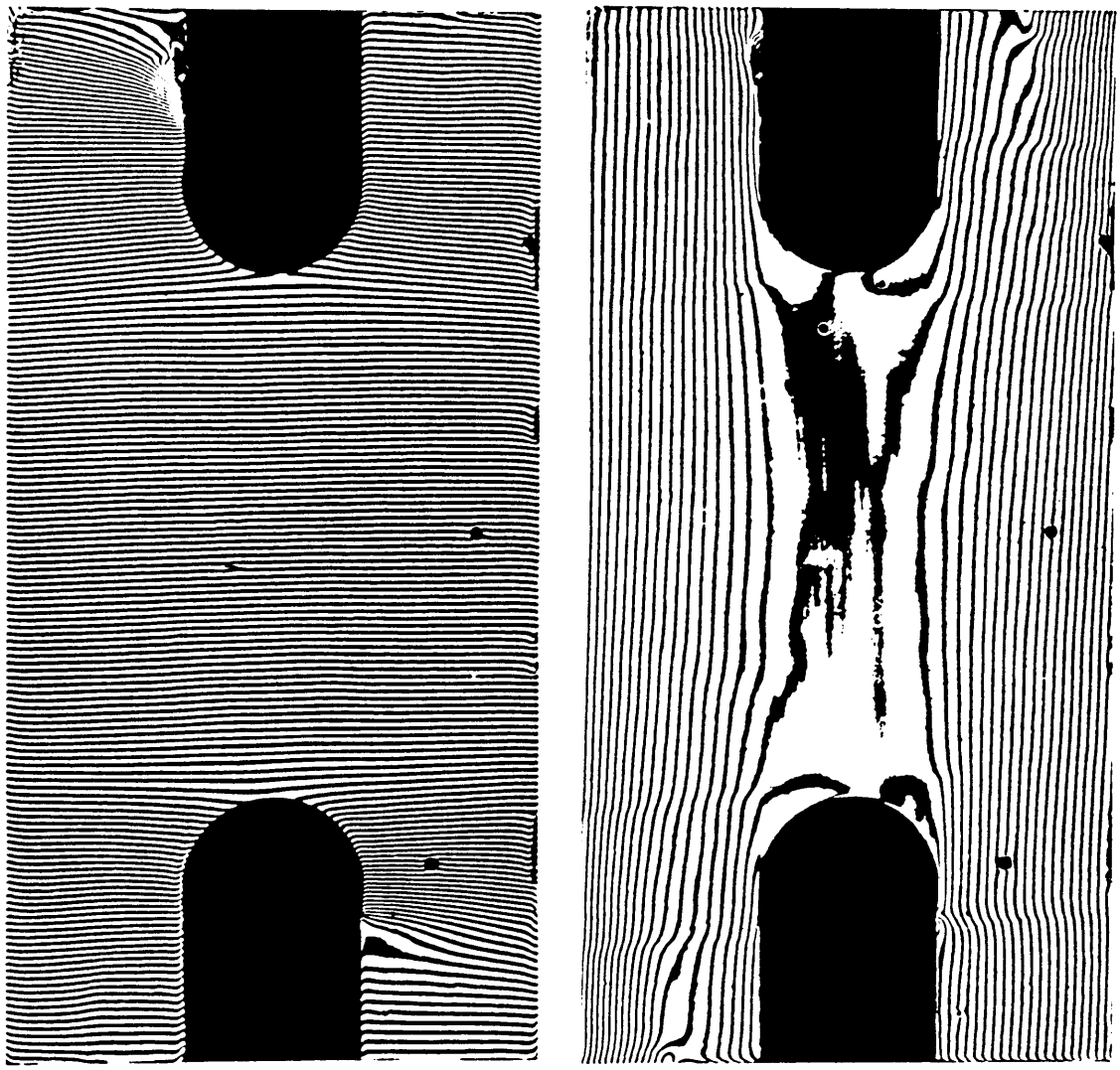

Fig. 31. The U and V Displacement fields for compact specimen I at 14630 kPa (2120 psi.) with a carrier pattern of rotation added.

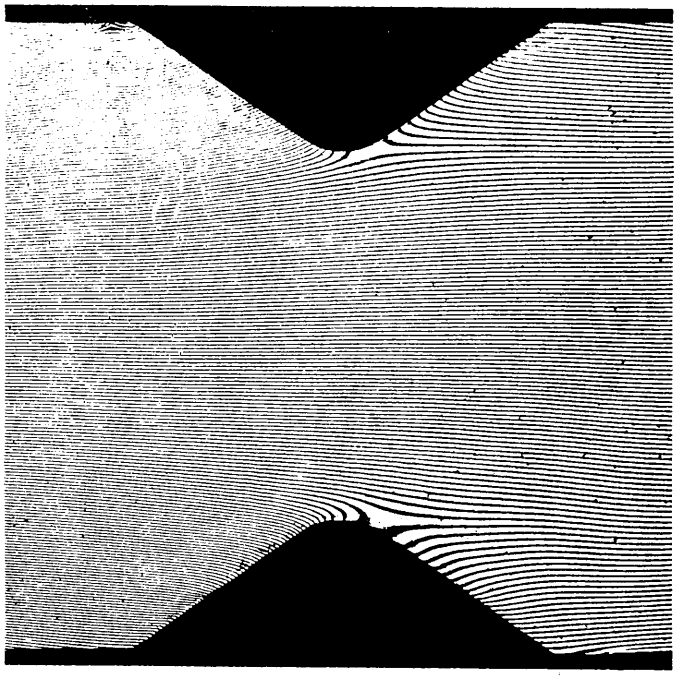

U Field

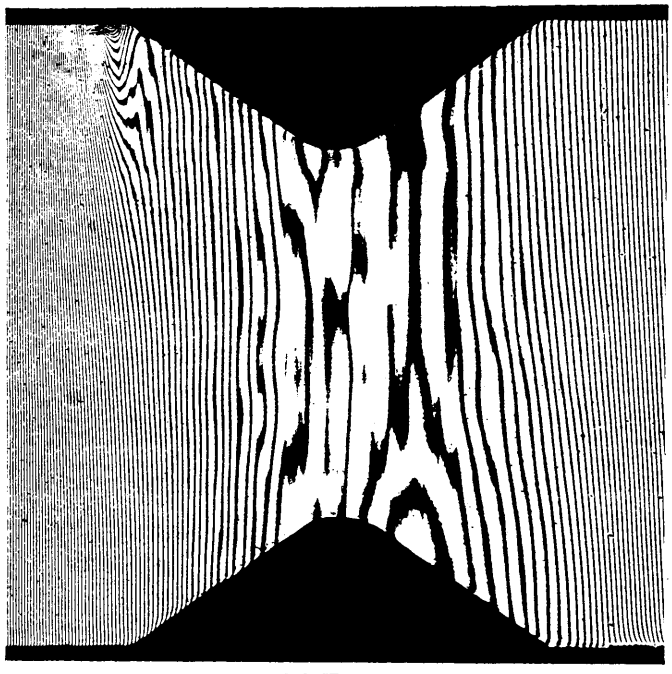

V Field

Fig. 32. The U and V displacement fields for the Iosipescu specimen at 12260 kPa (1778 psi.) with a carrier pattern of rotation added.

were small compared to the shear strains a relatively pure state of shear existed. Therefore the state of stress was not complex and normal stresses would not contribute to failure.

In addition, a perfectly uniform shear stress distribution across the test section would yield the most reliable shear strength values. A uniform distribution would insure that failure or yielding would occur in the test section at the average shear stress. If the distribution were not uniform, the failure would initiate at the location where the stress was maximum and not the average stress. The measured average shear stress then would not represent the actual shear strength of the material. The compact specimen produced a fairly uniform shear strain distribution in the test section and therefore the values obtained for shear strength would be quite accurate.

Comparing the results of the Iosipescu test with that of the compact specimens shows that for this laminate the compact specimens produced a more pure and uniform shear stress in the test section. Because of this it is believed that the compact specimen would produce more accurate shear strength measurements. Since the Iosipescu specimen is considered one of the most reliable shear strength measuring methods, the compact specimen merits serious attention for measuring shear strength.

High Strains Remote from the Test Section

For the measurement of shear stiffness the deformation of portions of the specimen outside the test section are not important unless they alter the loading in the test section. Deformation of remote areas however can strongly influence the accuracy or even the applicability of strength measurements with the compact specimen. The location of failure must occur as shear in the test section for strength measurements to be effective. Returning to the fringe patterns of Figs. 14 and 15, it can be seen that in specimen II the lower right and upper left arms of the specimen suffer from high shear strains as evidenced by the

strong fringe gradients in the U field in these areas. This strain resulted from the forces on these sections caused by the clamping devices. This phenomena was not evidenced in specimen I since the specimen was cemented to the load transfer fixture, reducing the shearing action of the clamping devices. At a higher load level though, the cement failed and this effect was observed. The shear stress in the arms were calculated to be 33% less than the shear stress in the test section. This value could be made smaller if the specimen was made wider or if the length of the test section were smaller. Reinforcing the vulnerable areas with tabs would strengthen then. The use of tabs will be discussed in more detail in the next section.

Other areas which suffered strong shear strains are the bottom left and top right arms of both specimens. These shear strains resulted from the transfer of the direct compressive load to shear. They are localized but quite high. A way to decrease these strains would be to widen the specimen in order to increase the area which is under direct compression. Another solution to lessen the effect of this shear would be to expand the region of direct compression all the way to the notch. End tabs could also improve the transfer of the compressive stress to shear stress in the test section.

Finally there were two areas which suffered from strong compressive strain. These regions are located directly under the area where the compressive load was applied to the specimen. Increasing the bearing area would reduce the compressive stress. Also tabbing these areas would increase the bearing area.

Specimen II was loaded to failure. Unfortunately the failure was not in the form of shear in the test section. The failure was located at one of the direct compression areas. It may have occurred as a result of a combined compressive and shear stress. It would seem that this failure may have been avoided by altering the geometry slight or reinforcing these

vulnerable areas. Future work will determine the appropriate corrective measures, suggestions will be given in this text in the recommendation section.

Incorporating Tabs for the Measurement of Shear Strength.

Tabs are often used in the materials testing community to reinforce certain areas of specimens to ensure that failure occurs in the prescribed test section. Tabs are recommended for the Iosipescu test for certain laminates by the ASTM proposal for the standardization of the Iosipescu test [2]. This scheme is easy to incorporate and for certain laminates essential for accurate shear strength measurements.

After closely analyzing the deformation of the compact specimen it was apparent that some areas remote from the test section showed excessive strain. In fact the failure of specimen II occurred in one of these areas. Reinforcing the specimen outside the test section could have prevented this form of failure. End tabs could be used to do this. Figure 33 shows a scheme that incorporates stiff, strong material (tabs) cemented to the compact specimen. Preparation of the specimen would still be simple and straight forward.

Tabs would serve a number of purposes. They would add material along the sides to decrease the shear stress on the arms of the specimen caused by the force from the clamping devices. The tabs would act to increase the bearing area at the sites of direct compression. Tabs would also act to distribute the shear forces along the length of the specimen so that areas under the direct compression would not have to do this alone. End tabs would also increase the thickness of the specimen in areas and prevent buckling of thin specimens.

Although incorporating tabs is relatively simple it is suggested that they only be used when the need arises. There are laminates which are inherently weak in shear and compression along certain directions. One such case would be a 0 deg unidirectional

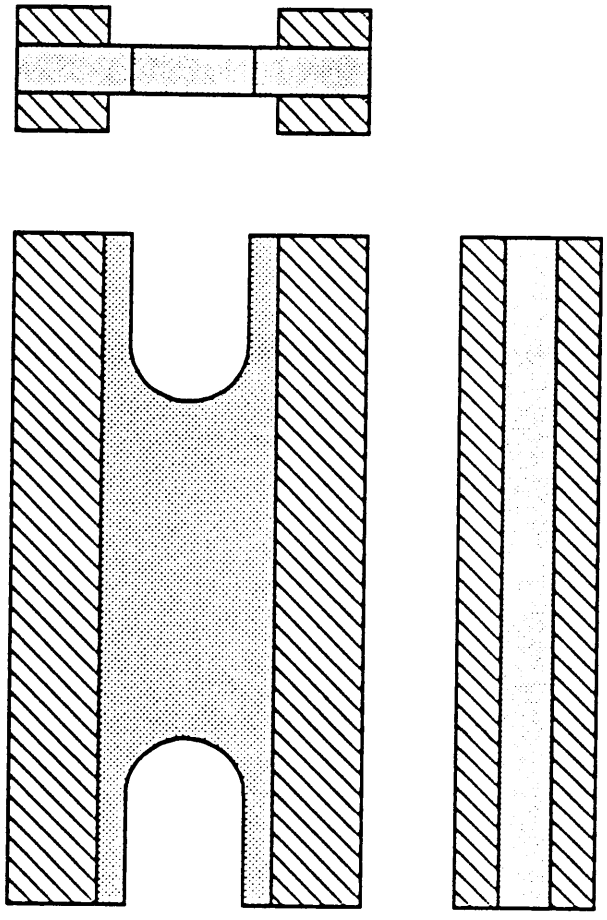

Fig. 33. A scheme that may be used to tab the specimen. This reinforces the weak areas of the specimen and could improve shear strength measurements.

laminate which would be strong in shear in the test section and weak at the direct bearing areas in compression and shear. In this case tabs may be essential for strength measurements.

Analysis of Specimen using Statics

Insight into the types and magnitudes of forces in the specimen and loading fixtures was obtained using a simple statics approach. Two assumptions were made in order to simplify the calculations. First, the force in the clamping device was assumed to be just enough to keep the specimen against the load transfer fixture. Second, there are no shear forces between the specimen and rail. This assumption gains validity when observing the specimen at high load levels as the specimen tries to separate from the load transfer fixture and a gap forms.

Starting with one on the load transfer fixtures, the load is applied as P in the top of Fig 34. To balance the moments on the fixture, C (clamping force) acts in the horizontal direction. Summing the forces in the vertical direction F (the bearing force on the specimen) must equal P. Then summing forces in the horizontal direction and moments, a force B occurs at the top corner of the specimen and is equal and opposite C. This compressive force on the rail can be observed at high load levels as the specimen bears only on a small area at these locations. Calculations in Fig. 34 show that forces B and C equal 1/4 P.

By transferring these forces to the specimen, as show in the figure, a pure shear state along a line connecting the notches is seen to balance all the external forces on the specimen. Then the average shear stress τ_{xy} times A (where A is the cross section area of shear) would be equal to the applied force P.

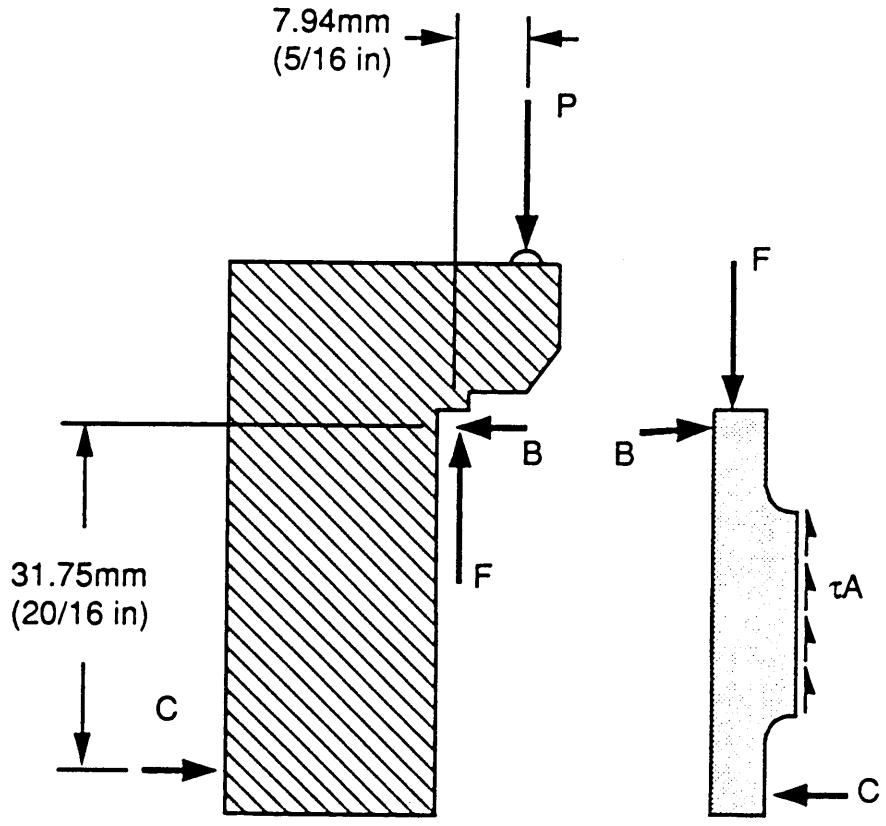

$$\Sigma F_x : B = C$$

$$\Sigma F_y : F = P$$

$$\Sigma M : 7.94\,P = 31.75\,C$$

$$: (5/16\,P = 20/16\,C)$$

$$C = 1/4\,P$$

Fig. 34. A simple static analysis of the load transfer fixture and compact specimen.

Effects of Ply Curvature

Since the three specimens, the two compact and the Iosipescu specimens, were cut from a cylinder there was some ply curvature in the test sections. Compact specimen I and the Iosipescu specimen were removed from the cylinder such that the plane of loading was not parallel to the plies along the entire test section. Because of this there is some coupling of the desired in-plane shear with undesirable interlaminar shear and normal stresses. The extent of this coupling is dependent on the angle between the ply and the plane of loading. The larger the angle the more interlaminar shear and compression results. Compact specimen I had larger curvature effects than the Iosipescu specimen because it had a longer test section. Compact specimen II was cut from the cylinder so that the plies along the test section were parallel to the plane of loading. This orientation is more desirable since a state of pure shear could exist in the test section without the coupling of other stresses.

Figure 35 shows the fringe patterns of the V displacements for the three specimens with a carrier of rotation added to isolated the normal strain ε_y. It was apparent that there is more normal strain in the test section for compact specimen I and the Iosipescu specimen than in compact specimen II. In addition, compact specimen I had the most serious curvature in the test section and also the largest normal strain ε_y. Specimen II showed virtually no normal strain. It is believed that the normal strains resulted form the curvature in the test section. This normal strain was very small however and its effect on shear stiffness and strength measurements is believed to be negligible.

Measurements on the Front and Back of the Compact Specimen

It is possible that a state of plane stress did not exist in the compact specimen. There could have been some difference in the deformation on the front and back sides of the specimens. The curves of stiffness in Fig. 27 show differences in stiffness values

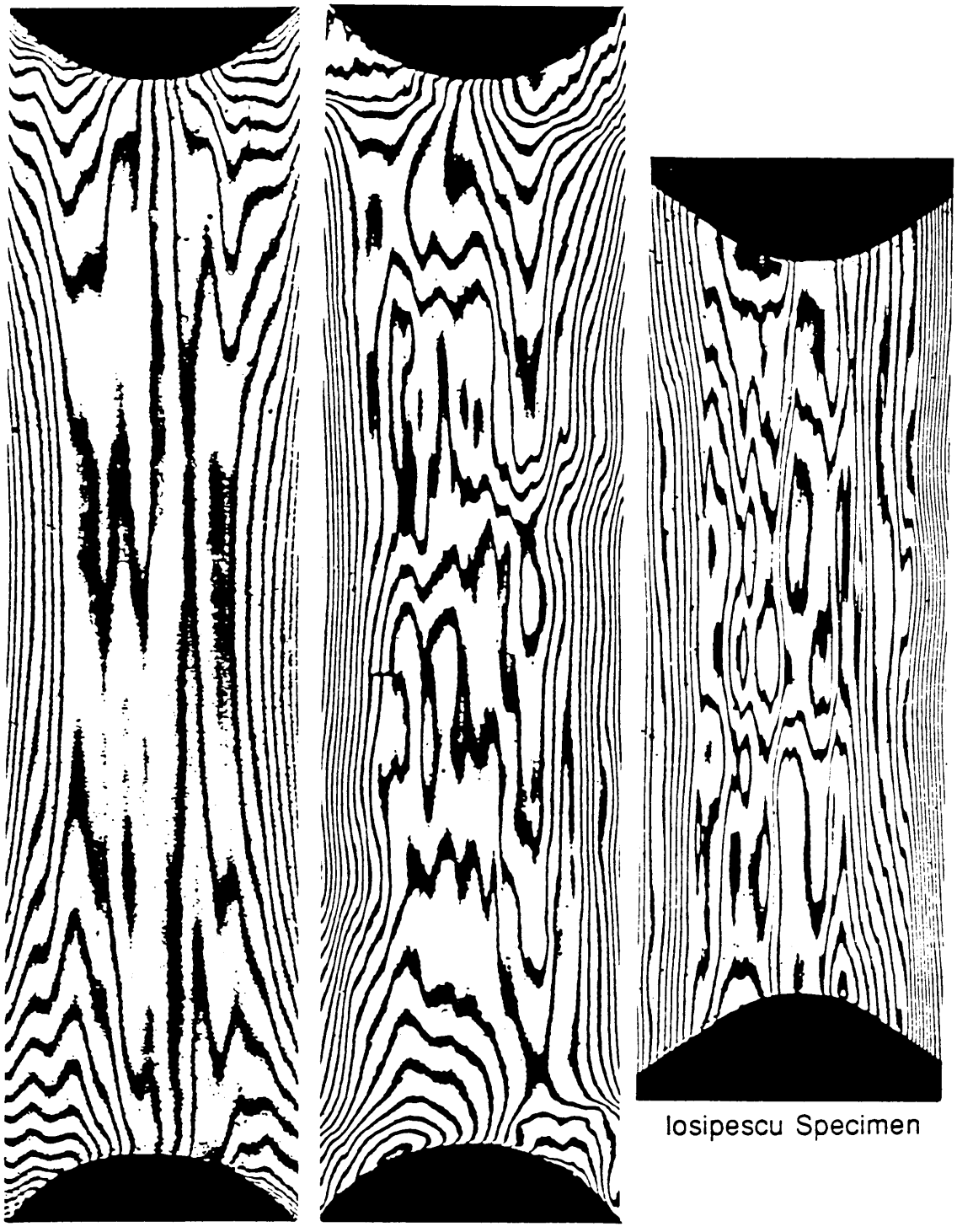

Fig. 35. The V field displacement patterns of the test sections for the three specimens at high load levels. The patterns have been modified with a carrier of rotation to reveal the normal strain ε_y .

which may have been caused by nonuniform loading through the thickness of the three specimens. Shear strains on the front and back surfaces may differ resulting from the curvature of plies in the test section causing some twist or bending as well as differences in shear strain. Also the bearing forces at the locations of direct compression could have been nonuniform. This nonuniformity may have resulted from the specimen or fixture surfaces not being truly flat or square. The extent of the nonuniform bearing is not clear, however, and a controlled test could be done in the future to investigate this. Another cause of differing shear strain measurements on the two sides of the specimen may occur as a result of a the loading plane which is not well aligned with the center of the specimen. This may result in shear strains being larger on one side of the specimen than the other. This effect could in the future be studied by a controlled test where the plane of loading is stepped away from the center of the specimen. Non symmetric laminates may also add coupling terms which could cause twist in the specimen. This twist could then conceivably contribute to sizeable differences in the deformation of the two sides.

Future work on the compact specimen should include some two sided measurements to support or dismiss the possibility of differing shear strain readings on the two surfaces. This could be performed simply with strain gages or if more insight is needed, with moire interferometry. Nevertheless, the proposed use of strain gages on both sides of the specimen for routine testing would circumvent this uncertainty.

Deformation at the Notch Tips

From a theoretical point of view the shear strain should be zero at the notch root since it is a free edge. The deformation analysis showed a trend that backs theory. Figures 31 and 32 illustrate that at the notch tips the shear strain goes to zero, as revealed by the hooked fringes in the U fields. The fringe gradients became zero approaching both notch

tips. The shear strains were relieved by the rigid body rotation of the material near the root satisfying the zero shear stress condition there. Ideally, the region where this rotation occurs should be minimized in order to get a more uniform shear stress distribution between the notch roots.

From a predictive point of view, reducing the notch radius would act to reinforce the notch root and reduce the extent of rotation which could relieve the shear stresses at the free edge. It is believed that this would yield a superior (more uniform) shear stress distribution on a line connecting the two notch tips. However, it is believed a less uniform distribution would occur on a transverse line such that at a small distance from the centerline connecting the notch tips the shear strain would be much smaller than the maximum shear strain. In other words a small notch radius would in effect reduce the width of the test section. For experiments that incorporate strain gages this could yield a considerable error. For practical purposes, the notch root diameter should be kept larger than the dimension of the strain gage. This would also accommodate small errors in gage alignment.

Another reason to keep the radius fairly large is that it incorporates more of the material into the test section. Larger strain gages could be used, and there would be less chance of isolating material anomalies in the larger area. In other words, with a larger test section more than one nonuniform zone could exist under the gage and more nearly average properties would be extracted for design purposes. With a small radius, it would be possible to isolated one compliant area and get erroneous stiffness measurements.

Normal Strain ε_y

The normal strain ε_y was analyzed more closely for the three specimens investigated. The normal strain in the test section seemed to be a material dependent

phenomena and not load induced. These strains nevertheless were two orders of magnitude smaller than the shear strains. Further analysis of the V field fringe patterns with carriers of rotation in Fig. 35 shows the vertical displacements. The carrier acts to subtract the uniform part of the vertical fringe pattern to enhance the normal strain information. It can be seen that on a line connecting the notch tips there was virtually no normal strain ε_y for compact specimen II. There was only one fringe order change across the test section. This is quite remarkable and represents a strain of only 22×10^{-6}. Compact specimen I and the Iosipescu specimen exhibited larger strains. The Iosipescu specimen has about a 4 fringe order change across its gage length which represents 164×10^{-6} strain. The compact specimen I has a 9 fringe order change across the test section which reveals a strain of 196×10^{-6}. These strains are more than 2 orders of magnitude smaller than the average shear strain.

Compact specimen I and the Iosipescu specimen have some undesired curvature in the test section. This may have had an influence on the state of shear in that area. Some coupling of the stresses might have occurred as a result of the curvature of the plies. The section on effects of ply curvature details this. In summary, it is believed that the curvature of the plies in the test section contributes to the normal strains ε_y. This curvature is small and likewise the normal strain ε_y is small.

Compact Specimen I vs II

Recall that the geometry and fixturing for the two compact specimens were the same except for their ply orientations. Otherwise the only other difference in the two tests was the use of cement to adhere specimen I to the load transfer fixtures. The deformation of specimen I was slightly different from that of specimen II up to the point that the cement failed (at an average shear stress of 3700 psi). The deformation at this and subsequent

load levels then became more similar to that of specimen II, since the boundary conditions were equivalent. Generally speaking, it is not advisable to change the applied loads on the specimen in the middle of the test. Therefore it is recommended that cement not be used. Thus testing for specimen II was superior to that of specimen I. In addition, other advantages of excluding the cement were the comparative ease of specimen preparation.

CONCLUSIONS

A new compact shear specimen was developed for the shear testing of fiber reinforced composite materials. A preliminary test was performed on a cross-ply laminate. The results were compared to the Iosipescu specimen. The compact specimen produced a more pure and uniform shear field in the test section. The advantages of the compact specimen confirmed in these tests are summarized here.

- The specimen is compact and easy to fabricate
- Fixturing is uncomplicated and inexpensive.
- There is a large area of pure and uniform shear.
- The specimen produces reliable stiffness measurements.
- Clamping forces don't effect the strains in the test section.
- Strain gages can be used for routine measurements.

In addition it is believed that the specimen has other advantages that were not confirmed in this study.

- The specimen could be used for shear strength measurements.
- Various material systems could be studied including isotropic and anisotropic materials.

Future work with the specimen will determine its ultimate usefulness. The following section will recommend appropriate measures to improve the test method.

RECOMMENDATIONS

The results of the initial test of the compact specimen were encouraging and informative. From the detailed analysis performed, a number of deficiencies of the test method were exposed. Refinement of the specimen and load mechanism could eliminate these deficiencies. Additional work on a variety of material systems are needed to verify the usefulness of the compact shear test method.

From the analysis it became apparent that altering the specimen geometry could improve the test method. It is recommended that the effects of the overall specimen size, the notch radius, and the test section size be investigated. The geometry used for the initial test was a preliminary one and not fixed. The overall size of the initial specimen was chosen to accommodate the cylinder material.

The specimen could be made smaller or larger depending on the material investigated. A smaller specimen would be required to test structures with small curvatures, while the size would not be as critical for flat laminates. As opposed to changes of scale the specimen could be enlarged or reduced in only one direction to strengthen certain areas. For shear strength testing it was found that the specimen did not fail in the test section but rather under one of the load bearing areas. This could have been prevented if the load bearing had been increased. One way of doing this would be to make the specimen wider thus increasing the bearing area. For the immediate future work, increasing the width of the specimen would improve the likelihood of shear failure in the test section.

The radius of the notches could have a large effect on the shear strain distribution in the test section. It is believed the smaller the radius the more likely the state of stress along the line connecting the notch tips would be pure and uniform. However, a smaller radius would decrease the width of the section, thus limiting the practicality of strain gage use. The optimal notch radius is then a compromise between the most uniform and pure shear state and the limitations of using strain gages, including the issue on anomalous variations in the gage area. Future work on the specimen geometry should include the investigation on the effects of changing the notch radius.

The notch radius would effect the width of the test section while the length of the test section is the notch spacing. Changing this length is likely to have an effect on the uniformity of shear along the line connecting the notches. It is believed that a longer test section would produce a more uniform shear state. Again, work is recommended to test the effects of the test section length on shear distribution and strength measurements. For immediate work it is my opinion that keeping the same length or slightly reducing it would be the right compromise for most measurements.

In addition to the specimen geometry, the fixturing could be altered to produce a better shear test. The load transfer fixtures for the initial test were rather crude yet the results were encouraging. Changes in the fixtures should be made in the future. The fixtures should be designed to accommodate specimens of different thicknesses. Also, a mechanism to index the specimens in order to fix their alignment should be added to the load transfer fixtures. This would ensure that under repetitive testing the loads would always be centered over the specimen. The fixture could also be altered to increase the bearing area on the specimen. This would reduce the chance of compressive failure at those zones and improve shear strength tests. In addition to the load transfer fixtures the clamping devises could also be alter in future work. The clamping fixtures used in the

initial test did not produce uniform pressure on the specimen. This may have effected the load transfer into the test section such that the shear on the front and back side may have been different. To test the effectiveness of the load transfer it is recommended that the deformation be investigated on both sides of the specimen. Future work should be performed to verify the state of shear on both surfaces of the specimen. The strain distributions should be analyzed on the two surfaces by moire interferometry, even though this would increase the difficulty of the test. An alternate approach may be to use moire on one side and strain gages on the other. If results indicate that the strain distributions on the two faces vary greatly then modifications to the loading fixtures would be required. These refinements of the test fixturing could in the future help the acceptance of the compact shear test method.

The optimal specimen size and shape would depend on the material tested. For instance a geometry best suited for a ninety degree unidirectional composite would not likely be suited for a zero degree specimen. Also the shear strain distributions in the test sections are likely to be quite different [22]. In addition, accurate shear strength measurements may be impossible for some laminates, while for others they would be routine. Future work needs to be performed to investigate the effects of different specimen material systems, fiber orientations and laminates. A comprehensive study of the compact specimen should be performed on a variety of fiber orientations for composites and also on different isotropic materials. It is recommended that five different composite systems be studied and compared to the Iosipescu test. These include 0 deg and 90 deg unidirectional, ±45 deg and 0,90 deg crossed-ply, and quasi-isotropic laminates. The shear strain distributions and shear strength measurements should both be compared for all of these materials. In addition, isotropic materials should also be tested and compared to results obtained from the Iosipescu specimen. Both brittle and ductile materials should be tested

for stiffness and strength. From these tests on different material systems it may turn out that the specimen geometry may have to be altered to achieve the best results. These alterations may come in the form of changing the specimen shape or simply by incorporating tabs. Nevertheless, at this stage the compact specimen should be viewed as a flexible testing scheme and not as a fixed one.

In addition to experimental investigation of the compact specimen, a numerical study could reveal some attributes and deficiencies of the test method. The compact specimen boundary conditions would be easy to model. By using an FE analysis such parameters as changing the notch radius, overall size, and fiber orientations could be investigated. These results, though, would need to be verified experimentally.

For work in the near future some recommended modifications of the compact shear test method are cited here. The width of the specimen and the notch radius should be varied. The fixtures should be redesigned to accommodate specimens of varying thickness. The clamping mechanisms should be modified so that uniform pressure is applied on the specimen. The shear distributions should be investigated on both faces of the specimen. A variety of material systems should be investigated including isotropic, and composite materials. Specifically both unidirectional and multi-directional laminates should be investigated. Tabs are recommended only when testing some laminates for shear strength such as 0 deg unidirectional laminates. These modifications will provide further insight into the usefulness of the compact double notched specimen.

PART 2

INTERLAMINAR SHEAR TESTING

The interlaminar shear response for the same composite cylinder tested in the previous section was determined. Twin objectives consisted of (1) investigating the phenomenological behavior of the composite material loaded in interlaminar shear, and (2) the determination of interlaminar shear moduli of individual plies and the effective modulus of the laminate.

To measure the shear strains on the micro-structural scale, or on the ply scale, detailed measurements were required. High sensitivity moire interferometry was used to obtain the interlaminar strains. Two different rail shear specimens and loading fixtures were designed especially for this test. This scheme was chosen because of the limited thickness of the material and the need for the shear response in numerous plies.

SPECIMENS AND LOADING

Two specimens were cut from the composite ring as illustrated in Fig. 36. A diamond impregnated saw was used to free the specimens from the cylinder and all the

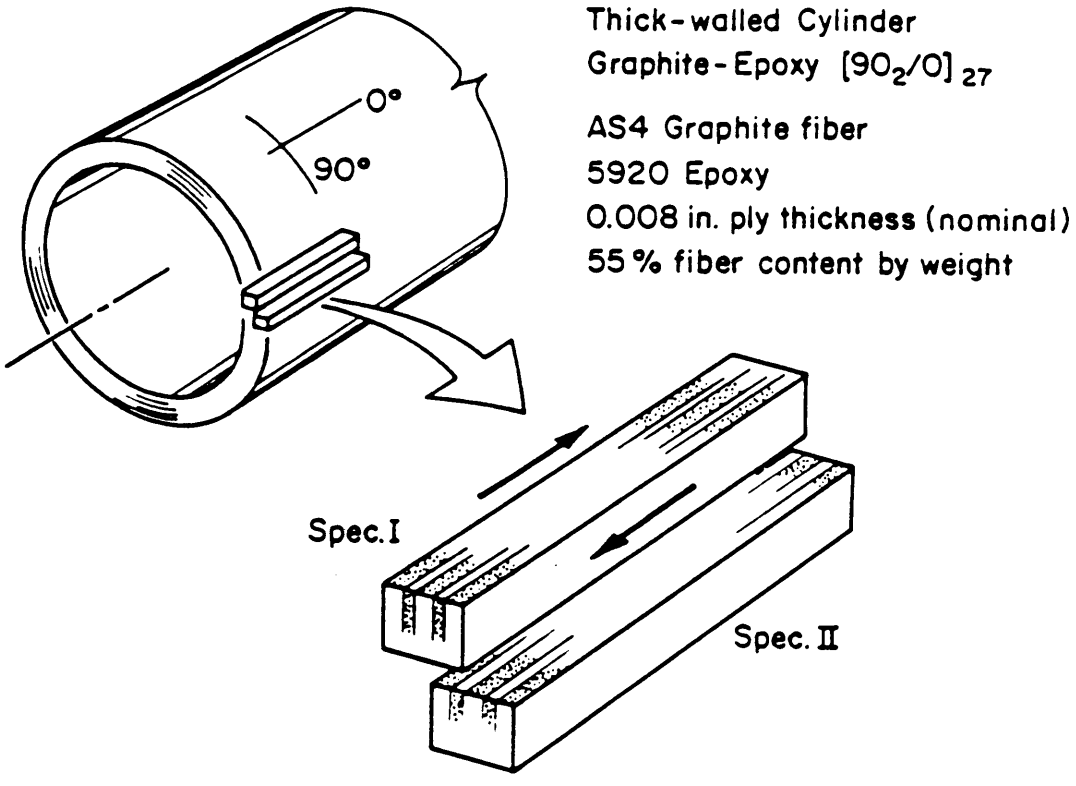

Fig. 36. Specimens were cut from a 200mm (8 in) outside diameter laminated composite tube.

sides were ground flat. Rails were cemented to both sides of the specimens as illustrated in Fig. 37.

Two different rail configurations were incorporated providing extremely different end conditions. Specimen I, shown in the top half of Fig. 37 was cemented to the rails with a stiff epoxy adhesive. It was subjected to direct compression on two opposite corners. Specimen II shown in the bottom half of Fig. 37 was cemented to the rails with a compliant acrylic adhesive. Additional adhesive was used at all four corners to alleviate abrupt load transfer and stress concentrations. After the specimens were cemented to the rails a 1200 l/mm cross line diffraction grating was replicated over the specimen surface as well as part of the rails.

The rails were loaded by a wedge type compression fixture. This was the same fixture used for the compact double-notched specimen. The displacements were obtained with moire interferometry.

QUALITATIVE ANALYSIS OF DEFORMATION

Figures 38 and 39 are the fringe patterns of the U and V displacement fields for specimens I and II respectively at roughly the same load levels. The patterns include the entire specimen, located between a portion of the two rails. The vertical fringes in the V field indicate shear deformation throughout the specimen. At the upper and lower ends of the specimen however strains become smaller and approach zero at the free edges. The shear strain is relieved at the ends by rigid body rotations caused by bending. This can be evidenced by the horizontal fringes in the V field near the free ends which act to cancel the vertical fringe gradient in the U field. Note, in specimen II there is a more pronounced

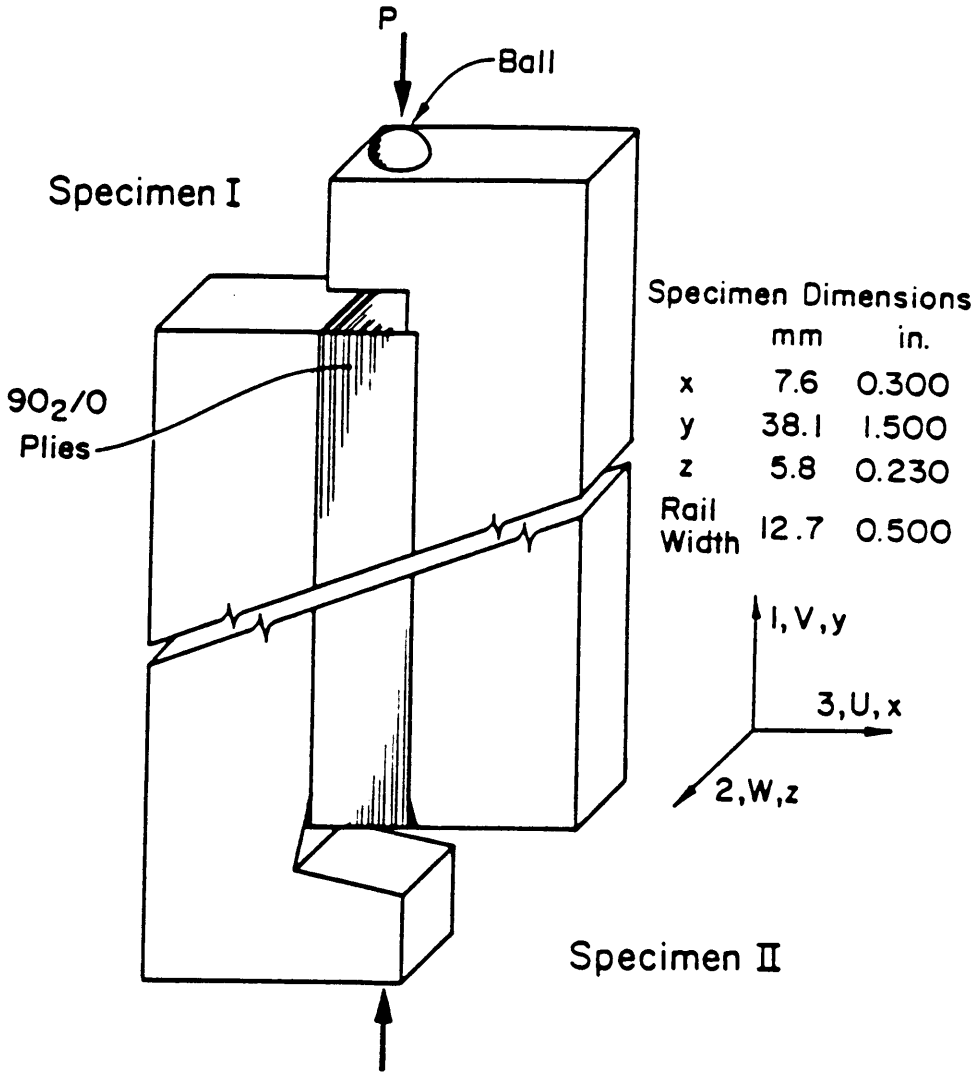

Fig. 37. The specimen configurations. Specimen I had steel rails attached to both sides with stiff cement. Specimen II was attached to the rails with compliant cement.

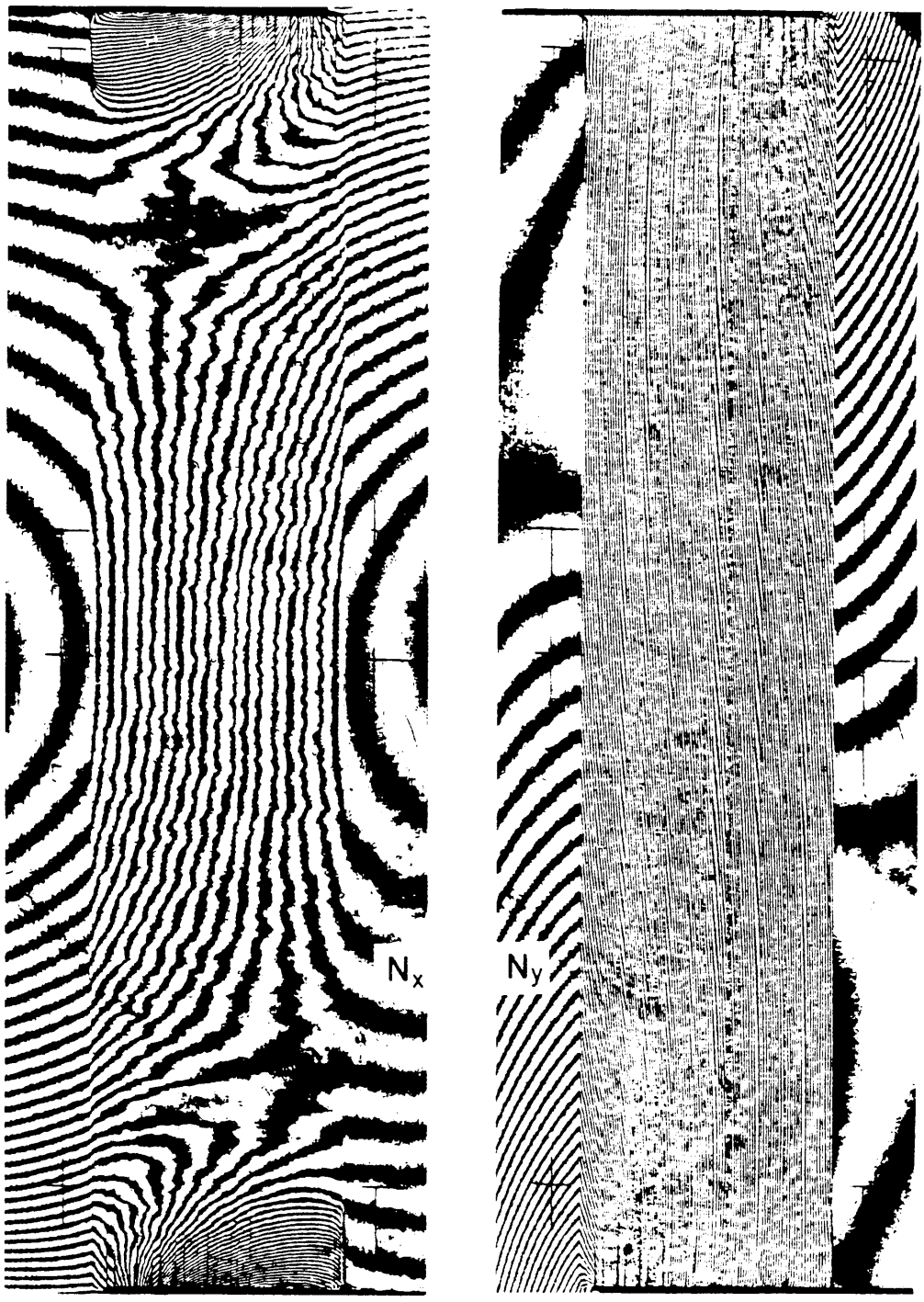

Fig. 38. N_x and N_y fringe patterns for specimen I, depicting the U and V displacement fields. The load level was 3.18 kN (714 lb).

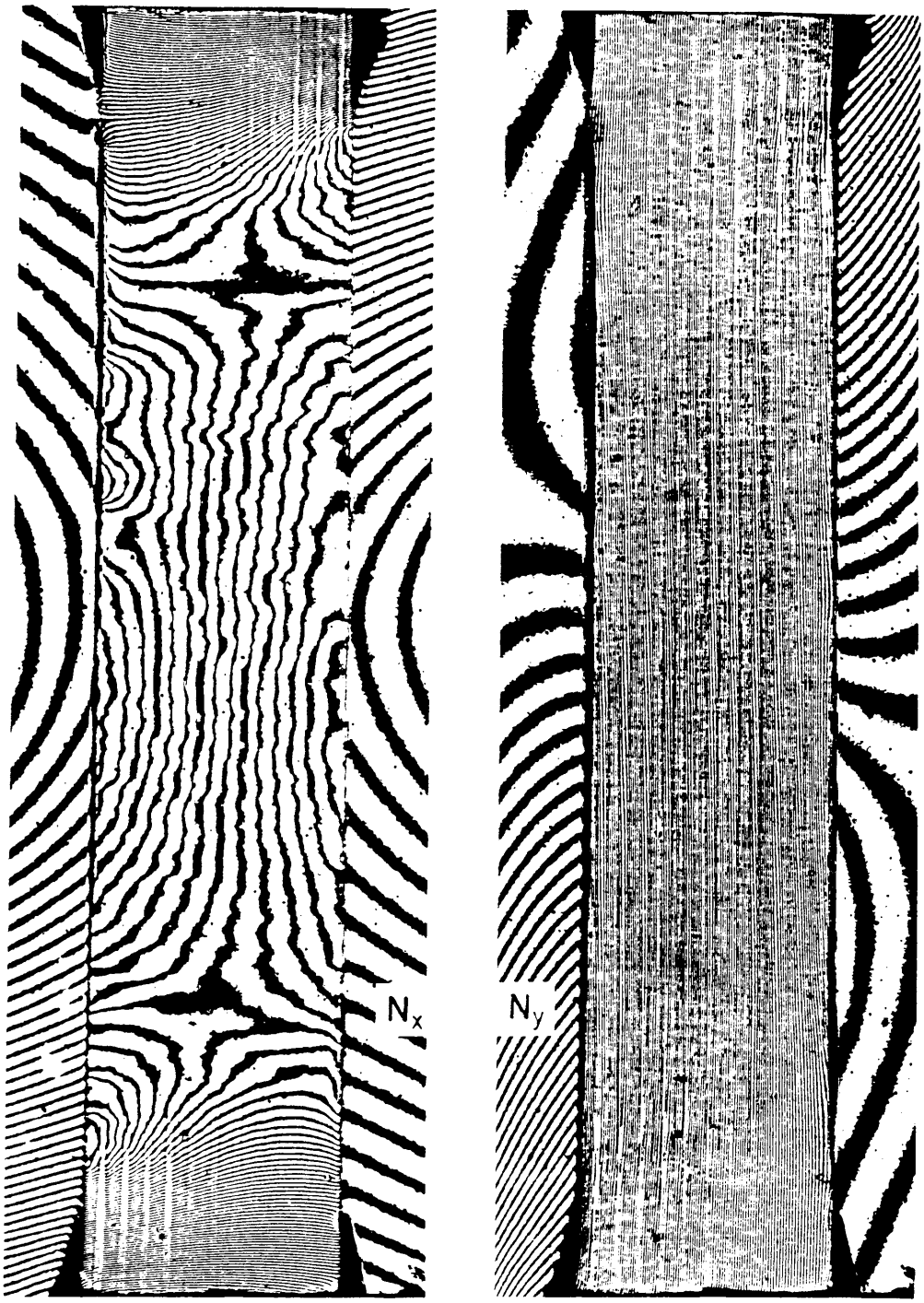

Fig. 39. U and V fringe patterns for specimen II. The load level was 3.14 kN (707 lb).

bending effect than in specimen I. This resulted from the more compliant rail condition of specimen II.

From the V fields in both specimens, the gradient in the x direction varies. This variation occurs on a ply by ply basis. In fact the shear strains in general are greater in the 90 deg plies than in the 0 deg plies, (by virtue of more closely spaced fringes in the 90 deg plies).

Normal strains exist in both specimens. Unlike the results of the in-plane work these strains occur over the entire specimen. The normal strain ε_y in specimen I is greater than that of specimen II. This resulted from the direct compression at the two opposite corners, where ε_y is greatest. The normal strain ε_x is also quite large in these zones.

The discontinuity of the fringes from the specimen to the rails at the upper left and lower right corners of specimen I indicates a crack has formed at that interface. Other vertical lines at the ends of the specimen do not represent cracks but zones of large out-of-plane deformations between 0 deg and 90 deg plies.

In both tests the rails did not remain perfectly rigid, as evidenced by the fringe patterns. Some bending occurred however the magnitude of deformation was small compared to that of the specimen.

Through the use of carrier fringes, discussed in the appendix, the micromechanical behavior can be accurately extracted. Figure 40 illustrates an enlarged central portion of the V field for specimen I, after a known carrier of extension was added. The pattern now is a series of sloped fringes. The slope of the fringe is related to the strain. The strains and locations of abrupt change in strain can be extracted with high fidelity. Strains are greater in the 90 deg plies than 0 deg plies and even greater in the resin rich zones between the plies.

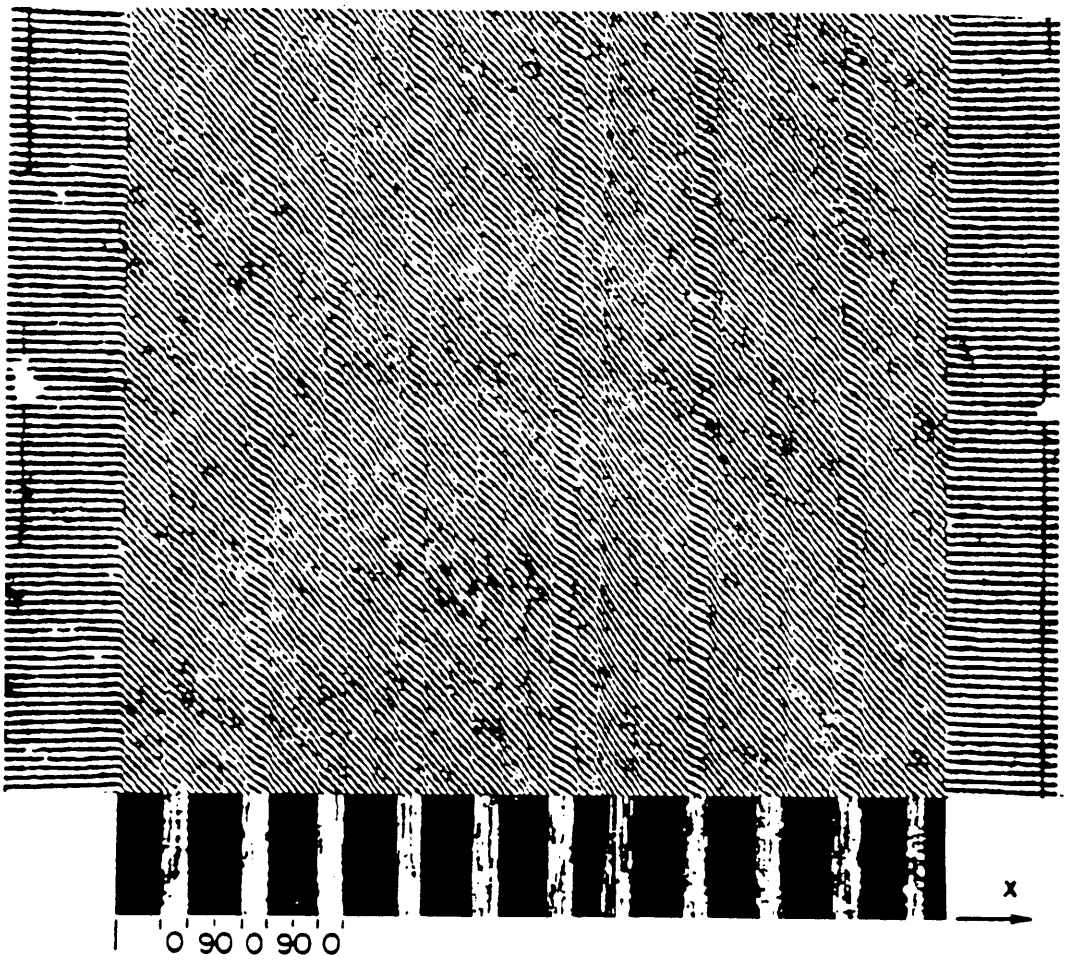

Fig. 40. The V displacement field with a carrier of extension for the central portion of specimen II. The insert at the bottom shows the ply sequence.

Figure 41 represents the same V field, but with a carrier of rotation added. The uniform fringe gradient in the horizontal direction was subtracted, creating a pattern in which normal strains ε_y can be extracted more easily.

QUANTITATIVE ANALYSIS OF DEFORMATION

Figure 42 shows the shear strain distributions along the length of specimens I and II for representative 0 and 90 deg plies. These graphs and all subsequent graphs of strain were plotted for the load levels pictured in Figs. 38, 39. The shear strains for the graphs were plotted by calculating the cross derivative terms from the two displacement fields along the length of the plies. The pertinent equations are given in Fig. 47 of the Appendix. The U field cross derivative term was measured from gradients in Figs. 38 and 39. The V field cross derivatives, however were extracted from patterns containing a carrier of extension as in Fig. 40. The curves in Fig. 42 have been smoothed and do not exhibit the local variations caused by the inhomogeneity of the material.

The shear strains in specimen I are more nearly constant along the length of the specimen than in specimen II. In both specimens the 0 deg plies exhibit smaller shear strains than the 90 deg plies. However in specimen II it is evident that two plies of the same orientation have different shear strain levels. The average shear strain of these two plies differ by about 12%. The symbol $\gamma_L{}^{av}$ represents the average shear strain wherein γ_{xy} is averaged along the length of the specimen for an individual ply. The cylinder material exhibits quite a variation of shear strain amongst nominally equal plies. This effect is caused primarily by local variations in the fiber volume fraction and the thickness of resin rich zones between plies. Accordingly, material properties calculated from these strains must be taken as representative rather than fixed values.

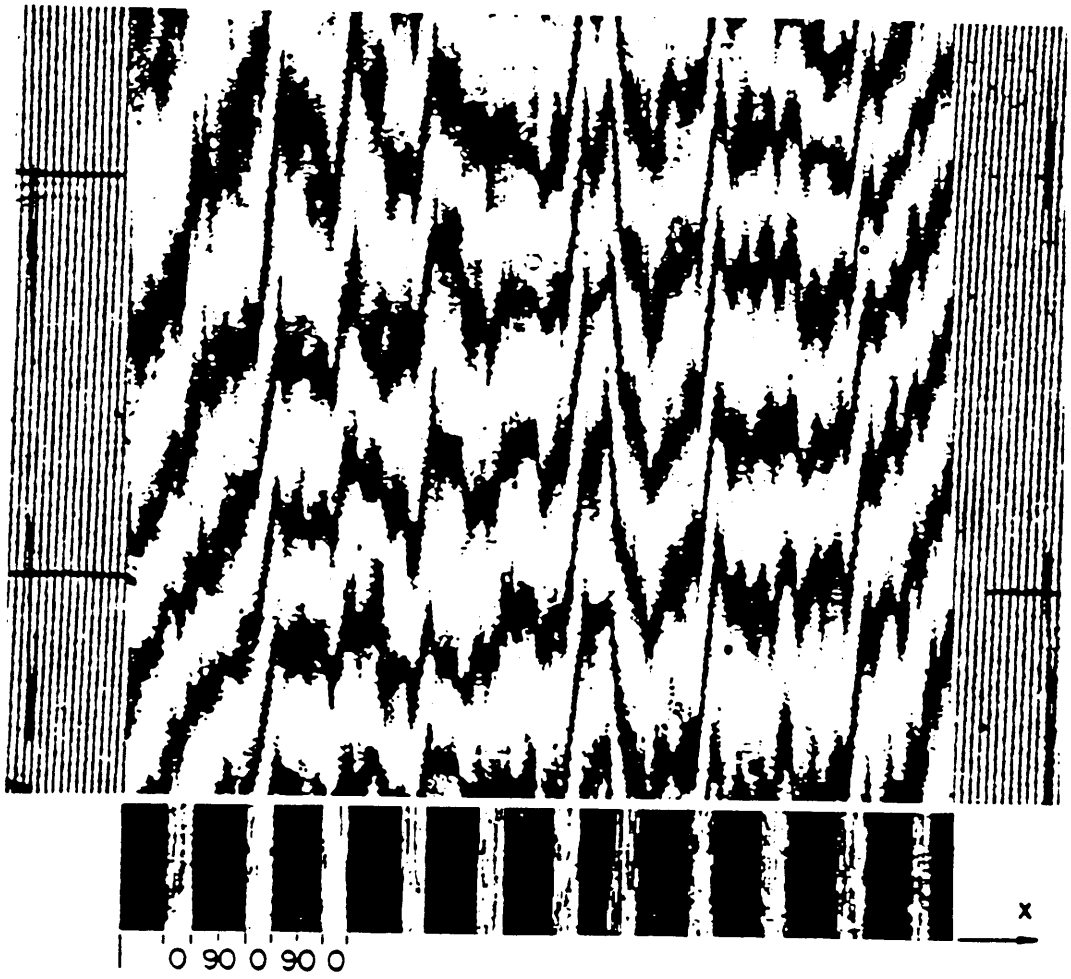

Fig. 41. The V displacement field with a carrier of rotation for the central portion of specimen II.

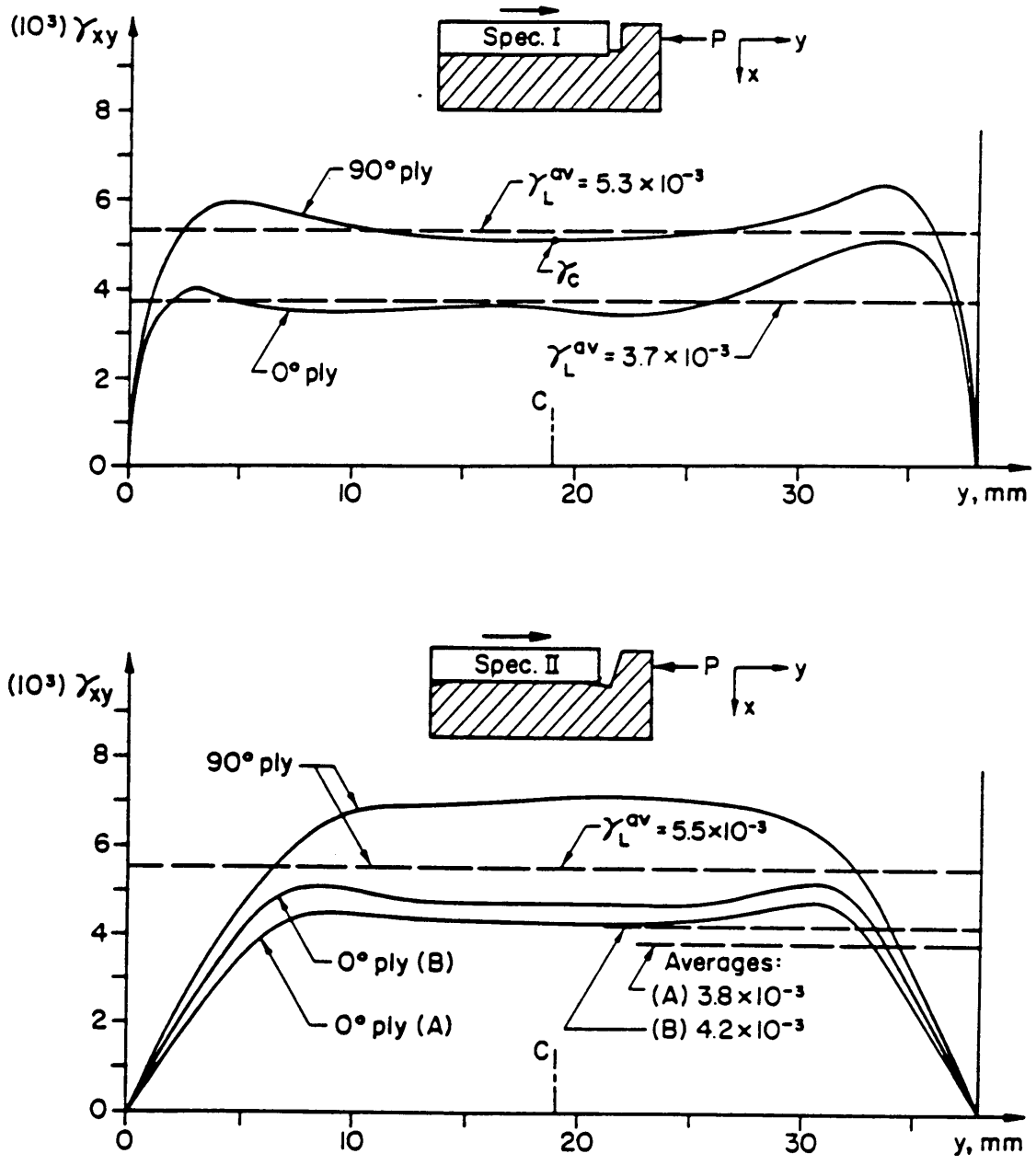

Fig. 42. The shear strain distributions in individual plies along the length of both specimens. The plies were located within the central third of each specimen.

Shear strains along the horizontal centerline of the specimen were plotted in Fig. 43. Matching the curve with the labeled ply sequence revealed the strains in the 90 deg plies were generally larger than in the 0 deg plies. Strains were even larger in the resin rich zones between the plies as indicated by the peaks in the curves. There is a dramatic difference in the shear strains of nominally equal plies. The average shear strain across the horizontal center line for the 0 deg plies was

$$(\gamma^{av})_0 = 3.6 \times 10^{-3}$$

with extremes of 28% higher and 17% lower. The average shear strain likewise for the 90 deg plies was

$$(\gamma^{av})_{90} = 5.0 \times 10^{-3}$$

with extremes of 18% higher and 14% lower. Table 4 shows these extreme values. The resin rich zones had shear strain values around 8×10^{-3}. The variability of the shear strains in equivalent plies is well documented.

In Fig. 43 an anomaly appears in the region of the sixth and seventh 0 deg plies. The strain was unusually large resulting from the defect in that area. The response was indicative of a resin rich region.

Returning back to Fig. 42 it should be noted that the plies were carefully selected for shear strain distribution plots. These particular plies exhibited a representative response, or one close to the average. Ply no. 5 of specimen I was chosen as the 0 deg ply and its neighbor the 90 deg ply. Similarly representative plies were chosen from specimen II.

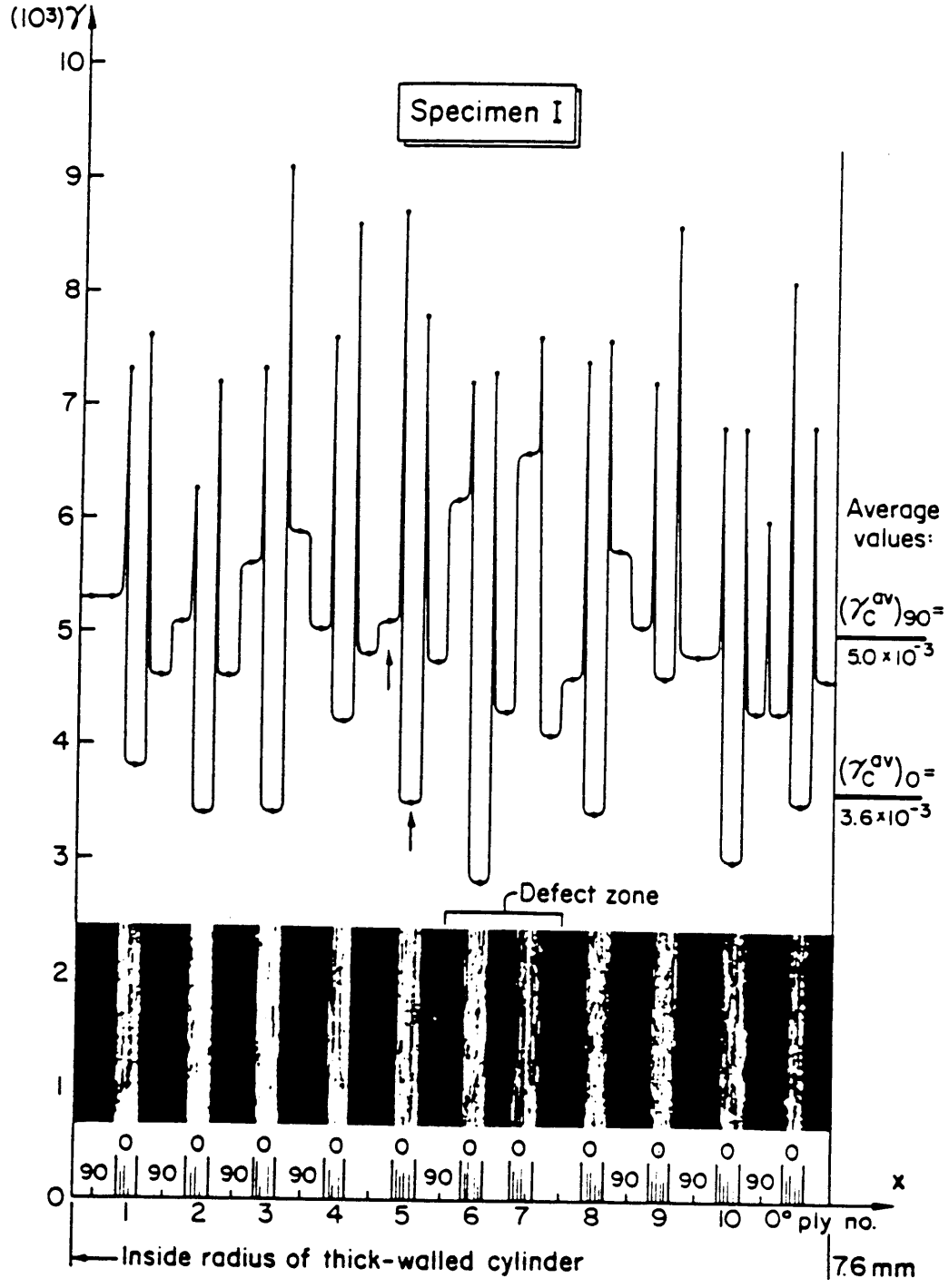

Fig. 43. Interlaminar shear strains across the width of specimen I at the center of its length. The insert is a photograph of the plies.

Linearity

The linearity of the interlaminar shear stress-strain response was verified. To test this the displacement ΔV across the full thickness of the specimen was measured across the central region of the specimen for three different load steps. These load steps were approximately P, 2P/3, P/3, where P was the load corresponding to Figs. 38 and 39. In specimen I the ratio of $\Delta V/L$, where L was the load, was constant to within $\pm 0.4\%$ and in specimen II to within $\pm 2\%$. These values fall within the measurement errors associated with extracting strains from the fringe patterns. Therefore for all practical purposes the interlaminar shear stress strain response is linear up to the load level investigated.

Interlaminar Shear Moduli of Individual Plies

The shear moduli of the individual plies were calculated on the basis of two specific propositions. Proposition 1. The shear modulus within any single ply is constant. This proposes that the shear stress is proportional to the shear strain at any point along the length of the ply, indicating that the average values are in the same proportion, or

$$G_a = \frac{\tau^{av}}{(\gamma_L)^{av}_a} \qquad (1)$$

where τ^{av} is the average shear stress on the ply (P/LT), and (a) designates a particular ply. Linearity of the material in interlaminar shear supports this proposition. Note also, curves (A) and (B) in Fig. 42 have a similar shape only differing in magnitude. This also supports the proposition.

This proposition does not account for the random variation of material properties associated with this composite material. In other words, the inhomogeneity of the composite which has been well established was not accounted for. This leads to a

somewhat artificial assumption. However representative values were extracted for design purposes.

Proposition 2. The shear modulus of any ply is inversely proportional to the shear strain at the horizontal centerline. This assumes that shear strains at the horizontal centerline are not anomalous values. It leads to the relationship

$$\frac{G_b}{G_a} = \frac{(\gamma_C)_a}{(\gamma_C)_b} \quad \text{or} \quad G_b = \frac{(\gamma_C)_a}{(\gamma_C)_b} \frac{(\tau^{av})}{(\gamma_L)_a^{av}} \tag{2}$$

where the subscript b designates any other ply of the same fiber orientation and γ_C is the shear strain measured at the horizontal centerline. To obtain representative values of G for all the plies, $(\gamma_C)_b$ is taken as the average value $(\gamma_C{}^{av})_{0,90}$. The subscript (0,90) represents a 0 deg or 90 deg ply. Then

$$G_{0,90} = \frac{(\gamma_C)_a}{(\gamma_C)_{0,90}^{av}} \frac{\tau^{av}}{(\gamma_L)_a^{av}} \tag{3}$$

Data for each ply was taken at its center, therefore the resin rich zones near the ply interface were not accounted for. An approach to extract the moduli which accounts for the resin rich portion will be addressed later in this text.

The shear moduli for 0 deg and 90 deg plies were calculated by Eq. (3), using values of $\gamma_L{}^{av}$ from Fig. 66 and $\gamma_C{}^{av}$ from Fig. 43. The same procedure was followed for specimen II. The results of the interlaminar shear moduli for 0 deg and 90 deg plies are given in Table. 2.

Table 2. Summary of interlaminar shear moduli.

		Specimen I		Specimen II	
	Property	Average Value	Extreme Variations	Average Value	Extreme Variations
RESIN-RICH ZONE EXCLUDED	$G_0 = G_{13}$ Center of Ply [Eq. 3]	3.7 GPa 540,000 psi	+ 17% - 28%	3.6 GPa 520,000 psi	+ 11% - 14%
	$G_{90} = G_{23}$ Center of Ply [Eq. 3]	2.8 GPa 400,000 psi	+ 14% - 18%	2.6 GPa 370,000 psi	+ 20% - 16%
	$G^{calc}_{[90_2/0]_n}$ by calculation	3.0 GPa 440,000 psi		2.9 GPa 420,000 psi	
RESIN-RICH ZONE INCLUDED	$G^{eff}_{[90_2/0]_n}$ by measurements [Eq. 4]	2.6 GPa 380,000 psi		2.8 GPa 400,000 psi	
	$G_0^{eff} = G_{13}^{eff}$	3.2 GPa 470,000 psi	+ 17% - 28%	3.4 GPa 500,000 psi	+ 11% - 14%
	$G_{90}^{eff} = G_{23}^{eff}$	2.4 GPa 350,000 psi	+ 14% - 18%	2.4 GPa 350,000 psi	+ 20% - 16%

Interlaminar Shear Modulus of the Laminate

The effective interlaminar shear modulus of the laminate, G^{eff}, is the value that would predict the macroscopic shear response of the laminate. It is an integrated or smeared value obtained from a ply by ply analysis of the laminate. G^{eff} can be determined by the equation

$$G^{eff}_{[90_2/0]_n} = \frac{\overset{av}{\tau}}{\gamma^{av}_{W,L}} \tag{4}$$

where $\gamma_{W,L}{}^{av}$ is the shear strain averaged along the width and length of the specimen. The subscript n represents the number of repeated ply sequences in the specimen, but the results are representative of the thick-walled cylinder. Averaging the shear strains, $\gamma_{W,L}{}^{av}$ can be determined in two steps.

In step 1, the shear strains across the width of the specimen at the horizontal centerline is given by

$$\overset{av}{\gamma_W} = \frac{\Delta N_y}{fW} \tag{5}$$

where ΔN is the change of fringe order at the horizontal centerline across the specimen width, W, and f is the frequency of the reference grating (2400 lines/mm).

In the second step, the averaging factors that account for variations along the specimen length are taken from Fig. 42 as $\gamma_L{}^{av}/\gamma_C$. Since this factor may be different for 0 deg and 90 deg plies, it is proportioned according to the relative number of these plies, then

$$\overset{av}{\gamma_{W,L}} = \frac{\Delta N_y}{fW}\left[\frac{1}{3}\left(\frac{\overset{av}{\gamma_L}}{\gamma_C}\right)_0 + \frac{2}{3}\left(\frac{\overset{av}{\gamma_L}}{\gamma_C}\right)_{90}\right] \tag{6}$$

where the subscripts 0 and 90 denote the corresponding plies. Then the effective interlaminar shear modulus is given by Eqs. 4 and 6. The results are given in Table 2.

The Shear Modulus for the Laminate Neglecting the Resin-Rich Zones

The shear modulus for the laminate (neglecting the resin-rich zones) was calculated. If the resin -rich zones were neglected the shear strain for the laminate could be calculated by

$$\overset{calc}{\gamma}_{[90_2/0]_n} = \frac{1}{3}\overset{*}{\gamma}_0 + \frac{2}{3}\overset{*}{\gamma}_{90} \tag{7}$$

where γ_0^* and γ_{90}^* are the average strains (at the center of the ply thickness) used in equation (3), or

$$\overset{*}{\gamma}_{0,90} = \left(\overset{av}{\gamma_C}\right)_{0,90} \frac{\overset{av}{(\gamma_L)_a}}{(\gamma_C)_a} = \frac{\overset{av}{\tau}}{G_{0,90}} \tag{8}$$

This then leads to the shear modulus for the laminate excluding the effects of the resin-rich regions.

$$\frac{1}{G^{calc}_{[90_2/0]_n}} = \frac{1}{3G_0} + \frac{2}{3G_{90}} \tag{9}$$

The values of the modulus are given in Table 2. These values are larger than those which include the resin-rich zones. In fact the ratio of the values are 0.864 for specimen I and 0.952 for specimen II.

Effective Moduli of Individual Plies

From the ratio k, effective values of the interlaminar shear modulus for individual plies can be defined. Essentially this accounts for the resin rich zones at the ply interfaces. The effective modulus for individual plies was determined by

$$G_{0,90}^{eff} = kG_{0,90} \tag{10}$$

Values of the effective ply moduli are given in Table 2 on this basis.

The specimen tested contained a nonuniform resin distribution characteristic of real laminates. The resin concentration was greater near the ply interface. The upper section of Table 2 relates to properties measured at the center of the plies, while the lower section offers values integrated through the entire laminate, including the resin-rich zones. In design practice the integrated values should be used. Values averaged from specimen I and II are the shear properties recommended for design purposes. Effective values are listed to only two significant figures. This is justified, in view of the variations within the material.

Normal Strains

In most regions on both of the specimens the normal strains were significantly smaller than the shear strains. In Fig. 44 the normal strains ε_y were plotted for specimen I. Strains down the center of the specimen are compressive except near the free edges where curiously they become tensile. These normal strains are an order of magnitude smaller than the shear strains. On the edge lines the strains are much larger near the points of load application. At the other end of this line the normal strains drop to zero. These results were extracted from the V field where a carrier of rotation was used to subtract the average shear fringe component as in Fig. 41.

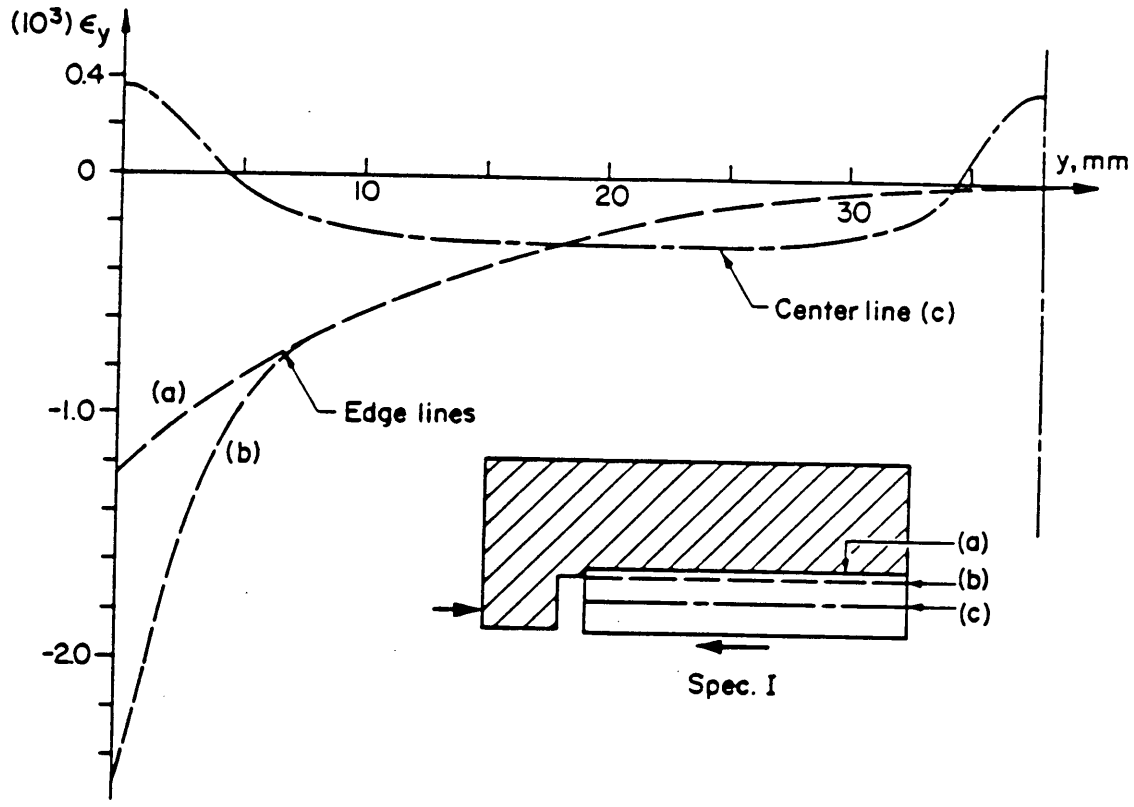

Fig. 44. Normal strain ε_y along the length of the specimen I at the centerline and two edge lines.

Figure 45 shows the plots of the normal strains ε_x along the vertical centerline of both specimens I and II. The strain were extracted form the U field fringe patterns in Figs. 38 and 39. Bending deformation of the fixtures for specimens I and II caused a tensile strain ε_x in the center of the specimens and compressive strains on the ends. In specimen II the compliant cement at the corners diminished the effect of the transverse constraint and the normal strains ε_x approach zero. Near the point of loading in specimen I strong compressive transverse strains occurred. In fact these strains are nearly as large as the shear strains in a small area near the zone of direct compression. Also at the ends of the specimen a different normal strain ε_x exists in the 0 deg and 90 deg plies. This divergence is illustrated in Fig. 45. It is believed however that this is associated with a free edge effect and it does not occur beneath the specimen surface.

Cracks between the specimen and the rails in Fig. 38 on specimen I suggests a tensile strain may have been present at lower load steps. They occurred because of the rigid body rotation at the ends of the specimen.

SPECIMEN I VS II

Judging by the shear strain distributions along the length of the specimens for individual plies, specimen I is the superior design. The distribution is more constant over a longer length. Also the deviation from the average shear strain value is less in specimen I. This improves the credibility of the averaging techniques.

Specimen I also experienced less bending than specimen II, as a result of differences in the compliance of the two boundary conditions. In each case, wider, stiffer rails would reduce bending. A combination of larger rails and stiff cement could improve the loading on the specimen.

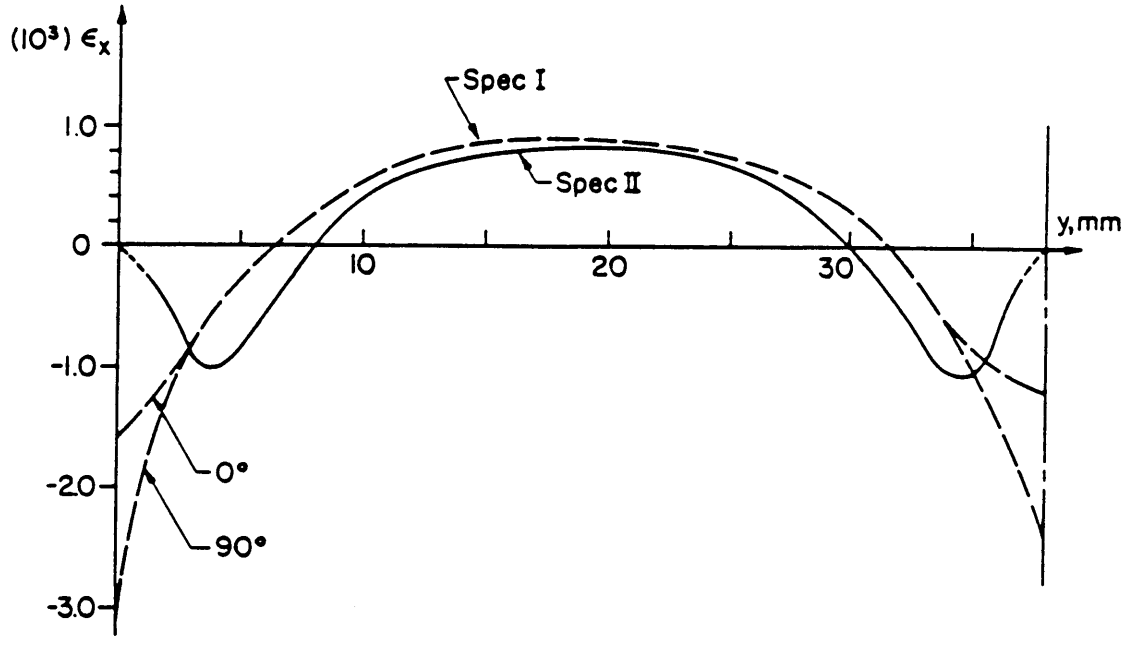

Fig. 45. Normal strains ε_x along the length and at the center of the widths of both specimens.

The results in Table 2 illustrate differences in measurements of moduli between specimen I and II of the order of 5%. These differences are not significant. The results of specimen I are thought to be more reliable. These differences though are trivial when point by point variations within nominally equal portions of the material are much larger.

CONCLUSIONS AND DISCUSSION

Detailed observation and measurement of the interlaminar shear response of the composite cylinder material was performed. The behavior of individual plies and of the resin rich interfaces between plies was observed quantitatively and qualitatively. The phenomenological response of the material in interlaminar shear was obtained as well as shear moduli for design purposes.

A major result observed in this work was the random variation of strains in nominally equal plies. The extreme variations are on the order of 20%. This variation is significant to our understanding of the characteristics of such composites. Variations within any given ply also exist, but they are much smaller.

The strains measured from the fringe patterns in the resin-rich zones between the plies were not entirely faithful to the actual deformation. This is due to the finite thickness of the diffraction grating which was replicated on the specimen surface. A shear lag through the grating thickness, results from abrupt changes in shear strain in the interface zones. The strains measured, therefore, in the resin rich zones, were smaller than the actual strains. The measurement of the shear strains at the center of the plies, however, are reliable since the width of the plies is many times larger than the thickness of the grating.

RECOMMENDATIONS

Future work with interlaminar shear should focus on specimen refinement. As pointed out in the previous section larger rails would prevent bending in the rails and reduce ε_x. Altering the length or width of the specimen could have a large effect on the shear strain distributions.

The compact specimen geometry discussed in the in-plane shear section could be utilized for interlaminar work. Additional material could be cemented to the sides of a representative cross section of the specimen material as illustrated in Fig. 46. This would effectively reduce the number of plies that could be investigated. The size of the test section would depend on the notch radius. This however would not be overly detrimental since representative values of moduli could still be obtained. The benefits of using the compact specimen should include a more pure state of shear, a more uniform state of shear, and possible interlaminar shear strength measurements.

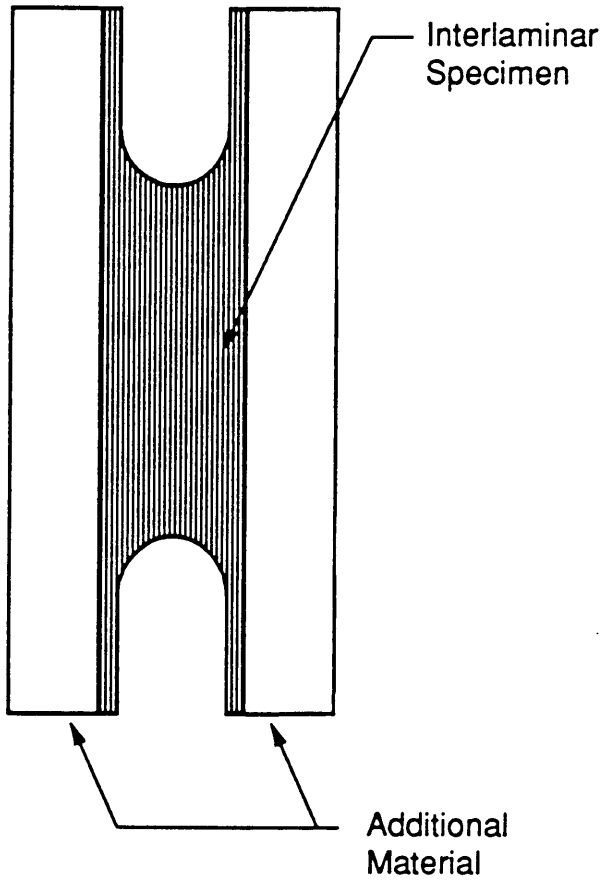

Fig. 46. The compact double-notched specimen applied to interlaminar shear testing.

REFERENCES

[1] Yeow, Y. T. and Brinson, H. F. "A Comparison of Simple Shear Characterization Methods for Composite Laminates", *Composites* 9 No 1 (January 1978) pp 49-55.

[2] ASTM D-30 Subcommittee on Shear Testing of Fiber Reinforced Composite Materials., Handout, Charlotte NC, Spring 1989.

[3] Lee, S. and Munro, M., "Evaluation of In-Plane Shear Testing for Composite Materials by the Decision Analysis Technique," *Composites*, 17(1):13 (January 1986).

[4] Beer, F. P. and Johnston, E. R., *Mechanics of Materials*, McGraw-Hill, New York, pp.67-70, (1981).

[5] Pagano, N. J. and Whitney, J. M., "Geometric Design of Composite Cylinder Characterization Specimens," *J. Comp. Mat'ls.*, 4, 538-548 (Oct. 1970)

[6] Chamis, C. C., and Sinclair, J. H., "10 - Deg Off Axis Test for Shear Properties of Fiber Composites" *SESA - Spring Meeting*, Dallas TX, May 1977 (also *Nasa-TND* 8215, April 1976)

[7] Petit, P. H. "A Simplified Method of Determining the In-Plane Shear Stress Strain Response of Unidirectional Composites" *ASTM STP* 460 (ASTM, 1969) pp 83-93.

[8] Whitney, J. M., Stansbarger, D. L., and Howell, H. B. "Analysis of the Rail Shear Test - Applications and Limitations" *Journal of Composite Materials* 5 (January 1971) pp 24-34.

[9] Garcia, R., Weisshaar, T. A. and McWithey, R. R., "An Experimental and Analytical Investigation of the Rail Shear Test Method as Applied to Composite Materials," *Experimental Mech* 20 No 8 (August 1980) pp 273-279.

[10] Chang, F. K. and Chen, M. H., "In Situ Ply Shear Strength Distributions in Graphite/Epoxy Laminated Composites," *Journal of Composite Materials* Vol. 21, No. 8 (August 1987) pp 708-732.

[11] Lockwood, P. A., "Results of the ASTM Round-Robin on the Rail Shear Test for Composites," *Composites Technology Review*, Vol 3, No. 2, (Summer 1981) pp. 83-86.

[12] Arcan, M., "A New Method for the Analysis of the Mechanical Properties of Composite Materials, *3rd Int. Congress Experimental Mechanics*, Los Angeles, 1973.

[13] Arcan, M., Hashin, Z. and Voloshin, A., "A Method to Produce Uniform Plane-Stress States with Applications to Fiber Reinforced Materials, *Exp Mech.* (April 1978), 18(4), 141-146.

[14] Adams, D. F. and Walrath, D. E., "Current Status of the Iosipescu Shear Test Method," *J. Comp. Mat.*, 21 494-507 (1987).

[15] Adams, D. F. and Walrath, D. E., "Iosipescu Shear Properties of SMC Composite Materials," *Proc. ASTM 6th Conf. on Composite Materials: Testing and Design*, Phoenix, AZ (May 12-13, 1981).

[16] Walrath, D.E., and Adams, D. F., "Verification and Application of the Iosipescu Shear Test Methods", Rep. No. UWME-DR-401-103-1, Composites Materials Research Group, Mechanical Engineering Department, University of Wyoming, June 1984.

[17] Iosipescu, N., "New Accurate Method for Single Shear Testing of Metals," *J. Materials*, Vol. 2, No. 3., Sept. 1967, pp 537-566.

[18] Slepetz, J. M., Zegeski, T. F., and Novello, R., "In-Plane Shear Test for Composite Materials," AMMRC TR 78-30, Army Materials and Mechanics Research Center, July 1978.

[19] Walrath, D. E., and Adams, D. F., "The Iosipescu Shear Test as Applied to Composite Materials", *Experimental Mechanics*, Vol. 23, No. 1, March 1983, pp 105-110.

[20] Pindera, M. J., Choksi, G. N., Hidde, J. S. and Herakovich, C. T., "A Methodology for Accurate Shear Characterization of Unidirectional Composites", *J. Comp. Mat.* Vol. 21, Dec. 1987, P. 1164.

[21] Herakovich. C. T., Bergner, H. W., Bowles, D. E., "A Comparative Study of Composite Shear Specimens Using the Finite-Element Method." *ASTM STP* 734. *American Society for Testing and Materials*. pp. 129-151 (1981).

[22] Pindera, M. J., Ifju, P. G., and Post, D., "Iosipescu Shear Characterization of Polymeric and Metal Matrix Composites," *Proceedings for the Spring SEM conference,* Cambrige Mass. (May 1989).

[23] Wang S. S. and Dasgupta, A., "Developement of Iosipescu-Type Test for Determining In-Plane Shear Properties of Fiber Composite Materails: Critical Analysis and Experiment," Rep. No. UILU-ENG-86-5021, Depts of TAM and Areo. and Astro. Eng., Univ. of Illinois (1986).

[24] Abdallah, M. G., Gardiner, D. S. and Gascoigne, H. E., "An Evaluation of Graphite/Epoxy Iosipescu Shear Specimen Testing Methods With Optical Techniques", *Proc. for the SEM Spring Conference*, Los Vegas, NV (June 1985).

[25] Post, D., "Moire Interferometry", *Handbook of Experimental Mechanics*, A. S. Kobayashi, Ed., Prentice Hall, Englewood Hills, NJ (1987).

[26] Guo, Y. and Post, D., "The Magic of the Carrier Pattern in Moire Interferometry," *Experimental Mechanics,* (to be published).

[27] Mckelvie, J., Walker, C. and Mackenzie, P. "A Workaday Moire Interferometer: Conceptual and Design Considerations; Operation; Applications; Variations; Limitations," *Proceedings of SPIE Conference*, Vol. 814-2, Aug. 1987.

[28] Guo, Y., "Developements in Moire Interferometry: Carrier Pattern Technique and Vibration Insensitive Interferometers," *Disertation at VPI and SU*, (February 1989).

FIGURE CAPTIONS

Fig. 1. The three independent states of shear stress which act on a composite. There is one state of in-plane and two states of interlaminar.

Fig. 2. The two rail shear test consists of a rectangular specimen with rails bolted to opposite sides. The loads are applied as shown by a universal testing machine resulting in shear along a vertical line down the center of the specimen.

Fig. 3. The Arcan test uses a butterfly shaped specimen with load fixtures bolted to its sides. The strains are obtained from gages located in the test section between the notches.

Fig. 4. The Iosipescu specimen is rectangular with opposing notches centered on the top and bottom. A special fixture applies the loads creating shear in the test section between the notches.

Fig. 5. The compact double-notched specimen and loading fixtures. The specimen is loaded at its corners by direct compression and held in static equilibrium by special clamping devices.

Fig. 6. An engineering drawing of the compact specimen used in this initial test.

Fig. 7. The Iosipescu specimen and loading fixture used in these experiments. The fixture was the second or modified Wyoming fixture.

Fig. 8. The specimens were cut from a thick-walled cross-ply graphite/epoxy cylinder. Two orientations were investigated for the compact specimen as show.

Fig. 9. The loads were applied to the compact specimen fixtures by a simple wedge type loading fixture.

Table. 1. The load steps recorded for the two compact specimens and the Iosipescu specimen.

Fig. 10. The U and V displacement fields for compact specimen I at 0 kPa (0 psi.).

Fig. 11. The U and V displacement fields for compact specimen I at 5516 kPa (800 psi.).

Fig. 12. The U and V displacement fields for compact specimen I at 14630 kPa (2120 psi.).

Fig. 13. The U and V displacement fields for compact specimen II at 0 kPa (0 psi.).

Fig. 14. The U and V displacement fields for compact specimen II at 5536 kPa (803 psi.).

Fig. 15. The U and V displacement fields for compact specimen II at 14310 kPa (2080 psi.).

Fig. 16. The U and V displacement fields for the Iosipescu specimen at 0 kPa (0 psi.).

Fig. 17. The U and V displacement fields for the Iosipescu specimen at 6005 kPa (871 psi.).

Fig. 18. The U and V displacement fields for the Iosipescu specimen at 12260 kPa (1778 psi.).

Fig. 19. Shear strain distributions along a line connecting the notch tips for compact specimen I at 0.66, 1.74, 2.87 kN (147, 390, and 645 lb.).

Fig. 20. Shear strain distributions along a line connecting the notch tips for compact specimen I at 3.03, 3.91 kN (680, and 880 lb.).

Fig. 21. Shear strain distributions along a line connecting the notch tips for compact specimen II at 0.66, 1.69 kN (147, and 380 lb.).

Fig. 22. Shear strain distributions along a line connecting the notch tips for compact specimen II at 2.87, 3.91 kN (645, and 880 lb.).

Fig. 23. Shear strain distributions along a line connecting the notch tips for the Iosipescu specimen at 0, 0.21 kN (0, and 48 lb.).

Fig. 24. Shear strain distributions along a line connecting the notch tips for the Iosipescu specimen at 0.44, 0.89 kN (98, and 200 lb.).

Fig. 25. Shear strain distributions along a line connecting the notch tips for the Iosipescu specimen at 1.33, 1.78, 2.60 kN (298, 400, and 585 lb.).

Fig. 26. The shear strain distributions along a line connecting the notch tips for the three specimens. The shear stress levels for compact specimens I, II, and the Iosipescu specimen were 14630, 14310, 12260 kPa (2122, 2076, and 1778 psi) respectively

Fig. 27. The shear stress, shear strain curves for the three specimens tested.

Fig. 28. The Normal strain ε_x distridutions along the line connecting the notch tips for the three specimens. The shear stress levels for compact specimens I, II, and the Iosipescu specimen were 14630, 14310, 12260 kPa (2122, 2076, and 1778 psi) respectively

Fig. 29. Normalized shear strain distibutions along the x axis for the three specimens. The shear stress levels for compact specimens I, II, and the Iosipescu specimen were 14630, 14310, 12260 kPa (2122, 2076, and 1778 psi) respectively

Fig. 30. A magnified view of the cross section of the composite cylinder. The photograph reveals areas of high resin content.

Fig. 31. The U and V Displacement fields for compact specimen I at 14630 kPa (2120 psi.) with a carrier pattern of rotation added.

Fig. 32. The U and V displacement fields for the Iosipescu specimen at 12260 kPa (1778 psi.) with a carrier pattern of rotation added.

Fig. 33. A scheme that may be used to tab the specimen. This reinforces the weak areas of the specimen and could improve shear strength measurements.

Fig. 34. A simple static analysis of the load transfer fixture and compact specimen.

Fig. 35. The V field displacement patterns of the test sections for the three specimens at high load levels. The patterns have been modified with a carrier of rotation to reveal the normal strain ε_y .

Fig. 36. Specimens were cut from a 200mm (8 in) outside diameter laminated composite tube.

Fig. 37. The specimen configurations. Specimen I had steel rails attached to both sides with stiff cement. Specimen II was attached to the rails with compliant cement.

Fig. 38. N_x and N_y fringe patterns for specimen I, depicting the U and V displacement fields. The load level was 3.18 kN (714 lb).

Fig. 39. U and V fringe patterns for specimen II. The load level was 3.14 kN (707 lb).

Fig. 40. The V displacement field with a carrier of extension for the central portion of specimen II. The insert at the bottom shows the ply sequence.

Fig. 41. The V displacement field with a carrier of rotation for the central portion of specimen II.

Fig. 42. The shear strain distributions in individual plies along the length of both specimens. The plies were located within the central third of each specimen.

Fig. 43. Interlaminar shear strains across the width of specimen I at the center of its length. The insert is a photograph of the plies.

Fig. 44. Normal strain ε_y along the length of the specimen I at the centerline and two edge lines.

APPENDIX

EXPERIMENTAL TECHNIQUES

PRINCIPLES OF MOIRE INTERFEROMETRY

Moire interferometry [25] was used to determine the horizontal and vertical displacements on the surface of the specimens tested. This is an optical technique using coherent light and features subwavelength sensitivity and high spatial resolution. It is capable of measuring deformations in composites on a micro-structural scale.

The principle and relevant equations of moire interferometry are depicted in Fig. 47. A crossed-line diffraction grating is replicated on The specimen and deforms with the loaded specimen. Input beams of collimated coherent laser light, B1 and B2, on a horizontal plane, diffract from the specimen grating and interfere with each other. The interference results in a fringe pattern which is a contour map of the U displacements. Additional input beams (not shown) in the vertical plane produce the fringe pattern for the V displacements. The patterns are photographed with a camera focused on the specimen surface.

$$f = \frac{2}{\lambda}\sin\alpha$$

$$U = \frac{1}{f}N_x \qquad V = \frac{1}{f}N_y$$

$$\epsilon_x = \frac{\partial U}{\partial x} = \frac{1}{f}\frac{\partial N_x}{\partial x}$$

$$\epsilon_y = \frac{\partial V}{\partial y} = \frac{1}{f}\frac{\partial N_y}{\partial y}$$

$$\gamma_{xy} = \frac{\partial U}{\partial y} + \frac{\partial V}{\partial x} = \frac{1}{f}\left[\frac{\partial N_x}{\partial y} + \frac{\partial N_y}{\partial x}\right]$$

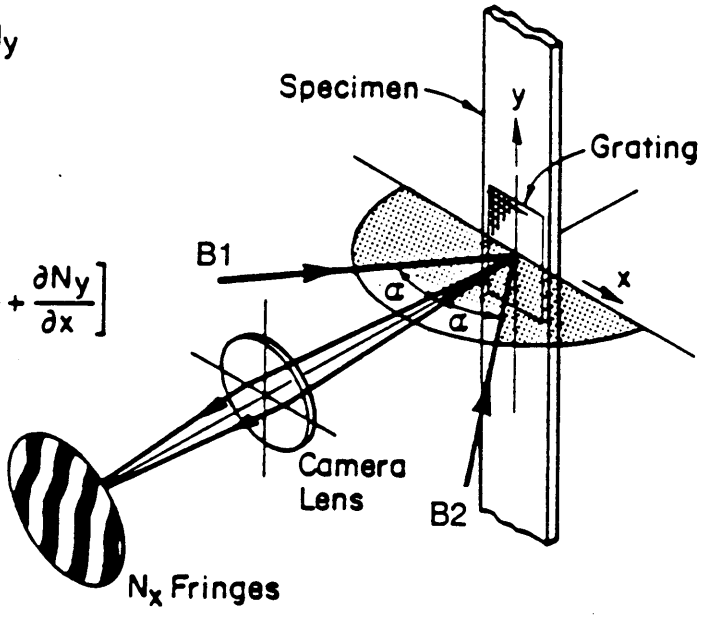

Fig. 47. Moire Interferometry and relevant fringe order/displacement/strain equations. f = 2400 lines/mm (60,960 lines/in.). Sensitivity = 0.417 μm/fringe order

In this work input beams created a virtual reference grating of 2400 l/mm (60,960/in). The sensitivity to displacements was 0.416 μm/fringe order. From the displacement information, strains on the face of the specimen were determined using the relationships in Fig. 47, where f is the frequency of the reference grating and N_x and N_y are the fringe orders for the U and V displacements respectively.

The process used to replicated the specimen grating is illustrated in Fig. 48. The grating mold was a 1200 l/mm crossed-line diffraction grating made with photo resist. Before replication it was coated with an ultra thin film of aluminum. The adhesive used for this process was an epoxy.

CARRIER PATTERNS

Carrier patterns can greatly simplify the extraction of the displacement information from a fringe pattern [26]. This is a technique used in moire interferometry to adjust the appearance of the fringe pattern without altering the displacement information. The carrier fringes can be introduced by the adjustment of beams B1 and B2 in Fig. 47. Carrier fringes transform the appearance of load-induced fringe patterns by adding or subtracting a uniform gradient of fringes across the field. There are two types of carrier patterns, rotation and extension. Carriers of rotation are created by rotating the reference grating with respect to the specimen grating. Carriers of extension result from changing the frequency of the reference grating in order to cause a frequency mismatch. Both of these carriers are simple to implement and usually only a thumb screw adjustment is needed to perform them. Both carriers of extension and rotation were used extensively for these experiments.

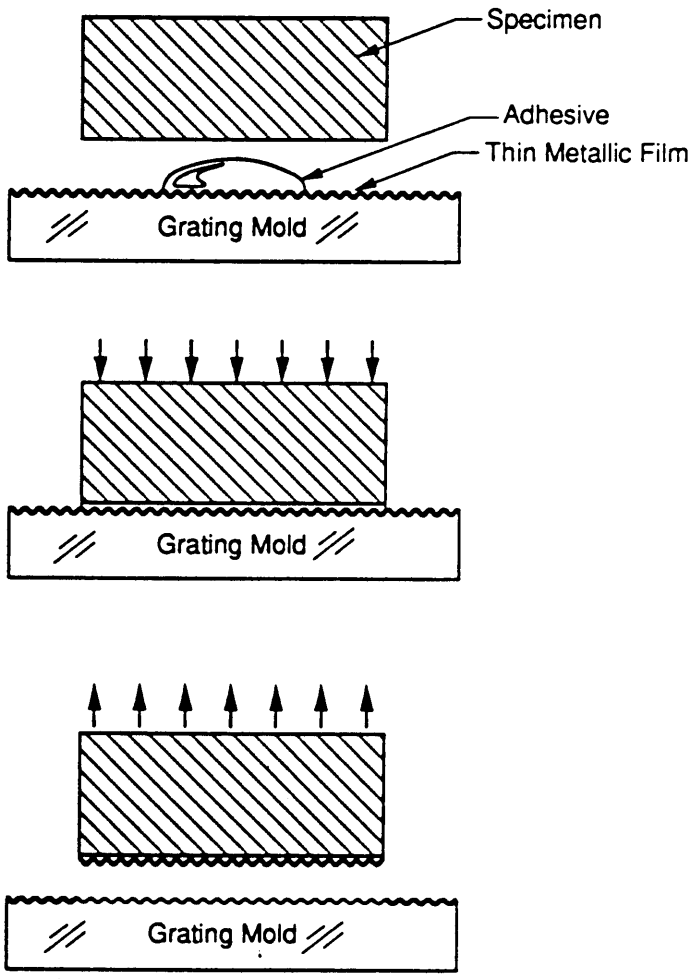

Fig. 48. The process used to replicate specimen gratings. Epoxy adhesive is pooled on an aluminized crossed-line photoresist diffraction grating. The specimen is lowered into the adhesive . A small pressure squeezes the adhesive into a thin film. When the epoxy cures the specimen is separated from the mold along with the reflective aluminum layer.

MOIRE INTERFEROMETRY OFF THE OPTICAL TABLE

Historically, moire interferometry experiments were performed on vibration isolated optical tables. This is because of the high sensitivity of the technique to vibrations. In fact, conventional moire interferometry systems have the same sensitivity to vibrations as to measurement of displacements. High frequency vibrations of the specimen as small in amplitude as $1/2\lambda$ will vibrate the fringe pattern and make photography difficult.

A recent push to take the technique off the optical table and onto the testing machine is under way. Mckelvie et al [27] have built a specialized interferometer to achieve this. This system incorporates quick exposure times to "freeze" vibrating or dancing fringes. Guo et al [28] have developed systems which have high sensitivity to measurements but reduced sensitivity to vibrations. A number of these systems have been investigated. They incorporate fiber optics and real reference gratings.

In this series of tests the Iosipescu specimen was loaded with a Tinius Olsen screw driven testing machine. A practical system was devised and incorporated to perform moire interferometry on this piece of equipment. The system is shown in Fig. 49. It uses a polarization preserving single mode optic fiber to bring laser light to the testing machine. The light is emitted from the fiber with both spatial and temporal coherence. All of the optics are secured to a rigid plate creating a compact interferometer. The system has an adjustment to precisely align the reference grating with the specimen grating. The adjustment essentially rotates the reference grating around the z-axis of the specimen. This adjustment also was used to add arbitrary carrier patterns of rotation to the displacement fields.

The resulting fringe patterns were then photographed using short exposure times to freeze dancing fringes. It is not certain how large of an amplitude or how quickly the

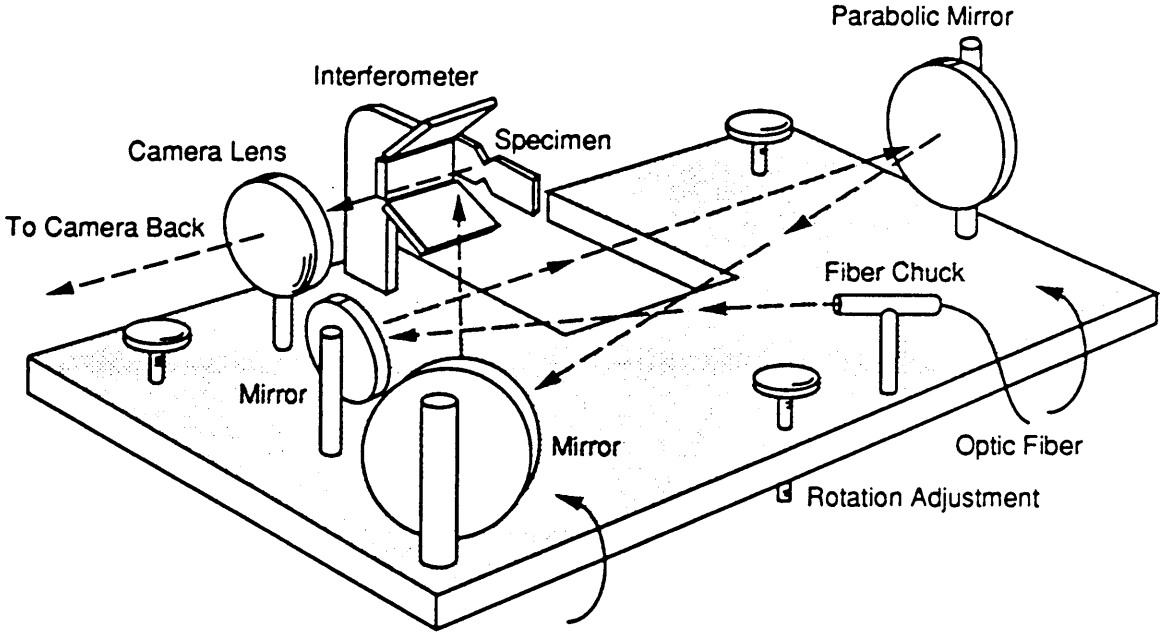

Fig. 49. A schematic drawing of the interferometer used on the testing machine. The rotation adjustment is shown.

fringes danced while the photographs were taken. Nevertheless, the contrast and resolution of the resulting fringe patterns were extremely good as can be seen in Figs 16, 17, and 18.

The vita has been removed from the scanned document